STATISTICAL PRINCIPLES OF NATURAL PHILOSOPHY

Guo Tao

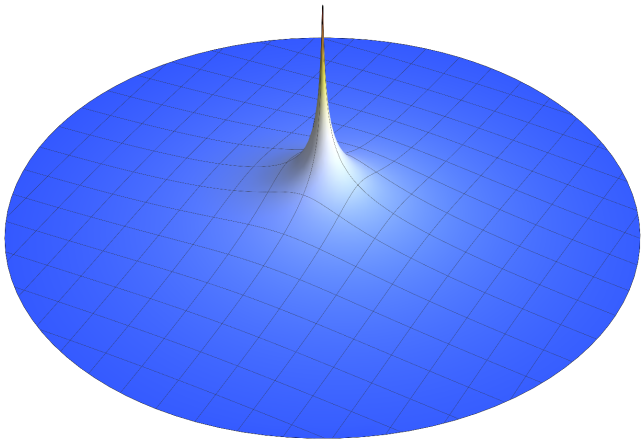

2020-4-22

SIMM

Shanghai · China

Title:

Statistical Principles of Natural Philosophy

Author:

Tao Guo[a,*]

Affiliation:

[a]Center for Drug Delivery System, Shanghai Institute of Materia Medica, Chinese Academy of Sciences, 501 Haike Road, Shanghai 201210, China

***Corresponding Author:**

Center for Drug Delivery System, Shanghai Institute of Materia Medica, Chinese Academy of Sciences, 501 Haike Road, Shanghai 201210, China; Tel: +86-18602131982; E-mail: gotallcn@gmail.com (Tao Guo)

Abstract

Currently, natural philosophy (Physics) is lacking a most fundamental model and a complete set of self-consistent explanations. This article attempts to discuss several issues related to this lack. Starting from the most basic philosophical paradoxes, I deduce a physical model (the natural philosophical outlook) to describe the laws governing the operation of the universe. Based on this model, a mathematical model is established to describe the generalized diffusion behavior of moving particles, for which the form without external field is simply verified. In this article, the gravitational force and relativistic effects are interpreted for the first time as a statistical effect of randomly moving particles. Thus, the gravitational force and special relativistic effects are integrated into a single equation (achieved by selecting an initial wave function with a specific norm when solving it), and the cause of stable particle formation is also revealed. The derived equation and the method of acquiring the initial wave function are fully self-consistent with the hypotheses stated in the physical model, thereby also proving the reliability of the physical model to some extent. Some of these ideas may have potential value as a basis for understanding the essence of quantum mechanics, relativity and superstring theory, as well as for gaining a further understanding of nature and the manufacture of quantum computers.

1. Introduction

"Birds flock and sing when the wind is warm, Flower-shadows climb when the sun is high"[1]; the Earth, our home, is overflowing with vigor! However, light years away, dead silence seems to prevail; from the human perspective, the Earth appears vast, but at the scale of the Solar System, it is merely a "little blue dot". By what forces are these mysterious phenomena, which are as far apart as Heaven and Earth in our eyes, arranged? How enormous is the universe? Why is it like this? Through what mechanism does it operate? Is there a beginning or an end? Where does the vast amount of energy in our universe come from? Will it ever run out? How do the concepts of time, space and speed come into being? Will the total entropy in the universe continue to increase? Etc. Throughout the history of human existence, these have been difficult questions to answer. "Know the enemy and know yourself, and you can fight a hundred battles with no danger of defeat"[2]; to explore the origin of the universe is the only way for human beings to conquer nature.

Since ancient times, human beings have gradually deepened their understanding of

the laws of nature and the universe, through a continuous process of development that can be roughly divided into the following three stages:

In the initial period of Aristotle, Ptolemy, Copernicus, Kepler and others, people's explorations of nature were restricted not only by the level of technological development at that time but also by various political conditions[3]. The explorations of nature and the universe were slow, and the levels of understanding gained were also relatively shallow. By the time of Galileo and Newton, technology had greatly improved, and a framework of relatively strict logic and scientific thinking methods had also been developed. Under the guidance of Newtonian mechanics and calculus, the understanding of nature greatly improved. However, Newtonian mechanics held that gravitation was generated directly by mass and was not affected by motion or energy. The laws of gravitation, inertia and acceleration were all developed based on simple rules of experience from the perspective of philosophy (i.e., axioms; although the definition of universal gravitation was formulated by Newton, Galileo had already established empirical rules in accordance with observation, and the essential nature of inertia or acceleration was not clear), and the universe as a whole was considered to be relatively static.

In modern times, Einstein's theory of general relativity emerged, and humans' ability to understand natural laws and predict natural phenomena improved tremendously. According to general relativity, a gravitation or space-time field is affected by matter, energy and motion, which leads to apparent "magical" changes in motion. On this basis, the existence of black holes and other celestial bodies was predicted[3,4]. With the subsequent rapid development of quantum mechanics, the human understanding of the universe at the microscale greatly improved, resulting in a new era of philosophy (the Copenhagen interpretation of quantum mechanics) as well as a large number of modern technological advances[3].

However, what are the physical principles behind quantum mechanics? How should quantum entanglement and Wheeler's delayed-choice experiment be perceived, and is the Dirac equation with special relativistic effects essentially correct or not? What is the more fundamental reason behind the curved nature space-time and the principles of special relativity? Furthermore, how can dark matter, dark energy and inexplicable repulsion, which often arise in discussions of modern cosmology, be explained? Etc.

In all this time, humans have made no effort to explore the answers to these

substantive questions (by establishing a more fundamental physical model) but rather have remained at the superficial surface of quantum physics. Based on classical physics (such as Newtonian mechanics), formulas have been deduced from a mathematical point of view, and the conclusions of special relativity and the constraints of Lorentz covariance have been added to various equations, yielding results that seem to be very fragmented (such as the Dirac equation and quantum field theory). All these practices have led to the emergence of various theories but have not fundamentally solved the problem[3,5]. The whole edifice of physics seems to have improved by virtue of various explanations, such as the so-called Standard Model of Particle Physics and superstring theory, but none of them is completely satisfactory. The Standard Model and various models of a Grand Unified Theory that have been developed to date merely integrate the previous models from the perspectives of mathematics and the surface nature of physical phenomena; as a result, they cannot perfectly explain gravitational effects (irreducible normalization after the introduction of gravitation). Superstring theory seems to encompass all known successful theories because it includes additional degrees of freedom (higher dimensions). However, the invocation of higher dimensions is not meaningful for solving more practical problems. Instead, because many additional false possibilities arise that make the equations extremely difficult to solve, the requirements in terms of the mathematical skills needed to pursue such theory have reached an amazing level. Moreover, a "string" is not and should not be considered the most basic physical morphology. In addition, the theory of loop quantum gravity is not perfect, and it seems to raise more difficulties than can be solved. In view of the above problems, it is necessary to further understand the essential nature of physical phenomena or physical constraints and to establish a more fundamental physical model.

Starting from the most basic philosophical paradoxes, this article probes into a series of even deeper and more essential problems in physics and attempts to establish a most fundamental physical model to describe the laws governing the operation of the universe. Based on this, a self-consistent mathematical equation is established in a concise form. This equation may be able to unify quantum mechanics and (general and special) relativity and solve the problem of the impossibility of renormalization when integrating quantum mechanics with general relativity. Furthermore, the cause of stable particle formation is also revealed. The frameworks of the physical and mathematical models derived in this article may provide guidance for the interpretation and prediction

of other natural phenomena. However, many viewpoints in this article are being put forward here for the first time, and hence, there must inevitably be some immature ideas and even defects. I earnestly request that my readers may read these with an open mind, not allowing instances of imprecision or individual mistakes in some of the more complicated details to prevent them from being willing to offer constructive suggestions for correcting some rough or flawed aspects of the main idea of this article.

2. Methods

This article expounds on many ideological experiments based on philosophical paradoxes. Mathematica 12.1 for Mac and Linux (*Wolfram Research Inc.*) were used for all of the mathematical calculations, and the operating systems were macOS High Sierra 10.13.6 and Red Hat Enterprise Linux Server (Release 6.3, Kernel Linux 2.6.32-279.el6.x86_64). The solutions to each specific problem can be found in the Supplementary Information. If no specific parameters are specified, the default values in the software system were used. The effective number of significant figures in the numerical methods was no less than 6. In addition, it should be noted that some "abnormal" parameter configurations or script details described in the Supplementary Information of this article actually arose from empirical actions taken to deal with software bugs (for instance, in Fig. 5, different line width settings were used for different midlines, such as the lines at $x = 0$, in the same graphics because this was the only way to ensure that the midlines would look consistent and equal in width). If the results in this article are to be reproduced completely, the software version used must be identical to that used here.

3. Results and Discussions

3.1 Can the World be Understood?

The innate knowledge possessed by human beings is perceptual knowledge that corresponds to external stimuli and is established through long-term interaction and internalization between an organism and its natural environment constrained by the elimination mechanism of nature[6,7]. Therefore, such innate knowledge shows excellent reliability. The acquired knowledge or experience accumulated by human beings through a model of innate cognition (even if such a cognitive model includes more or less subjective factors) should still be reliable and applicable in practice if such practice is based on the same cognitive model. Moreover, in view of the relative stability and repeatability of certain external conditions (i.e., the translation invariance of time and

space), the innate knowledge and acquired experience possessed by human beings should also be reliable throughout the whole range of human practice.

Therefore, the theories established by human beings, even if they are cognitions only from the perspective of human beings on Earth, who in some sense are equivalent to cosmic dust, and even if they contain many limitations or mistakes (such "mistakes" are relative; they are related to the fact that the appearances and forms of things as reflected in the human consciousness are not, in fact, the original appearances and forms of those things), as long as they can effectively explain and predict the phenomena we observe, are successful theories, even though we cannot confirm whether they represent completely correct truth[6].

3.2 The World from the Perspective of Philosophical Paradoxes

The reason why the world has infinite energy and runs endlessly must be that there exists a series of philosophical paradoxes restricting each other[8,9]. Only under such contradictory constraints can the world become balanced and logical (self-consistent). Under the guidance of this perspective, this article summarizes three axioms, as follows:

AXIO 1: Substances exist in the world.

Whether substances exist in the world is an ancient topic of philosophical discussion. However, this debate serves as the original basis for all rational inference and logical extrapolation in this article. There are only two possible situations: either some substance exists in the world or there is no substance at all. The fact is obvious: there are some substances that exist in this world. On average, however, these substances are so sparse that they are almost nonexistent[10]. As a result, the world (or at least within the range of human observation) is as sparse as though it is without substance.

AXIO 2: These substances are inhomogeneous.

If the world is full of substance, then there are only two possibilities for its distribution: it is either homogeneous or inhomogeneous. Obviously, the distribution of substance in this world is inhomogeneous within the range of our observation. However, there is no reason that any one of these inhomogeneous substances should be favored more than another, that is, substances should have no greater opportunity to be distributed in one place than another. Therefore, it should be considered that the probability of the distribution of substances in every location (not limited to only 3 dimensions) is equal, or homogeneous, from a large-scale perspective[11,12]. To satisfy

both of these properties of inequality of distribution and equality of probability, the substances in this world must exist in quantum form. This fact does not require discussion because it has been verified by various physical experiments. There is no reason for the world to "favor one substance more than another", and similarly, it should be probabilistic identical between different "quantum dots". The fact that the above two properties of "inequality of distribution" and "equality of probability" are both satisfied also necessitates that the world is a paradoxical body with uniform probability but inhomogeneous characteristics at the microscale (or in several dimensions).

AXIO 3: These substances are moving.

This seems to be another topic of philosophical discussion, but I give it new connotation here. The substances observed in the world are moving, or from the perspective of human understanding, the substances that exist in the world are moving. In any case, the world can be interpreted as dynamic rather than static. Then, what is the most reasonable movement pattern?

The current understanding is as follows: Photons, which have no stationary mass, are the fastest substance in the universe. It is impossible to accelerate species with stationary masses (such as electrons) to the speed of light. If they were to reach this speed, their masses would become infinite, and their energy consumption will also become infinite (according to the conclusions of relativity). Therefore, there is no species that can move faster than the speed of light, even if there is, it cannot transmit information. However, from this point of view, the essential nature of quantum entanglement cannot be understood, the phenomenon of Wheeler's delayed-choice experiment is astonishing, and the mechanism by which the influence of gravitation can reach out beyond a black hole is not easy to explain, ect.

Therefore, this point of view is abandoned here, and it is instead considered that photons are the fastest species that can transmit information that have been found or perceived by human beings at present, that photons have a light mass (see Section **3.7** for further speculations on photonic structure), and that motion cannot substantially change the physical mass of an object. Particles at a smaller mass level than photons, even if they can transmit information, cannot be perceived (or consciously perceived) by human beings at present, and their limiting speed is faster. Therefore, once the speed of a particle is sufficiently fast, it must "split" into particles of lower mass levels, until the speed reaches infinity and the mass becomes infinitesimal (in the framework based

on the assertion that "the substances in this world must exist in quantum form", Section **3.3.5.2** will confirm that it is possible that particles of lower mass levels can form a particle of a higher mass level and that the opposite process can also occur).

From this point of view, the whole universe will exhibit motion-related phenomena as follows: For a particle with infinitesimal mass, its speed can reach infinity. So, no matter how large the space in which it exists is, such an infinitesimal particle can instantaneously exist at any position. Therefore, it can be everywhere at once, relative to it, any arbitrarily large space is also an infinitesimal space in which the concepts of time and distance do not apply, and such a particle is infinitely large relative to any such space, meaning that no motion in space can be perceived for space at all. Since there is no concept of space or time in the case of infinitesimal particles, there is also no concept of energy. If the universe is composed of infinitely many such moving particles (because they are infinitesimal particles, there are no collisions between them), then it will not consume any so-called energy and can continue to exist and run forever. However, once a particle of a larger mass level (a particle swarm of infinitesimal particles) is observed, its speed will decrease (the relationship between the mass of the undisturbed particle swarm and the average speed of the constituent particles obeys the Maxwell distribution; see Part 1 of the Supplementary Information for details). Simultaneously, the concepts of time, space, speed, mass and energy will arise. Therefore, there is no inherent concept of time, space or speed and no inherent concept of mass or energy in the universe; all of these concepts instead arise from the representations of the universe that are observed from various perspectives. Although a particle is infinitesimal, it is infinite relative to the universe; although the universe is infinitely great, it is infinitesimal relative to the infinitesimal particles. As the velocity of a particle approaches infinity, the very concept of motion will be lost. The universe is both large and small; substances both move and do not move within it; and the concepts of time, space, speed, mass and energy are both extant and absent. Thus, the nature of the universe is described by several pairs of mutually constraining paradoxes.

The validity of the above three axioms is obvious, and their existence depends on the constraints imposed by their counterparts in the mutually constraining paradoxes introduced above. Here, only the meaningful sides of these paradoxes are selected for further investigation. In addition, under the constraints of logic, the concepts derived from the 3 axioms are also contradictory constraints. Only logic that is constrained by

paradoxes is complete and self-consistent. On the basis of the above three axioms, this article makes reasonable inferences and extracts the following 3 hypotheses:

HYPO 1: The universe is composed of infinitely many uniform particles with infinite speed and infinitesimal mass.

The concepts of "infinity" and "infinitesimal" are equivalent to those in mathematical analysis. The statement that the masses of the particles are uniform refers to these masses relative to their standard deviation, and the concept of "uniform particles" discussed below also has the same meaning.

HYPO 2: The speeds of these infinitesimal particles in 3-dimensional space are equal, and the directions of their motion are random.

As mentioned in **AXIO 2**, these infinitesimal particles are formed in accordance with the same law; therefore, their masses and speeds (or norms of momenta) should be either strictly equal or equal relative to their standard deviations (the concepts of equal masses and speeds discussed below also have the same meaning), and the probabilities of the possible directions in each dimension are also equal because there is no reason for them to be uneven.

HYPO 3: There is no interaction between infinitesimal particles.

In the world we observe, interaction forces exist everywhere. However, this is not necessarily true for infinitesimal particles. For infinitesimal particles, it is assumed that there is no traditional interaction between them (such as gravitation) and that any observed macroscopic force (or interaction) is caused by a statistical effect of these infinitesimal moving particles. This assumption does not conflict with the classical force concept but will be helpful for establishing a general equation and expanding the self-consistent range of theory.

These are the 3 basic characteristics (hypotheses) extracted from the 3 basic axioms regarding the nature of the world. Next, a model will be built on the basis of these 3 hypotheses.

3.3 Model Building Based on Philosophical Paradoxes

On the basis of the above 3 axioms and 3 hypotheses, this article infers that there are only four possibilities regarding the scale (large or small) of space (in any dimension) and the number (many or few) of particles in any local domain and that these four possibilities are independent in different local domains. This is because the world is dynamic (in infinite dimensions) and inhomogeneous, and motion and inhomogeneity

are two independent properties. Because of the movement of particles, when a certain number of particles are observed without any spatial differences, the concept of velocity will be generated in the world. In infinite dimensions, the concept of velocity will be characterized in terms of the concepts of time and distance. Due to the inhomogeneity of the distribution of particles, when a certain number of particles are observed with spatial differences, the concept of density will be generated in the world. In infinite dimensions, the concept of density will be characterized in terms of the concepts of scale (another single degree of freedom different from distance) and the number of particles with spatial differences (disguised distance in another degree of freedom). If the latter two degrees of freedom are fixed (that is, the two degrees of freedom or the entities they represent are used as references to determine the object under inspection), then they will be characterized in terms of the degrees of freedom of distance in the other two dimensions. Therefore, there are four independent dimensions in this world, being three dimensions characterized in terms of the concept of space in our consciousness and one dimension characterized in terms of the concept of time in our consciousness. In principle, these 3-dimensional space and 1-dimensional time coordinates can describe all natural phenomena. Even methods operating in the so-called multidimensional space of string theory have the ultimate purpose of solving problems in 4-dimensional space-time.

To understand the world more easily and intuitively, humans tend to project various abstract results and conclusions into the world we are familiar with. In principle, if a 4-dimensional curvilinear coordinate system is adopted through coordinate transformation, the necessary mathematical operations may be simple, but this conceptualization will lead to difficulties in understanding the problem. Einstein's general relativity uses a 4-dimensional curvilinear coordinate system (space-time), which is an "immersive perspective" with a sense of participation. Although individual immersive physical events (such as the constant speed of light) are consistent with physical observations, difficulties will eventually arise in understanding the essence of physical problems. In absolute space-time, the coordinate system consisting of 3 spatial dimensions and 1 time dimension is the "God perspective", which is helpful in allowing people to look at and understand problems from a macroscopic perspective. Of course, no matter which perspective is adopted, it does not affect the descriptions of physical phenomena in 4-dimensional space-time. Finally, the evolution of various phenomena

should ultimately be measured and understood in the flat coordinate system that we are familiar with at present.

It should be emphasized that the "God perspective" (or "absolute space-time") mentioned here also has relativity. When absolute space-time is used as the reference system, the particles in it should satisfy the conditions given by **HYPO 1–3** (this system can also be regarded as the classical "inertial reference system" here). This means that if the entire swarm of existing particles moves as a whole, then absolute space-time will also move with it; it would be meaningless if absolute space-time (or the corresponding absolute coordinate system) did not follow the overall movement of the particle swarm.

Since our goal is to understand and grasp the world, it is unnecessary to use a relatively variable view of space-time. Sometimes, the concept of absolute space-time is more advantageous for building models and understanding laws. In view of the above analysis, the physical and mathematical models presented in this paper will be established in the 4-dimensional (3 dimensions of space plus 1 dimension of time) absolute coordinate system.

3.3.1 Physical Model

Here, **HYPO 1–3** are combined to form the physical model considered in this article: The universe is composed of infinitely many uniform particles with infinite speed and infinitesimal mass. The speeds of these infinitesimal particles in 3-dimensional space are equal, and the directions of their motion are random. There is no interaction between infinitesimal particles. No additional rules are needed.

3.3.2 Special Relativistic Effects on Infinitesimal Particles

It will be proven that (special) relativistic effects exist in the abovementioned physical model (Section **3.3.1**). Once again, it is emphasized that the speeds of these particles (throughout this article, the "infinitesimal particles" described in the above physical model are called "particles", "1st-order particles" or "tiny particles", while larger finite-mass-level particles composed of k particles are called "kth-order particles") are exactly the same (or $\sigma_1 \ll c$, where c is the mean value of the particle speeds and σ_1 is their standard deviation), and the directions of their motions in 3-dimensional space are random. Therefore, these particles can be represented by random vectors with equal norms in Euclidean space. In this article, statistical methods will be used to prove the existence of special relativistic effects in the vector swarm composed of such a group of vectors. When a group of particles in the same 3-dimensional space is moving

in one direction on average (i.e., their centroid is moving in one direction), they will lose some probability of movement in other directions due to statistical effects, i.e., the movement trends in other directions will decrease, giving rise to a special relativistic effect. This phenomenon will be quantitatively explained in detail below.

Note that the velocity of a *k*th-order particle is the velocity of the overall center of mass of the *k* particles, which is the average of the velocity vectors of all these particles. Moreover, the projection of the velocity vector of a *k*th-order particle onto one of the three equivalent coordinate axes of the 3-dimensional Cartesian coordinate system is the mean value of the projection (onto the same axis) of the velocity vectors of the 1st-order particles forming the *k*th-order particle, which follow the same distribution; therefore, it approximately follows a normal distribution (central limit theorem). There are three equivalent (approximate) normal distributions, one on each of the three axes, which are not completely independent. However, James Clerk Maxwell[13] proved that these distribution can, in fact, be equivalently treated as completely independent. This is because randomly selecting a vector is equivalent to randomly determining a three-axis coordinate; moreover, the problem of the momentum transfer of gas molecules participating in random collisions is also equivalent to the problem discussed in this article. Accordingly, the speeds of *k*th-order particles follow the Maxwell distribution. Suppose that the standard deviation of the projection (treated as a random variable; the same is done below) of the velocity of any one of the *k* equivalent particles forming a *k*th-order particle onto each equivalent coordinate axis is σ. Then, the standard deviation of the projection of the velocity of a *k*th-order particle onto each equivalent coordinate axis is $\frac{\sigma}{\sqrt{k}}$, namely, the projection onto each coordinate axis follows a normal distribution with a standard deviation of $\frac{\sigma}{\sqrt{k}}$. As a result, the speed of *k*th-order particles follows the Maxwell distribution with scale parameter $\frac{\sigma}{\sqrt{k}}$ (see Part 1 of the Supplementary Information for details).

As already mentioned, it is assumed that the speed of all particles is c ($c > 0$) and that the directions of their movement are evenly distributed in 3-dimensional space. Among the possible systems composed of randomly moving particles, the system with an average velocity of 0 (i.e., the "absolute space-time" mentioned earlier) is called the

stationary reference system (denoted by $\mathcal{R}_0$), and a 3-dimensional Cartesian (rectangular) coordinate system *Oxyz* is established for it. A particle swarm formed by a subset of particles in a certain period of time and moving at an average velocity u is called a moving reference system (denoted by $\mathcal{R}_u$). Let the direction of the velocity of $\mathcal{R}_u$ be parallel to the z-axis in the direction of increasing z. Then, the mean value of the velocity component of the particles in $\mathcal{R}_u$ along the z-axis must be u. Under the assumptions that all particles in $\mathcal{R}_u$ are represented by vectors with their starting points at the origin of the coordinate system and that the point (0, 0, u) is taken as the dividing point of the z-axis, the vectors in $\mathcal{R}_u$ can be separated into two groups: the components of the vectors above this dividing point and the components of the vectors below it. These vectors randomly enter $\mathcal{R}_u$ from $\mathcal{R}_0$ with equal probability. Therefore, the distribution of the vectors in $\mathcal{R}_u$ can be thought of as a mixed distribution of the vector distribution of the components above the dividing point and the vector distribution of the components below the dividing point. When the mean value of the components on the z-axis of this mixed distribution is u, the mixture weights w can be determined. With this value as the reference, the distribution of the vectors that form the mixed distribution on the x-axis (or y-axis) can be determined; thus, their standard deviation σ_u can also be obtained. When the standard deviation of the components on the z-axis of this mixed distribution is also σ_u, then the speed of kth-order particles (of mass μk, where μ is the mass of a single particle; the same is true below) in $\mathcal{R}_u$ follows the Maxwell distribution with scale parameter $\sigma_{u,k}$, where

$$\sigma_{u,k} = \frac{\sigma_u}{\sqrt{k}}. \tag{1}$$

Therefore, $\sigma_{u,k}$ is directly proportional to the average speed $\overline{v}_{u,k}$ of the kth-order particle, namely,

$$\overline{v}_{u,k} = 2\sqrt{\frac{2}{\pi}}\sigma_{u,k}. \tag{2}$$

By substituting Eq. 1 into Eq. 2, we obtain

$$\overline{v}_{u,k} = 2\sqrt{\frac{2}{\pi}} \cdot \frac{\sigma_u}{\sqrt{k}}. \tag{3}$$

The distribution of the vectors in $\mathcal{R}_0$ is relatively simple. Suppose that the standard deviation of their components on the x-axis (or y- or z-axis) is σ_0; similarly, the average velocity of the kth-order particles that is formed by them is

$$\overline{v}_{0,k} = 2\sqrt{\frac{2}{\pi}} \cdot \frac{\sigma_0}{\sqrt{k}}. \tag{4}$$

When particles of the same mass level are formed in both $\mathcal{R}_u$ and $\mathcal{R}_0$, the ratio between their average speeds (Eq. 3 to Eq. 4) is

$$\frac{\overline{v}_{u,k}}{\overline{v}_{0,k}} = \frac{\sigma_u}{\sigma_0}. \tag{5}$$

Therefore, the ratio of σ_u to σ_0 is the ratio between the average speeds of particles of higher mass levels in $\mathcal{R}_u$ and $\mathcal{R}_0$. A more detailed introduction will be presented in the following.

As mentioned above, in the 3-dimensional Cartesian coordinate system constructed in the stationary reference system $\mathcal{R}_0$, if the moving reference system $\mathcal{R}_u$ moves along the z-axis at velocity u, then the x- and y-coordinates are equivalent; hence, only the x-coordinate is considered in the following. In view of the nature of probability theory, in $\mathcal{R}_0$, if the components of these vectors along the z-axis are uniformly distributed in the interval $[-c, c]$, then the probability density on the x-axis is

$$\mathcal{D}(\theta,\eta) = c \cdot \cos\theta \cdot \sin\cos^{-1}\eta, \tag{6}$$

where the random variables are $\Theta \sim U(-\pi, \pi)$ and $H \sim U(-1, 1)$. Note that in this article, random variables (vectors) are expressed in capital letters, and the values of random variable (vectors) are expressed in the corresponding lower-case letters. The component distribution of the vectors whose components are above $(0, 0, u)$ on the x-axis is denoted by $\mathcal{D}_1$, and its probability density is written as

$$\mathcal{D}_1(\theta,\eta) = c \cdot \cos\theta \cdot \sin\cos^{-1}\eta, \tag{7}$$

where the random variables are $\Theta \sim U(-\pi, \pi)$ and $H \sim U(\frac{u}{c}, 1)$. Correspondingly, the component distribution of these vectors on the z-axis is denoted by $\mathcal{D}_3$, namely, $\mathcal{D}_3 \sim U(u, c)$. The component distribution of the vectors whose components are below $(0, 0, u)$ on the x-axis is denoted by $\mathcal{D}_2$, and its probability density is written as

$$\mathcal{D}_2(\theta,\eta) = c \cdot \cos\theta \cdot \sin\cos^{-1}\eta, \tag{8}$$

where the random variables are $\Theta \sim U(-\pi, \pi)$ and $H \sim U(-1, \frac{u}{c})$. Correspondingly, the component distribution of these vectors on the z-axis is denoted by $\mathcal{D}_4$, namely, $\mathcal{D}_4 \sim U(-c, u)$. When the mean value of the components of the mixed distribution consisting of

$\mathcal{D}_3$ and $\mathcal{D}_4$ on the z-axis is u, the corresponding mixture weights are $\frac{c+u}{2c}$ and $\frac{c-u}{2c}$, respectively. Note that $\mathcal{D}_1$ and $\mathcal{D}_2$ are randomly selected from the vector swarms with the same characteristics as $\mathcal{D}_3$ and $\mathcal{D}_4$, respectively. Then, the mixed distribution consisting of $\mathcal{D}_1$ and $\mathcal{D}_2$ can be calculated in accordance with these two weights (the analytical form of this mixed distribution cannot be given in this article at present); then, it can be found that the standard deviation of the velocity components on the x-axis of the particles in $\mathcal{R}_u$ is

$$\sigma_u = \frac{\sqrt{c^2 - u^2}}{\sqrt{3}}. \tag{9}$$

By evaluating the ratio between Eq. 9 and the standard deviation of the velocity components on the x-axis of the particles in $\mathcal{R}_0$, we can obtain the corresponding scale factor, namely,

$$\boxed{\frac{\sqrt{c^2 - u^2}}{c}}. \tag{10}$$

This is equivalent to the additive inverse of the Lorentz factor when c represents the speed of light. Obviously, the ratio of the standard deviations of the velocity components on the y-axis is also this scale factor, as shown in Eq. 10. This same factor can also be obtained by evaluating the ratio of the standard deviation of the velocity components on the z-axis of the mixed distribution in $\mathcal{R}_u$ to the standard deviation of the velocity components on the z-axis in $\mathcal{R}_0$. The detailed Mathematica code for the above calculation can be found in Part 2 of the Supplementary Information. This result implies that when a subset of the particles in the reference system $\mathcal{R}_0$ composed of particles moving at the same speed (such as c) and in random directions forms a reference system $\mathcal{R}_u$ moving at speed u, the speed of the moving aggregate particle of a larger mass level in $\mathcal{R}_u$ will be relatively decreased, with a degree of deceleration corresponding to the value determined by the scale factor given by Eq. 10.

In this article, we will not discuss further special relativistic effects (such as time expansion and length contraction) based on this logic. It is obvious that from the deceleration effect, all other related phenomena follow.

The abovementioned results prove that vectors with equal norms in Euclidean space exhibit special relativistic effects. In a stationary (inertial) reference system, if particles of different mass levels are moving in accordance with the relationship

determined by Eq. 40 below, they will be considered to have different average velocities based on the corresponding Maxwell distributions. When the average velocity of a larger-mass-level particle composed of $\mathcal{K}$th-order particles is measured in a moving reference system $\mathcal{R}_u$ with velocity u, the corresponding degree of deceleration is determined by the average speed $c_{\mathcal{K}}$ of the $\mathcal{K}$th-order particles in accordance with the scale factor $\frac{\sqrt{c_{\mathcal{K}}^2 - u^2}}{c_{\mathcal{K}}}$, and when the average velocity of a larger-mass-level particle composed of $\mathcal{L}$th-order particles is measured similarly, the corresponding degree of deceleration is determined by the average speed $c_{\mathcal{L}}$ of the $\mathcal{L}$th-order particles in accordance with the scale factor $\frac{\sqrt{c_{\mathcal{L}}^2 - u^2}}{c_{\mathcal{L}}}$. If a moving species in a moving reference system $\mathcal{R}_u$ consists entirely of photons (an energy group of photons), then the degree of reduction in their average velocity is calculated using the Lorentz factor given in Eq. 10 (or determined by special relativity). At present, human beings can detect only photons and photon-level formations (such as electromagnetic waves and atomic clocks); from this point of view, the quantitative relationship given by special relativity is extremely accurate! It is also noted that in $\mathcal{R}_u$, the slowdown on all three axes is the same. This means that there is no difference in physical laws that can be perceived between $\mathcal{R}_u$ and the stationary reference system $\mathcal{R}_0$. Therefore, when another moving reference system $\mathcal{R}_{u'}$ appears in $\mathcal{R}_u$, $\mathcal{R}_u$ can, in turn, be treated as a stationary reference system, which is a useful feature. This reveals that any reference system that satisfies the conditions given in **HYPO 1–3** can be regarded as a stationary reference system, regardless of whether it is an absolutely stationary reference system. Therefore, the particles in $\mathcal{R}_0$ can also be regarded as formed by the particles in $\mathcal{R}_u$. Special relativistic effects are statistical effects of moving particles. If the equation established in this article can capture the statistical effects of moving particles, then it can also describe the effects of (special) relativity.

3.3.3 Establishment of the Classical Diffusion Equation

To comprehensively describe the above physical model, we should establish a four-parameter equation, including time, for the law governing the motion of each particle, i.e., $\wp(x, y, z, t)$. For a system with n particles, it is necessary to establish an equation with $3n + 1$ degrees of freedom in the same time dimension, where $n \to +\infty$. This is obviously extremely unrealistic. Attempting to establish equations in

accordance with this idea will only increase the complexity of the solution. For example, in superstring theory, equations with even tens of degrees of freedom are often established. Although such equations can be "all inclusive" to a great extent, the difficulty of solving them is already unimaginable and has given rise to the rhetorical statement that “String theory is 21st century physics that fell accidentally into the 20th century”[5]. By extrapolation, equations established in accordance with the above approach may be expected to be difficult to solve even in the 210th century!

In this article, we take the second best approach. We do not expect to describe all of the motion characteristics of all particles; instead, we wish only to describe the laws of particle motion succinctly and practically, to establish an equation that does not fundamentally fail to capture any critical motion characteristics of particles and can be described (solved) in actuality to the greatest possible extent. To do so, it may be appropriate to approach the problem from the perspective of statistics, that is, to establish a mathematical model with certain statistical characteristics on the basis of the physical model.

Theoretically, infinitely many aggregations of any number of particles can be found in infinite 4-dimensional space-time, although the greater the difference between the degree of aggregation and the total average density in space-time, the lower the formation probability of the corresponding particles, and the more unstable they will be in the time dimension. However, it is difficult to describe this situation with a specific function. Therefore, this article does not seek functions that apply at the micro level or for uncertain cases but rather seeks statistical description functions that are relatively certain by expanding the considered scope to cover a sufficiently large range of cases. Regardless of how these particles move in 3-dimensional space, their trajectories are continuous, which will lead to diffusion (or agglomeration) behavior that is the generalized diffusion of randomly moving particles. Here, each moving particle is regarded as a vector, whose direction is the same as the movement direction of the particle and whose norm is equal to the movement speed. Therefore, the generalized diffusivity of randomly moving particles is equivalent to the generalized diffusivity of random vectors (in direction). Thus, the "random vectors" and "randomly moving particles (or velocities)" mentioned below have the same meaning. Considering particles of the same mass and speed, the generalized diffusivity of the corresponding random vectors is equivalent to the generalized diffusivity of random momenta (which

are also vectors). It is considered that the scale of the "generalized diffusivity of vectors" is simply the scale that is most suitable for describing the invariant laws for randomly moving particles. More information will be lost if the scale is even slightly more macroscopic (e.g., the scale can be approximately described by real diffusion), and there will be no invariant statistical law to follow if the scale is even slightly more microscopic (for example, the scale described at the beginning of this paragraph). At this scale, the external behavior of the vectors in a tiny space cannot be considered isotropic. When the randomly moving particles are not disturbed, according to the Maxwell distribution, the total vector in a certain domain always points in an uncertain direction, and the norm is directly proportional to $\sqrt{k}$, where k is the number of vectors (see Part 1 of the Supplementary Information for details). Although the direction of the total vector in a tiny space cannot be determined from the Maxwell distribution, we hope to use appropriate constraints to obtain the distribution rules governing the norm and direction of the total vector at any position in space.

First, we determine the constraints acting on spatial vectors. Let the density of the vector sum at some point in space be denoted by $\boldsymbol{\mathcal{X}}$, which is a function of position and time, namely, $\boldsymbol{\mathcal{X}}(x, y, z, t)$. It is defined as follows: At a certain time t, let $\boldsymbol{\mathcal{Y}}(\mathcal{V})$ be a function of the sum of all vectors in the closed domain $\mathcal{V}$ containing $\mathcal{P}(x, y, z)$; then, $\boldsymbol{\mathcal{X}}(x,y,z,t)=\lim_{\mathcal{V}\to\mathcal{P}}\frac{\boldsymbol{\mathcal{Y}}(\mathcal{V})}{\mathcal{V}}$) (in the following, $\boldsymbol{\mathcal{X}}$ is also a function of the spatial coordinates (x, y, z) and the time coordinate t). The situation in which particle position aggregation is dominant will be studied in the following.

$\boldsymbol{\mathcal{X}}$ is a statistical average vector. When the system is undisturbed, the relationship between $\boldsymbol{\mathcal{X}}$ and the number of vectors follows the Maxwell distribution. As illustrated in Fig. 1a, it is assumed that there are two microdomains $\mathcal{V}_\mathrm{A}$ and $\mathcal{V}_\mathrm{B}$ of the same size along the normal direction on both sides of the segmentation surface Φ. If the sum of all vectors in $\mathcal{V}_\mathrm{A}$ is $\overrightarrow{\mathrm{OA}}$ and the sum of all vectors in $\mathcal{V}_\mathrm{B}$ is $\overrightarrow{\mathrm{OB}}$, then their sum is $\overrightarrow{\mathrm{OC}}$, and their difference is $\overrightarrow{\mathrm{AB}}$. Let the sum and difference vectors intersect at point M (Fig. 1b). In view of the previous assumption that the domains $\mathcal{V}_\mathrm{A}$ and $\mathcal{V}_\mathrm{B}$ on both sides of Φ are equal, there is no need to consider statistical effects before the particles move. Due to the characteristic that the distribution of the velocity directions is homogeneous, both vectors must tend to approach their average value $\overrightarrow{\mathrm{OM}}$, that is, both $\overrightarrow{\mathrm{OA}}$ and $\overrightarrow{\mathrm{OB}}$ will tend towards $\overrightarrow{\mathrm{OM}}$. Accordingly, the rate of change in $\boldsymbol{\mathcal{X}}$

along the normal direction at a particular point should be related to the time-dependent rate of change in $\mathcal{X}$. This time-dependent rate of change is also affected by another inherent factor (i.e., the velocity of the particles forming $\mathcal{X}$), the concrete value of which is temporally uncertain. Therefore, the above two rates of change should be directly proportional when the differences between particles caused by density (including position aggregation and direction aggregation) are neglected.

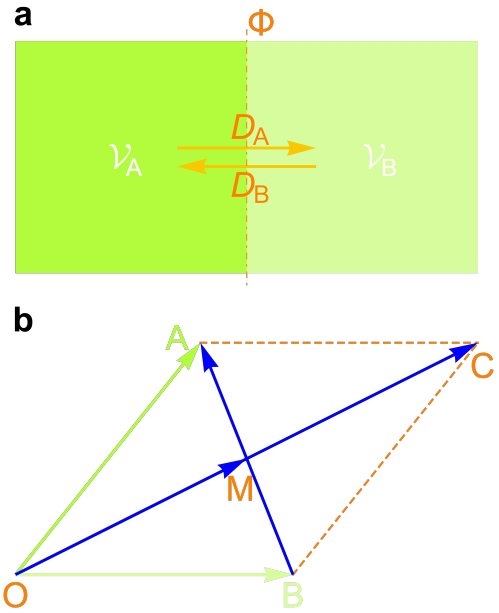

Figure 1 | Illustration of the principle of the generation of a mutual diffusion potential in microdomains $\mathcal{V}_A$ and $\mathcal{V}_B$.

In view of the similar calculus properties of vector and scalar, the derivation method for real diffusion is imitated here. If a domain $\mathcal{W}$ is enclosed by a closed surface Σ, then during the infinitesimal period $\mathrm{d}t$, the directional derivative $\frac{\partial \boldsymbol{\mathcal{X}}}{\partial \boldsymbol{N}}$ of $\boldsymbol{\mathcal{X}}$ along the normal direction of an infinitesimal area element $\mathrm{d}S$ on the surface Σ is directly proportional to the vector $\mathrm{d}\boldsymbol{\mathcal{X}}$ flowing through $\mathrm{d}S$ along the normal direction in the closed domain $\mathcal{W}$ enclosed by Σ (Fig. 2), under the assumption that the coefficient is a positive real number D.

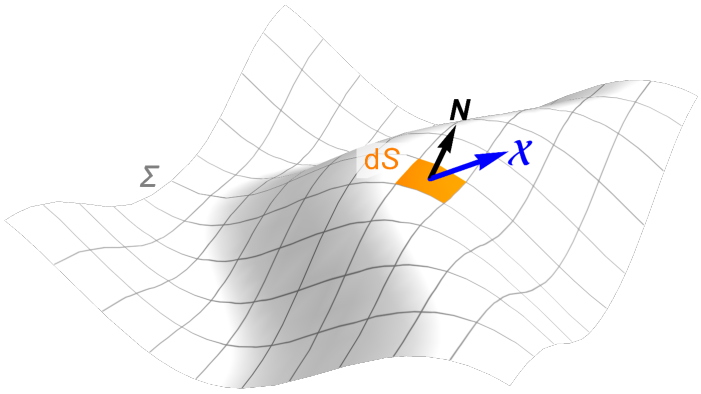

Figure 2 | Illustration of the diffusion of the vector sum density $\boldsymbol{\mathcal{X}}$.

From time t_1 to time t_2, when the influence of the vector density on D is not considered (i.e., the diffusion coefficient is the same at every position), the variation of the vector sum $\boldsymbol{\mathcal{A}}$ inside the closed surface Σ is

$$\delta\boldsymbol{\mathcal{A}} = \int_{t_1}^{t_2}\left(\oiint_{\Sigma} D\frac{\partial\boldsymbol{\mathcal{X}}}{\partial\boldsymbol{N}}\mathrm{d}S\right)\mathrm{d}t. \tag{11}$$

According to the Gauss formula, the right-hand side of Eq. 11 can also be written in the form

$$\int_{t_1}^{t_2}\left(\iiint_{\mathcal{W}} D\Delta\boldsymbol{\mathcal{X}}\,\mathrm{d}x\,\mathrm{d}y\,\mathrm{d}z\right)\mathrm{d}t, \tag{12}$$

where Δ is the Laplace operator, which describes the second derivative with respect to the position (x, y, z). And the left-hand side of Eq. 11 (namely, $\delta\boldsymbol{\mathcal{A}}$) can be written as

$$\delta\boldsymbol{\mathcal{A}} = \iiint_{\mathcal{W}}\left(\int_{t_1}^{t_2}\frac{\partial\boldsymbol{\mathcal{X}}}{\partial t}\mathrm{d}t\right)\mathrm{d}x\,\mathrm{d}y\,\mathrm{d}z. \tag{13}$$

By setting Eq. 13 equal to Eq. 12 and transforming the order of integration, we can obtain

$$\int_{t_1}^{t_2}\iiint_{\mathcal{W}}\frac{\partial\boldsymbol{\mathcal{X}}}{\partial t}\mathrm{d}x\,\mathrm{d}y\,\mathrm{d}z\,\mathrm{d}t = \int_{t_1}^{t_2}\iiint_{\mathcal{W}} D\Delta\boldsymbol{\mathcal{X}}\,\mathrm{d}x\,\mathrm{d}y\,\mathrm{d}z\,\mathrm{d}t. \tag{14}$$

Based on the observation that t_1, t_2 and the domain $\mathcal{W}$ are all arbitrary, the following equation can be written:

$$\frac{\partial\boldsymbol{\mathcal{X}}}{\partial t} = D\Delta\boldsymbol{\mathcal{X}}. \tag{15}$$

It is clear that the above conclusion still holds when $\boldsymbol{\mathcal{X}}$ is dominated by the aggregation of the velocity direction rather than the position of the particles. This is because this situation is also a statistical characteristic of a large number of particles, and the

diffusion behavior does not discriminate between these two types of aggregation.

To facilitate the task of vector decomposition in the following, a 3-dimensional vector needs to be converted into a plane vector. Next, we determine the constraints acting on plane vectors. Although the operation in Eq. 15 is performed using 3-dimensional vectors, when differential operations are performed on a spatial vector, the (sum or) difference operations are always performed at two points on the vectors that are separated by an infinitesimal distance; thus, all 3-dimensional vectors can exhibit only relative 2-dimensional characteristics. Consequently, by solving this differential equation, only 2-dimensional constraints can be obtained. Therefore, only the derivatives of plane vectors are needed to act as the derivatives of the 3-dimensional vectors (in this case, plane vectors can retain the important information, such as the norms of the vectors and the included angle between them). Moreover, the function of plane vectors obtained by solving the partial differential equation expressed in terms of plane vectors is unique and corresponds to the 3-dimensional vectors obtained from a differential equation of the same form. It is assumed that the function of plane vectors describing the density of the vectors or momenta is $\mathcal{M}(x, y, z, t)$, which corresponds to $\mathcal{X}$ at the point (x, y, z, t) (unless otherwise stated, in the following, $\mathcal{M}$ is a function of the spatial coordinates (x, y, z) and the time coordinate t). Thus, the abovementioned $\mathcal{X}$ can be replaced with $\mathcal{M}$. After this replacement, it is obvious that the norm of the plane vector will not change, but its direction will be reoriented. Finally, Eq. 15 can be written as

$$\left|\frac{\partial \mathcal{M}}{\partial t}\right| = D\left|\Delta \mathcal{M}\right|. \tag{16}$$

Now, let us determine the constraints on the direction of the plane vector $\mathcal{M}$. In view of the continuity of the trajectories of infinitesimal particles, since $\mathcal{M}$ is also characterized in terms of the statistical properties of an enormous number of particles, it should also be smooth. According to the theory of plane curves, the first and second derivatives of a plane vector in any direction in space are vertical. If an equation relating these derivatives is established following the above derivative relationship (Eq. 16), the direction needs to be adjusted to be consistent; then, this relationship can be written in the form

$$\frac{\partial \mathcal{M}}{\partial t} = \boldsymbol{i} D \Delta \mathcal{M}. \tag{17}$$

where $\boldsymbol{i}$ is the imaginary unit. By multiplying both sides of Eq. 17 by $\boldsymbol{i}$, the form of the Schrödinger equation can be obtained:

$$\boldsymbol{i}\frac{\partial \boldsymbol{\mathcal{M}}}{\partial t} = -D\Delta\boldsymbol{\mathcal{M}}. \tag{18}$$

Eq. 18 describes the distribution of a moving particle swarm (including the direction of movement) in space following the same diffusion coefficient; in other words, it is the classical diffusion equation. However, when the particle swarm is moving faster or more particles are aggregating in a certain microdomain, the effect on diffusion is not clear. To more comprehensively describe this kind of diffusion process (which is called generalized diffusion), further analysis is needed.

3.3.4 Construction of the Generalized Diffusion Equation

To construct the generalized diffusion equation, we need to take into account many aspects, including whether the generalized diffusion coefficient $Đ$ should vary and how to describe it to include the effects of general relativity (gravitation) and special relativity.

The classical view is that regardless of how large the target norms of vectors are, they follow a diffusion equation with the same diffusion coefficient (the Schrödinger equation). However, this article adopts an alternative viewpoint: $Đ$ should vary with the value of the target vector. As derived above, when the influence of the vector sum density (including the aggregation densities of position and direction; the same is also considered below) on D is not considered, the diffusion equation for the vectors conforms to the form of the Schrödinger equation. However, when the vector sum density is large, the effect on D cannot be ignored. Suppose that, as illustrated in Fig. 1a, the vector sum density in the microdomain $\mathcal{V}_A$ is greater than that in $\mathcal{V}_B$. If both microdomains exist in the same background field, there is a cost for the higher density in $\mathcal{V}_A$. If this high density is maintained at the next moment (in terms of probability, more uncertainty is introduced into the unit volume), which will inevitably affect the (average) movement speed of the particles, the overall movement speed of the particles in $\mathcal{V}_A$ will decrease (Section **3.3.2**). As mentioned above (or in Eq. 31 below), the particle speed is what determines D; therefore, the law governing the diffusion rate towards the right (D_A) is not the same as the law governing the diffusion rate in $\mathcal{V}_B$ towards the left (D_B) (under the assumption that $Đ$ is a combination of D_A and D_B). Therefore, it is necessary for the generalized diffusion coefficient to vary in time with

the vector sum density to reflect this inequality.

In view of the above considerations, choosing the appropriate quantitative function to describe this phenomenon is the main problem to be solved in this article. First, the momentum vector in the microdomain is decomposed.

3.3.4.1 Vector Decomposition

Let us determine the distribution function for particles with equal probability in a certain domain, as follows: Suppose that the whole domain contains n particles in total. For convenience of description, the whole domain is also partitioned into n boxes of equal size. The gaps between boxes and the wall thickness are both 0. Now, let us determine the probability of k ($k \in \mathbb{N}$; the same also holds below) particles in a local area containing $\mathcal{M}$ boxes (suppose that the particles are small enough to fall into the box, not the wall). In view of the statement described above, the probability of particles existing in each domain is the same. Accordingly, the total number of possible cases describing how n particles can be randomly distributed among n boxes is n^n, there are $\binom{n}{k}$ total ways that k particles can be randomly chosen from among n particles, there are $\mathcal{M}^k$ total ways in which the k chosen particles can be randomly distributed among $\mathcal{M}$ boxes, and there are $(n-\mathcal{M})^{n-k}$ total ways in which the remaining $n - k$ particles can be randomly distributed among the remaining $n - \mathcal{M}$ boxes. Therefore, the probability $P(\mathcal{M}, k)$ of k particles existing in $\mathcal{M}$ boxes can be expressed as

$$P(\mathcal{M},k)=\frac{\binom{n}{k}\mathcal{M}^k(n-\mathcal{M})^{n-k}}{n^n}. \tag{19}$$

Suppose that the number n of particles in the whole domain is infinite; then, by taking the limit of Eq. 19 as $n \to +\infty$, we find that

$$P(\mathcal{M},k)=\frac{e^{-\mathcal{M}}\mathcal{M}^k}{k!}, \tag{20}$$

where $\mathcal{M}$ denotes the number of boxes comprising the local domain of interest (the size of the volume in 3-dimensional space), k denotes the number of particles in that domain of $\mathcal{M}$ boxes, and P denotes the probability that k particles exist in that domain. Eq. 20 is the (position-based) Poisson distribution.

It is considered that this is the most appropriate method of partitioning a whole domain (the domain can be the whole universe or simply a broad range including the

objects of investigation) into the uniform boxes with the same number as that of particles. In addition to reducing the parameters involved and facilitating discussion, the reasons are as follows: if the boxes are slightly larger, they will not ensure the accuracy of the following vector decomposition; if they are slightly smaller, they will not adequately reflect the grouping effect of the particles. Therefore, in this article, the whole domain is divided into a number of uniform boxes equal to the number of particles it contains, and this partitioning serves as the basis for all of the following discussions. In this article, the whole domain (environment) is called the T-domain, and the local domain (target) is called the S-domain; the set of all particles contained in the T-domain is called the T-particle swarm, and the subset of particles contained in the S-domain is called the S-particle swarm.

Next, we will investigate the equiprobability distribution of the static particle swarm in the abovementioned S-domain $\mathcal{V}$. In Eq. 20, $\mathcal{M}$ denotes the number of boxes (volume) spanned by some S-domain (which belonged to the domain in which the target particles are distributed). Put another way, when the T-domain is partitioned into uniform boxes following the above method, $\mathcal{M}$ can also denote the average relative density of the particles in the S-domain $\mathcal{V}$, where the reference density is the average density of the T-particle swarm in the T-domain. $\mathcal{M}$ represents the corresponding multiple of the average density, k denotes the number of particles in one box, and P is the probability of k particles existing in that box. Thus, the distribution of the S-particle swarm in $\mathcal{V}$ is a Poisson distribution with density intensity $\mathcal{M}$. Next, we will analyze the Poisson distribution formula given in Eq. 20. In fact, it is the proportion of each term determined by k (when $e^{\mathcal{M}}$ is expanded as a power series) to the value of $e^{\mathcal{M}}$. The meaning here is that it is also the proportion of the number of boxes containing k particles each to the total number of boxes in $\mathcal{V}$ when the S-particle swarm of relative density $\mathcal{M}$ is distributed among the reference boxes determined by the above criteria and spanned by the S-domain $\mathcal{V}$ (supposing that the number of boxes spanned by $\mathcal{V}$ is sufficiently large). According to mathematical analysis, we can see that the power series expansion for this case is unique, and obviously, this ratio distribution is also unique. If the right-hand side of Eq. 20 is multiplied by k, the result, denoted by $R(\mathcal{M}, k)$, takes the following form:

$$R(\mathcal{M},k)=\frac{e^{-\mathcal{M}}\mathcal{M}^{k}}{(k-1)!}. \tag{21}$$

In this way, termwise addition (by k) based on this expression offers a possible form for the decomposition of $\mathcal{M}$ into infinite items. Because the power series expansion above is unique, this decomposition form of power series is also unique. According to the previous statement of physical meaning, the meaning of Eq. 21 is the relative density contributed by the particles in the boxes that contain k particles each to the total relative density $\mathcal{M}$ (the average relative density in $\mathcal{V}$) after the particles of relative density $\mathcal{M}$ are dispersed among the (infinitely many) reference boxes spanned by $\mathcal{V}$ with equal probability. Multiplying Eq. 21 by the number of boxes contained in $\mathcal{V}$ yields the total number of particles in the boxes containing k particles each. Since the distribution of particles in this form is definite (following the Poisson distribution), from this point of view, the decomposition of the relative density $\mathcal{M}$ in this form is also unique.

If $\boldsymbol{\mathcal{M}}$ is a complex number (or plane vector), Eq. 21 can be written in vector form as follows:

$$R(\boldsymbol{\mathcal{M}},k)=\frac{e^{-\mathcal{M}}\boldsymbol{\mathcal{M}}^{k}}{(k-1)!}. \tag{22}$$

The form obtained by dividing Eq. 22 by k is still the ratio of each term (complex) determined by k (when $e^{\mathcal{M}}$ is expanded as a power series) to the complex of $e^{\mathcal{M}}$. There is one more dimension here, and the power series expansion is still unique. Similarly, the termwise addition of Eq. 22 also provides a decomposition form for the vector $\boldsymbol{\mathcal{M}}$. This power series decomposition form is also unique.

Now, we study the distribution of the velocity of the moving S-particle swarm in the abovementioned S-domain $\mathcal{V}$. If the particles of the T-particle swarm are moving randomly in the T-domain, the distribution of the S-particle swarm in a time slice in a sufficiently small S-domain (when the particle speed is fast enough) can also be approximately regarded as the equiprobable distribution. At the human scale, the number of S-particles in almost every "microdomain" of the universe can be regarded as approaching infinity; therefore, the distribution of the moving S-particle swarm in a certain microdomain $\mathcal{V}$ can be described by Eq. 20. The moving particles in each type of box partitioned by k in one S-domain $\mathcal{V}$ can form a component vector, and these components can be added together to form the total vector in $\mathcal{V}$. Once the total 3-dimensional vector $\boldsymbol{\mathcal{Y}}$ of the moving S-particle swarm in $\mathcal{V}$, which includes the specific number of particles, is determined, the norm of each component vector should be (approximately) directly proportional to the number of particles forming it when the

number of particles is large (see Part 3 of the Supplementary Information for details). It should be noted that even for $k = 1$, the number of samples in $\mathcal{V}$ should be very large. Therefore, the ratios between the norms (mathematical expectations) of the component vectors in various boxes partitioned by k are uniquely determined by the form of the power series determined by Eq. 20. As the limiting value $\boldsymbol{\mathcal{X}}$ of the quotient of $\boldsymbol{\mathcal{Y}}$ and $\mathcal{V}$, it can still be considered as a sum of 3-dimensional vectors in the S-domain $\mathcal{V}$. Therefore, there is also a form of component vectors with the ratios of norms determined by Eq. 20 spanning various boxes partitioned by k. When the 3-dimensional component vectors (spanning various boxes partitioned by k) of the 3-dimensional vector $\boldsymbol{\mathcal{X}}$ are mapped to the 2-dimensional component vectors (spanning various boxes partitioned by k) of the plane vector $\boldsymbol{\mathcal{M}}$, it is obvious that there is also a corresponding 2-dimensional form of component vectors with the ratios of norms determined by Eq. 20 but the direction is not determined. From the abovementioned decomposition method of scalar $\mathcal{M}$ (Eq. 21), it can be seen that if the ratios of norms of the component vectors of $\boldsymbol{\mathcal{M}}$ follow the Poisson distribution, it is necessary to use a unique and specified form of power series, that is, the method for calculating the norms of the component vectors determined by Eq. 22. At this time, the direction of each component vector is uniquely determined. Therefore, the plane mapping of the sum of all the vectors in the boxes containing the same number k of particles is the component vector determined by k in Eq. 22. When k takes all values in $\mathbb{N}$, the termwise sum of these terms is the unique decomposition of $\boldsymbol{\mathcal{M}}$, namely,

$$\boldsymbol{\mathcal{M}} = \sum_{k=1}^{\infty} \frac{e^{-\mathcal{M}} \boldsymbol{\mathcal{M}}^k}{(k-1)!}. \tag{23}$$

Regardless of whether the moving particles are dominated by position or direction aggregation, as long as their vectors are equal, their influences on diffusion and relativistic effects are the same; therefore, the position or direction aggregation are equivalent (When it is equivalent to position aggregation, the velocity direction is uniform distribution; when it is equivalent to velocity direction aggregation, the position is uniform distribution. The equivalent velocity direction or position aggregation represented by equal momentum in this article are both this meaning). The average velocity of the particles in each S-domain $\mathcal{V}$ is regarded as 1, so the number of particles is numerically equal to the magnitude of the momentum. Accordingly, the equivalent numbers of vectors distributed in various boxes are directly proportional to

the norms of vectors, and it is also comparable between S-domains. As mentioned above, $\mathcal{M}$ represents the relative density of particles in the S-domain $\mathcal{V}$, which is a concept of multiples. It is obvious that $\boldsymbol{\mathcal{M}}$ should also be a relative vector. The essence of the determination of the number of reference boxes for scalar $\mathcal{M}$ is the maximum number of boxes that can be occupied by particles in the T-domain. Here, when the particles in the S-domain $\mathcal{V}$ (which contains n particles in total, and the velocity of each particle is c) are thought of as a system with an average velocity of 1, the maximum number of boxes occupied (after expansion) is nc, namely, the number of reference boxes of vector $\boldsymbol{\mathcal{M}}$, and the direction of vector $\boldsymbol{\mathcal{M}}$ is the same as that of the absolute sum of vectors located at that place. Therefore, $\boldsymbol{\mathcal{M}}$ in Section **3.3.3** should be exactly the relative vector sum density. As mentioned above, the sum and difference operations between two spatial vectors are performed in their shared plane. In this plane, they can be decomposed respectively into a sum of plane vectors, as described in Eq. 23. Therefore, the two sets of plane component vectors can also serve as their respective spatial component vectors to correspondingly perform sum, difference or derivative operations.

3.3.4.2 Description of Diffusion

Suppose that the standard deviation of the projection (treated as a random variable; the same is done below) of the velocity of any one of the k equivalent particles forming a kth-order particle onto each equivalent coordinate axis is σ. As mentioned earlier, the speed of kth-order particles follows the Maxwell distribution with scale parameter $\frac{\sigma}{\sqrt{k}}$ (in this case, it is unnecessary to consider the situation in which direction aggregation is dominant; the diffusion coefficient is the inherent statistical effect in the system, and only the average speed needs to be calculated in accordance with its definition). Then, the average speed of kth-order particles is

$$\overline{v} = 2\sqrt{\frac{2}{\pi}} \cdot \frac{\sigma}{\sqrt{k}}. \tag{24}$$

For k_1th- and k_2th-order particles, the ratio of their average speeds is

$$\frac{\overline{v}_1}{\overline{v}_2} = \frac{\sqrt{k_2}}{\sqrt{k_1}}. \tag{25}$$

Because the sizes, or masses, of all 1st-order particles are the same, if the masses of a

k_1th-order particle and a k_2th-order particle are m_1 and m_2, respectively ($m \propto k$), then according to the relationship shown in Eq. 25, the ratio of their average speeds can be written as

$$\frac{\overline{v}_1}{\overline{v}_2} = \frac{\sqrt{m_2}}{\sqrt{m_1}}. \tag{26}$$

See Part 1 of the Supplementary Information for the detailed calculation and derivation process. According to Eq. 26, when the mass of a kth-order particle is m, compared with that of a 1st-order particle, its average speed is

$$\overline{v} = \frac{\kappa_1}{\sqrt{m}}, \tag{27}$$

where κ_1 is a constant coefficient.

The diffusion coefficient is defined as follows: it is the mass or mole number of a substance that diffuses vertically through a unit of area along the diffusion direction per unit time and per unit concentration gradient. Therefore, it is believed that such real diffusion, in the traditional view, is consistent with the essence of vector diffusion described here. According to the Einstein-Brown displacement equation, the diffusion coefficient is

$$D = \frac{\overline{x}^2}{2t}, \tag{28}$$

where $\overline{x}$ is the average displacement of kth-order particles along the direction of the x-axis. To replace the average displacement $\overline{x}$ in Eq. 28 with the average velocity (namely, $\overline{V}$) of kth-order particles, this diffusion coefficient can be transformed into

$$D = \frac{\overline{V}^2}{2} t^1. \tag{29}$$

The unit of the diffusion coefficient D is $m^2 \cdot s^{-1}$. By combining Eq. 28 and Eq. 29 (where t^1 and the t implied in $\overline{V}^2$ are consistent, so t^1 = 1 s), the abovementioned diffusion coefficient can also be regarded as follows: it is the average area over which kth-order particles spread out on a plane per unit time. This average area is related to the speed of a single kth-order particle. If the (average) speed of a single kth-order particle is $\overline{v}$, then the statistical average speed of these particles in one direction is

$$\overline{V} = \frac{\overline{v}}{2}. \tag{30}$$

The *k*th-order particle swarm spreads in the plane at this rate. By substituting Eq. 30 into Eq. 29 and combining t^1 = 1 s into the coefficient, which we then denote by κ_2, we can obtain

$$D = \kappa_2 \overline{v}^2, \tag{31}$$

where κ_2 is a constant coefficient with units of seconds (s).

By substituting Eq. 27 into Eq. 31, the diffusion coefficient of a (*k*th-order) particle swarm of (average) mass *m* is obtained:

$$D = \kappa_2 \left(\frac{\kappa_1}{\sqrt{m}} \right)^2 = \frac{\kappa_1^2 \kappa_2}{m}. \tag{32}$$

The above equation (Eq. 32) can also be thought of as the apparent diffusion coefficient of particle(s) with mass *m* described by 1st-order particle swarm (which forms a particle of mass *m* after collapse) without relativistic effects. Moreover, the specific form of this coefficient is given in the Schrödinger equation without relativistic effects (i.e., in the case of the apparent diffusion described by a 1st-order particle swarm). By comparing the diffusion coefficient in Schrödinger equation with Eq. 32, the following relationship can be immediately obtained:

$$\kappa_1^2 \kappa_2 = \frac{\hbar}{2}, \tag{33}$$

where $\hbar$ is the reduced Planck's constant.

3.3.4.3 Construction of the Generalized Diffusion Equation

Previously, we have adopted the assumption that there is no interaction between infinitesimal particles. Even if there are interactions between particles of larger mass levels (this article claims that these "interactions" are produced by statistical effects), there is also a continuous process of particle disappearance and generation, meaning that in fact, there is no interaction. In addition, considering that the essence of these "interactions" is gravitation (that is, the statistical effects of moving particles; other forces can be treated similarly), it is equivalent to the concept that there is no interaction between particles of various mass levels. In a time slice of a microdomain, the decomposition of velocity given by Eq. 23 must be exhibited, and all boxes containing the same number of particles in different microdomains containing different densities of vectors are equivalent. This is because there should be no differences between boxes

of the same type (i.e., containing the same number of particles) when the Poisson distribution determines the numbers of boxes of different types in different microdomains of different vector densities. Although the moving particles are distributed throughout the microdomains with the same probability, when k particles are counted, their average speed will inevitably slow down. The particles in various boxes partitioned by k move at their average speed (the centroides of boxes containing k particles each are, on average, located at the center of each box). Among all boxes of the same type (i.e., containing k particles), the average speed of each kth-order particle is the same and must conform to the diffusion form of the Schrödinger equation determined by the diffusion coefficient for particles of this type. Therefore, according to the particle numbers k in the previously partitioned boxes, from 1 to ∞, we study the corresponding term $R(\mathcal{M}, k)$, which is the component vector of $\mathcal{M}$. First, we investigate the diffusion of individual term, and then, we add them together.

Here, all the particles in each box containing k particles are regarded as forming a kth-order particle of a larger mass level, and together, all kth-order particles in all boxes containing k particles in microdomain $\mathcal{V}$ are called the kth-order particle swarm in that microdomain. Based on the above discussion, it can be considered that the average speed of each (kth-order) particle in the kth-order particle swarm is the same when there is no external disturbance, and all of them have the same diffusion coefficient. According to the relationship given in Eq. 32 (the diffusion coefficient is inversely proportional to the mass of a kth-order particle, or the number of 1st-order particles forming a kth-order particle), if the diffusion coefficient of a 1st-order particle swarm is D_1, then the diffusion coefficient of a kth-order particle swarm is

$$D_k = D_1 \cdot \frac{1}{k}, \tag{34}$$

where $\frac{1}{k}$ is called the diffusion coefficient factor.

When it is not necessary to consider the influence of the deceleration effect of the statistical speed due to particle aggregation on diffusion, the diffusion behavior of interest is that of a 1st-order particle swarm, which is consistent with the description of diffusion given by the Schrödinger equation. Therefore, the diffusion coefficient is

$$D_1 = -\frac{\hbar}{2m}. \tag{35}$$

The diffusion equation determined by this coefficient describes the dynamics of the probabilistic diffusion of a target object (or the aggregation after collapse) of mass *m* on the basis of the apparent diffusion rate (after deceleration) determined by the 1st-order particles forming it (before collapse); however, the distribution characteristics of the target object in its dispersion space is determined by the diffusion behavior of the 1st-order particles in the background field. When $k>1$, according to the above discussion, the diffusion coefficient of a *k*th-order particle swarm can be obtained by substituting Eq. 35 into Eq. 34, namely,

$$D_k = -\frac{\hbar}{2m}\cdot\frac{1}{k}. \tag{36}$$

This is equivalent to the proportional decline in the apparent diffusion rate of a target object (or the aggregation after collapse) of mass *m* due to the slowdown in the speed of the *k*th-order particles forming the target object. The meaning of the diffusion equation determined by this diffusion coefficient is similar to the case for 1st-order particles as considered above, that is, the dynamics of the probabilistic diffusion of a target object (or the aggregation after collapse) of mass *m* are described on the basis of the apparent diffusion rate (after deceleration) determined by the *k*th-order particles forming it (before collapse); however, the distribution characteristics of the target object in its dispersion space is determined by the diffusion behavior of the *k*th-order particles in the background field.

By taking the second partial derivative of $R(\mathcal{M}, k)$ (this is the plane vector sum in the boxes containing *k* moving particles, namely, the *k*th-order particle swarm, which is one of the component vectors in the whole microdomain $\mathcal{V}$) with respect to position (x, y, z) and considering the intermediate variable $\mathcal{M}$, we obtain the following expression:

$$\frac{\partial^2 R(\mathcal{M},k)}{\partial \mathcal{M}^2}\cdot T^2(\mathcal{M}) + \frac{\partial R(\mathcal{M},k)}{\partial \mathcal{M}}\cdot \Delta\mathcal{M}, \tag{37}$$

where $T^2(\mathcal{M}) = \left(\frac{\partial \mathcal{M}}{\partial x}\right)^2 + \left(\frac{\partial \mathcal{M}}{\partial y}\right)^2 + \left(\frac{\partial \mathcal{M}}{\partial z}\right)^2$. It should be emphasized that the absolute sizes of the two (infinitesimal) microdomains $\mathcal{V}_1$ and $\mathcal{V}_2$, which are selected to compare their differences, are equal when calculating the derivative of the vector $\mathcal{M}$. After multiplying Eq. 37 by the diffusion coefficient for the particle swarm of each order (Eq. 36) and then adding the products for all orders together, the complete

generalized diffusion expression (including coefficients) can be obtained as follows:

$$-\frac{\hbar}{2m}\sum_{k=1}^{\infty}\left[\frac{1}{k}\cdot\frac{\partial^2 R(\boldsymbol{\mathcal{M}},k)}{\partial\boldsymbol{\mathcal{M}}^2}\cdot T^2(\boldsymbol{\mathcal{M}})+\frac{1}{k}\cdot\frac{\partial R(\boldsymbol{\mathcal{M}},k)}{\partial\boldsymbol{\mathcal{M}}}\cdot\Delta\boldsymbol{\mathcal{M}}\right]. \tag{38}$$

The diffusion calculated in this way is the generalized diffusion from the whole (infinitesimal) microdomain $\mathcal{V}_1$ to $\mathcal{V}_2$. Eq. 38 can be simplified as follows:

$$-\frac{\hbar e^{-\boldsymbol{\mathcal{M}}}}{2m}\left[\Delta\boldsymbol{\mathcal{M}}-T^2(\boldsymbol{\mathcal{M}})\right]. \tag{39}$$

By combining the left-hand side of Eq. 18 with Eq. 39, a complete expression for the generalized diffusion equation for vectors is obtained:

$$\boxed{\boldsymbol{i}\frac{\partial\boldsymbol{\mathcal{M}}}{\partial t}=-\frac{\hbar e^{-\boldsymbol{\mathcal{M}}}}{2m}\left[\Delta\boldsymbol{\mathcal{M}}-T^2(\boldsymbol{\mathcal{M}})\right]}. \tag{40}$$

Therefore, the expression for the generalized diffusion coefficient with relativistic effects (including gravitation) is

$$\boxed{Đ=-\frac{\hbar e^{-\boldsymbol{\mathcal{M}}}}{2m}}. \tag{41}$$

The diffusion coefficient here is not a constant but rather a natural exponential function that varies with the relative vector density of moving particles. Hence, the generalized diffusion equation and the generalized diffusion coefficient $Đ$ for vectors have been determined. The norms of the spatial vectors in an undisturbed microdomain can be determined in accordance with the Maxwell distribution, while the norms and directions of the spatial vectors in the complex plane can be determined in accordance with Eq. 40. Thus, the basic effective information for a spatial (moving) particle swarm has been derived.

Returning to the vector decomposition presented in Section **3.3.4.1**, we will now prove that Eq. 23 is the unique form of the plane decomposition when the 3-dimensional vector $\boldsymbol{\mathcal{X}}$ is mapped to the plane vector $\boldsymbol{\mathcal{M}}$. It can be seen from the above that the ratios between the norms of the plane component vectors obtained through such mapping follow a Poisson distribution, whereas the directions are unknown. Suppose that there are many sets of directions conforming to this distribution of norms of the plane component vectors. Since the result of generalized diffusion is definite, all these sets of directions should be equivalent. When they are operated on in the manner shown in Eq. 38, it can be seen that the identical Eq. 39 cannot be obtained after substituting the component vectors with different sets of directions. Therefore, Eq. 23 given in this

article is the unique decomposition result that satisfies the necessary conditions.

For Eq. 39, the overall diffusion potential is reflected in the term $\Delta\mathcal{M}$ without considering its own "gravitation" (particle agglomeration), and the remaining terms arise from relativistic effects. This is because the special relativistic effect mentioned in Section **3.3.2** arises only when the scenario in $\mathcal{R}_u$ is evaluated from $\mathcal{R}_0$. If the particles in $\mathcal{R}_u$ are observed together with those in $\mathcal{R}_0$, the velocity sum of some particles in $\mathcal{R}_u$ will be slightly different from the situation described in the case of the previously discussed special relativistic effect. In this case, all moving particles in $\mathcal{R}_u$ will have an additional velocity component u along the z-axis. However, the diffusion of these particles will still follow the rule that applies in $\mathcal{R}_0$. Obviously, when such a moving particle swarm (sum of the vector swarm) is decomposed into plane component vectors, the same rule must be followed. The vector decomposition in Eq. 23 is unique. The total vector in all boxes containing k vectors is the sum of the vectors in $\mathcal{R}_0$, which is converted from the vectors in $\mathcal{R}_u$. The statistical effects of these moving particles can be incorporated into Eq. 38 by multiplying the second derivatives of the component vectors (after comparative treatment) by different diffusion coefficients according to the classification standard based on k and summing the results. It can be clearly seen from the above proof process for special relativity that the principle of the special relativistic effect of moving particles in space is a statistical effect of randomly moving particles. More precisely, it is a statistical effect that arises from direction aggregation being dominant. It should be noted that when direction aggregation is dominant, this special relativistic effect manifests, while in general, the possible aggregation effects also include the situation in which position aggregation is dominant. Here, these two (aggregation) effects are collectively called the general relativistic effect. From this perspective, these two aggregation effects are unified, and both conform to the law given by Eq. 10. Therefore, the proof process for the special relativistic effect is also the proof process for the general relativistic effect. Both of these effects are, in essence, a statistical effect of moving particles. Obviously, the treatment presented in this article (Eq. 40) can also cover all possible aggregation effects, that is, all relativistic effects are included. By contrast, equations that are subject to the constraints of Lorentz covariance (such as the Dirac equation and quantum field theory) are not sufficient to reflect all relativistic effects.

3.3.5 Further Study of Eq. 40

3.3.5.1 The Relationship with the Schrödinger Equation

By expanding the right-hand side of Eq. 40 using the power-series representation of $e^{-\mathcal{M}}$, we can obtain the following form:

$$\begin{aligned} i\frac{\partial \mathcal{M}}{\partial t} &= -\frac{\hbar}{2m}\left(1-\mathcal{M}+\frac{\mathcal{M}^2}{2}+\cdots\right)\left[\Delta\mathcal{M}-T^2(\mathcal{M})\right], \\ &= -\frac{\hbar}{2m}\left[\Delta\mathcal{M}-T^2(\mathcal{M})-\mathcal{M}\cdot\Delta\mathcal{M}+\mathcal{M}\cdot T^2(\mathcal{M})+\cdots\right]. \end{aligned} \tag{42}$$

When only the first term to the right of the equals sign in the second line of Eq. 42 is considered, this equation has the form of the Schrödinger equation without an external field. Thus, it can be concluded that Eq. 40 is the result of adding several corrections to the Schrödinger equation. When the norm of the wave function $|\mathcal{M}| \to 0$, obviously, $T^2(\mathcal{M})$ is an infinitesimal of higher order than $\Delta\mathcal{M}$ (this is similar to the case of the sine and cosine wave functions when the velocity is small but the acceleration is large). Moreover, the terms after $-T^2(\mathcal{M})$ to the right of the equals sign in the second line of Eq. 42 are all related to $\mathcal{M}$, and the product of each term and $\mathcal{M}$ is also an infinitesimal of higher order than $\Delta\mathcal{M}$. Therefore, when $|\mathcal{M}|$ is sufficiently small, Eq. 40 can be approximated to take the form of the Schrödinger equation without an external field; however, when $|\mathcal{M}|$ is larger, the relativistic effect (the statistical effect of moving particles) in Eq. 40 is nonnegligible, and this equation cannot be replaced by the Schrödinger equation.

3.3.5.2 Nondispersive Particle Swarm

Creation and annihilation operators for particles are included in quantum field theory, but such descriptions are rigid. By contrast, the equation (Eq. 40) presented in this article naturally contains the processes of the appearance and disappearance of particles and can even give their half-lives (we will not study this problem in detail here). Eq. 40 is the equation describing the generalized diffusion of a particle swarm. When

$$\Delta\mathcal{M}-T^2(\mathcal{M})=0, \tag{43}$$

$\mathcal{M}$ does not vary with time *t*, and a particle swarm that meets this condition is a nondispersive particle swarm. Such a particle swarm can also be regarded as a particle of a higher mass level, which is composed of a set of particles of a lower mass level that obey statistical laws.

Under the assumption that $\mathcal{M}$ is a function only of position (*x*, *y*, *z*), a general

analytical solution containing 9 arbitrary constants (Eq. 44) can be obtained by solving Eq. 43 using the method of separating variables:

$$\begin{aligned}\mathcal{M}(x,y,z) = &-\frac{1}{2}\ln\frac{C_1^{\,2}+C_2^{\,2}-\left[C_1\cos\left(\sqrt{C_7}\,x\right)+C_2\sin\left(\sqrt{C_7}\,x\right)\right]^2}{C_7}\\ &-\frac{1}{2}\ln\frac{C_3^{\,2}+C_4^{\,2}-\left[C_3\cos\left(\sqrt{C_8}\,y\right)+C_4\sin\left(\sqrt{C_8}\,y\right)\right]^2}{C_8}\\ &-\frac{1}{2}\ln\frac{C_5^{\,2}+C_6^{\,2}-\left[C_5\cos\left(\sqrt{C_9}\,z\right)+C_6\sin\left(\sqrt{C_9}\,z\right)\right]^2}{C_9}.\end{aligned} \tag{44}$$

Based on the equivalence of the three coordinate axes, C_7, C_8 and C_9 are complex constants that are not equal to 0, such that the sum of any two of these constants is equal to the additive inverse of the third; thus, it should hold that $C_7 : C_8 : C_9 = 1 : (-1)^{\frac{2}{3}} : (-1)^{\frac{4}{3}}$. However, it is very difficult to eliminate all possible arbitrary constants under certain initial conditions, and doing so is neither the focus nor the interest of this article. Therefore, without affecting the further discussion of the problem, the concrete form of the actual analytical solution will not be explored here, and a numerical solution will be adopted instead.

To investigate the shape of a nondispersive particle swarm in detail, it is again assumed that $\mathcal{M}$ is a function only of position (x, y, z) and that the position aggregation of moving particles is dominant. In 3-dimensional space, the following initial conditions are specified for Eq. 43:

$$\begin{cases}\mathcal{M}(0,0,0) = 1+2\boldsymbol{i}, \\ \mathcal{M}(x,y,z) = 0,\ x^2+y^2+z^2 = 4^2.\end{cases} \tag{45}$$

To numerically solve the simultaneous equations given in Eq. 43 and Eq. 45 (see the description of the process of generating Fig. 3 in Part 8 of the Supplementary Information for the detailed Mathematica code for the solution process), the distribution of mass density ($|\mathcal{M}|^2$) can be obtained, as illustrated in Fig. 3.

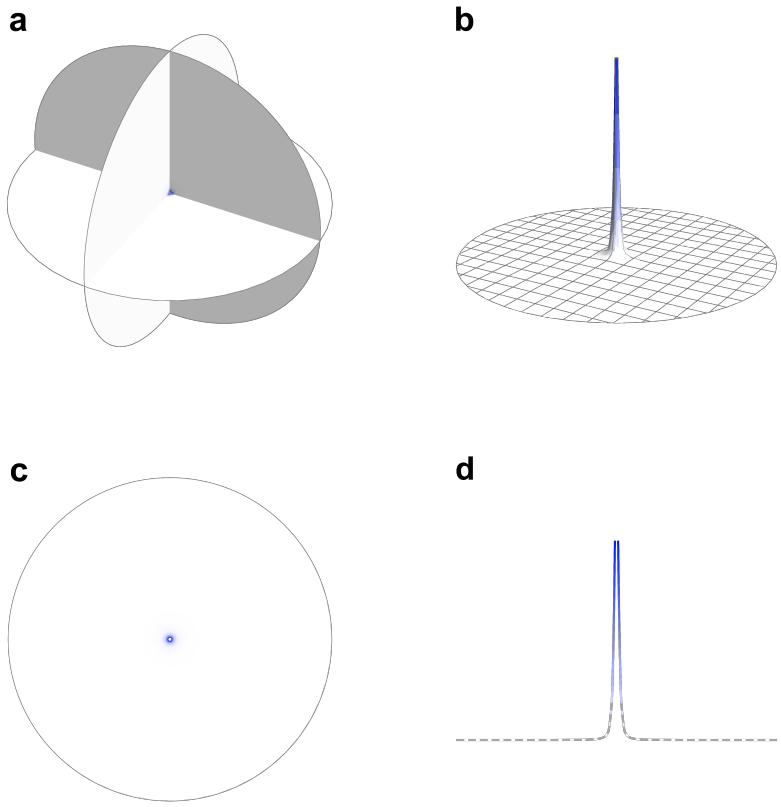

Figure 3 | Distribution of mass density for a particle swarm meeting the conditions given by Eq. 43 and Eq. 45 (shown from various perspectives): **a**, 3-dimensional density distribution; **b**, 2-dimensional density distribution at $z = 0$; **c**, 2-dimensional density distribution on the plane at $z = 0$; **d**, 1-dimensional density distribution at $y = 0$ and $z = 0$. For convenience of comparison, the three (two) coordinate axes in each figure are displayed at a scale of 1:1.

It can be seen from the figure that the mass of such a stable particle is almost entirely concentrated in a small spherical area near the center of a larger spherical region and that the rest of this region is very sparse (with a very low mass density), similar to the structure of an atom. This result further qualitatively shows that we can study not only the distribution of electrons but also the distribution of nuclear mass by solving Eq. 40.

It should be noted that for the boundary condition $\mathcal{M}(0,0,0) = 1 + 2\boldsymbol{i}$ given in Eq. 45, the value on the sphere described by $x^2 + y^2 + z^2 = 0.04^2$ is assigned to be $1 + 2\boldsymbol{i}$ in the solution process to approximate this condition. It can be inferred that when the radius of this (inner boundary) sphere approaches infinitesimal, what is shown in Fig. 3 is still similar to this shape. Moreover, the equations for the 2-dimensional case under the same conditions are also solved in this article; see Part 3 of the Supplementary

Information for details. Without affecting the discussion of the problem, only a small value ($\sqrt{5}$) as the norm of initial wave function and a relatively larger radius (0.04) of the inner boundary sphere are taken for the initial conditions. If the norm is further increased or the radius of the inner boundary sphere is further reduced, there will be a more obvious contrast in mass density, but the difficulty of solving the equation and drawing the graph will also be greatly increased. In addition, the value of the function on the sphere with a radius of 4 is 0 with the above boundary conditions, which is also approximately consistent with the actual situation. In reality, the mass density environment around the research object is complex. Even if this complex environment is not considered, the object will exist in a background field with a nonzero mass density. In this case, the outer boundary condition should be a constant value close to 0 or a wave function with a norm close to 0 at infinity (when $\mathcal{M}$ is a function of position (x, y, z) and time t).

Based on the analysis of the above equation (Eq. 40), the formation mechanism for particles of a large mass level in the universe can be estimated as follows: As particles of a lower mass level in the universe undergo randomly fluctuating movements, if they meet the appropriate external conditions, they will have the chance to form many standing waves with the same distribution. When the external conditions change, these standing waves will undergo generalized diffusion over time. Some of them will disappear; some of them will form particle swarms that also essentially meet the above conditions. These particle swarms will become larger-mass-level particles that will decay extremely slowly (the decay rate depends on the value of $e^{-\mathcal{M}}$ in Eq. 40 and the conformity of the particle shape to the condition given in Eq. 43) and thus will continue to stably exist in the universe for a long time (if the external or boundary conditions do not change significantly). At different positions and under different external conditions, standing waves of different densities may form. Once the above conditions are essentially met, these standing waves can persist for a long time, thus forming more stable particles of different mass levels. Thus, it can be concluded that the concept of macroscopic mass is a characterization of a number of agglomerated lower-mass-level particles in a certain domain, while the concept of macroscopic energy is a characterization of a number of nonagglomerated lower-mass-level particles in a certain domain. Moreover, the boundary between these two concepts is extremely blurred. It should be noted that due to limitations of computing scale, it is impossible to simulate

or watch the process of the generation of particles from uniformly distributed energy or other conditions described in this article; therefore, the above possible generation process is merely hypothesized, and its veracity remains to be investigated.

3.3.5.3 Method of Acquiring the Initial Wave Function

Obviously, the initial conditions for the solution to Eq. 40 place constraints on the norm of the wave function. The following presents the method of acquiring the initial wave function when the position aggregation of lower-mass-level particles is dominant (mostly, in this case). To eliminate D by solving the simultaneous equations given by Eq. 29, Eq. 32 and Eq. 33, we can obtain

$$\bar{V}^2 t^1 = \frac{\hbar}{m}. \tag{46}$$

Note that $t^1 = 1$ s in Eq. 46; we ignore it for now. By replacing m in Eq. 46 with the mass $\mathfrak{M}$ in a certain domain $\mathcal{V}$ and extracting the roots of both sides of the equation, we can obtain a quantitative expression for the average velocity $\bar{V}$ of the particle swarm in this domain after finding the norm of both sides of the equation:

$$\left|\bar{V}\right| = \sqrt{\frac{\hbar}{\mathfrak{M}}}. \tag{47}$$

From a statistical point of view, the norm of the vector sum in a certain domain is $\left|\mathcal{X}\right| = \left|\bar{\mathcal{X}}\right| \cdot k$ in a system with identical norms and identical probabilities of all directions in space, where $\left|\bar{\mathcal{X}}\right|$ is the average contribution of each particle to the total norm of the vector sum in the domain and k is the number of vectors. If these random vectors are regarded as representing the random movements of small particles moving with the same speed in space, then the total momentum of the particle swarm in domain $\mathcal{V}$, or the sum of the total velocity in domain $\mathcal{V}$ from a statistical point of view, is

$$\left|V\right| = \left|\bar{V}\right| \cdot k, \tag{48}$$

where k is the number of particles in domain $\mathcal{V}$. By substituting Eq. 47 into Eq. 48 and replacing k with $\frac{\mathfrak{M}}{\mu}$, we obtain

$$\left|V\right| = \sqrt{\frac{\hbar}{\mathfrak{M}}} \cdot \frac{\mathfrak{M}}{\mu} = \frac{\sqrt{\hbar \mathfrak{M}}}{\mu}, \tag{49}$$

where μ is the mass of a single particle.

From the perspective of Max Born's interpretation of the wave function, after the wave function of a system is normalized (let it be denoted by ψ_1), the mass density of

the wave function everywhere it reaches is expressed as follows:

$$\rho_m = \left|\psi_1\right|^2 \cdot m, \tag{50}$$

where m is the mass of the target object (the same as the m given in Eq. 40). In fact, even from the perspective of statistics in accordance with the logic of this article, the square of the speed or the square of the norm of the wave function is also directly proportional to the mass; see Part 1 of the Supplementary Information for details.

Since the wave function represents the velocity or velocity density per unit volume, if ψ_0 is used to denote the wave function at a certain point, then by substituting Eq. 50 into Eq. 49, the norm of the wave function at a certain point can be obtained as follows:

$$\left|\psi_0\right| = \frac{\sqrt{\hbar m}}{\mu} \cdot \left|\psi_1\right|. \tag{51}$$

In view of the discussion presented in Section **3.3.4.1**, a further operation on ψ_0 is needed to obtain the relative wave function $\mathcal{M}_0$ (ψ_0 is divided by the speed of a single particle and the number of particles per unit volume in background field, and $\mathcal{M}_0$ is assigned to the same direction as ψ_1). If the system is composed of particles at the photon level, $\mathcal{M}_0$ can be written as

$$\boxed{\mathcal{M}_0 = \hat{\lambda} \cdot \frac{\sqrt{\hbar m}}{c \cdot \overline{\rho}_{m,0}} \cdot \psi_1}, \tag{52}$$

where c is the speed of light, $\overline{\rho}_{m,0}$ is the average mass density over a range larger than $\mathcal{V}$ (the background field) and is generally accepted to be $\overline{\rho}_{m,0} = 2 \times 10^{-28}\,\mathrm{kg \cdot m^{-3}}$, and $\hat{\lambda}$ is the unit coefficient, whose value is $1\,\mathrm{m^{-3} \cdot s^{-\frac{1}{2}}}$. The purpose of this coefficient is mainly to correct the dimensional difference caused by the conversion of the diffusion coefficient into a velocity and to compensate for the specification of the unit volume implied in the conversion relationship. The method described above is the acquisition method for the initial condition for Eq. 40.

In the case of a low mass density (such as the electron distribution outside the nucleus of an atom), the norm $\left|\mathcal{M}\right|$ of the wave function is extremely small in the initial condition obtained from Eq. 52 (electrostatic interaction is not considered in the

initial condition; however, even if the electrostatic interaction with the nucleus were to be considered in the calculation process, the norm of the wave function would still be small, as detailed in Section **3.6**). As mentioned before, in this case, Eq. 40 is almost the same as the Schrödinger equation. That is, Eq. 40 will reduce to the Schrödinger equation when solving for the electron distribution outside the nucleus of an atom, while the case of the application of an external electromagnetic field to the atomic system needs to be investigated separately. It should be noted that, as mentioned above, when the target system (background field) is composed of particles at the photon level, c in Eq. 52 is equal to the speed of light, while if the target system is composed of particles at another mass level, c is equal to the speed of particles at that mass level. The background domain here can be either the whole universe or a smaller range that encompasses the research objects. Once the background domain is defined, the corresponding average mass density $\overline{\rho}_{m,0}$ of the background field can be determined. In addition, as seen from Eq. 40 and the acquisition method for the initial wave function, only when both the position aggregation and direction aggregation are at a maximum is $e^{-\mathcal{M}}$ infinitesimal and can a particle swarm ($\left|\mathcal{M}\right|^2$) that does not satisfy the condition in Eq. 43 be completely nondispersive. In other words, for a particle swarm for which only direction or position aggregation is dominant, diffusion cannot be completely prohibited when the shape of the particle swarm does not satisfy the condition described in Eq. 43.

3.3.5.4 Further Discussion

The way in which the initial wave function $\mathcal{M}_0$ is acquired from Eq. 52 reflects the way in which the wave function at a point is calculated. Therefore, to judge whether the wave function $\mathcal{M}$ at a point changes with the selections of the reference system or the minimum reference particles, it is necessary only to examine whether the method of acquiring the initial wave function $\mathcal{M}_0$ has changed. In view of the discussion in Section **3.3.2**, in any stationary (inertial) reference system, the synchronous change in movement and time from which movement is measured, from which the obtained speed of light c and the velocity determining $\mathcal{M}$ are both constant; in addition, the speed of light is included in Eq. 52, and other parameters are not limited by the reference system. Therefore, in any reference system, as long as the conditions **HYPO 1–3** are satisfied, Eq. 40, which is deduced in this article, and Eq. 52, which is the acquisition method for

the initial wave function, are applicable. Moreover, let us consider the case of particles of different mass levels being thought of as the minimum (infinitesimal) reference particles in the same reference system. There is no need to consider the mass of an infinitesimal particle in the acquisition method for the initial wave function; regardless of which mass-level particle is treated as the minimum reference particle, the synchronous change in movement and time from which movement is measured, from which the obtained speed of light c and the velocity determining $\mathcal{M}$ are both constant; in addition, the other parameters in the acquisition method for the initial wave function $\mathcal{M}_0$ are not limited by the selection of the minimum reference particle. Therefore, regardless of how large the particles are that are regarded as the minimum reference particles, Eq. 40 and Eq. 52 are still applicable. In summary, the gravitational effect between various particles can be regarded as a statistical effect of moving particles; it can be considered that there is no interaction between particles of any mass level. This is self-consistent with the hypothesis stated in **HYPO 3**. In this way, particles can be constructed step by step, and particles of a high mass level can form particles of a higher mass level under appropriate conditions. The whole universe is quantized regardless of the mass level, and each mass level is also equivalent. This is self-consistent with the statement that "the substance in the world is quantized", which is the axiomatic inference (or hypothesis) derived from **AXIO 2**.

When direction aggregation is dominant, the form of Eq. 43 allows the velocities of some particles to be extremely fast, while the velocities of other particles that are not far from them decrease rapidly. Particles with a very fast velocity can also have a higher mass density than their surroundings, and under certain conditions, the mass and velocity can mutually transform (as long as the condition of Eq. 43 is met). The above conclusion is consistent with the hypothesis of "high-speed and random motion of particles in the universe" mentioned above.

To summarize the results stated above, in any reference system that satisfies the conditions of **HYPO 1**–**3**, no matter what the mass level of the basic (infinitesimal) reference particle considered in this article actually is, and no matter how slow the "absolute" movement speed of that particle, from the perspective of human understanding, the particle mass at this level is infinitesimal, and the speed is infinite (corresponding to the expansion of the self-consistent range). At the same time, this conclusion also gives legitimacy to the vector decomposition in the (infinitesimal)

microdomain $\mathcal{V}$ introduced in Section **3.3.4.1** and the viewpoint that "the absolute coordinate system needs to move along with the whole particle swarm". In this way, Eq. 40, which is derived in this article, and Eq. 52, which is the acquisition method for the initial wave function, can be applied not only in a local space but also in a broader space (or in various inertial reference systems), and they can also be applied not only in a low-mass-level particle system but also in a high-mass-level particle system (i.e., either low-mass-level particles or high mass-level particles can be treated as infinitesimal particles). Based on the above conclusions, we infer that Eq. 40 and the abovementioned physical model are completely equivalent.

3.4 A Simple Verification of the Mathematical Model

It can be seen from the above discussion that Eq. 40 can completely describe all objects and phenomena in nature and that the situation described by Eq. 40 is logically self-consistent with the physical model (hypotheses) given at the beginning of this article; however, its reliability in real situations should be further tested. In this article, the description of the time-dependent diffusion of a 1-dimensional Gaussian wave packet without an external field with even parity along the *x*-axis and the initial condition e^{-2x^2} is solved for comparison with known theories to guide further discussion. For convenience of operations, we adopt natural units (i.e., $\hbar = c = 1$) and set $m = 1$ eV for all evaluations in this section, while the International System of Units is still adopted in other sections.

As mentioned above, to correctly solve Eq. 40, it is necessary to give the equation an initial condition with an appropriate norm in accordance with Eq. 52, which is different from solving the Schrödinger equation. In the following, the average electron mass density outside the nucleus of the hydrogen atom is taken as a reference to determine the norm of the wave function for the initial condition of the Gaussian wave packet e^{-2x^2} in the case of time-dependent diffusion. It is assumed that these two kinds of problems are essentially the same; both of them concern the movements of particles at the photon level. Let $m = 9.109\ 389\ 7(54) \times 10^{-31}$ kg, which is the electron mass; then, the coefficient pre the normalized wave function ψ_1 in Eq. 52 can be evaluated to be approximately 1.63×10^{-13}. The normalized norm of the above Gaussian wave-packet is $\sqrt{\frac{2}{\pi}}$. Therefore, the approximate value $\mathcal{M}_0(x,0)=10^{-13}e^{-2x^2}$ of the same order of magnitude can be taken as the initial condition without affecting the discussion

of the problem (after verification, when the coefficient of e^{-2x^2} is less than 10^{-3}, the maximum relative deviation between the contours for the wave packet obtained using these two methods is less than 1.14% in all ranges; see Part 6 of the Supplementary Information for details). For comparison, the case of a larger norm in the initial conditions (such as $\mathcal{M}_0(x,0)=e^{-2x^2}$) is also evaluated. At the same time, the Schrödinger and Dirac equations are used to solve for the description of the time-dependent diffusion of this wave packet. For the Dirac equation, the case in which the two components of the wave function are equal (i.e., $\chi_1(x,0)=\chi_2(x,0)=\frac{\sqrt{2}}{2}e^{-2x^2}$) is taken as the initial condition here (see the description of the process of generating Fig. 4 in Part 8 of the Supplementary Information for the detailed Mathematica code for the solution process).

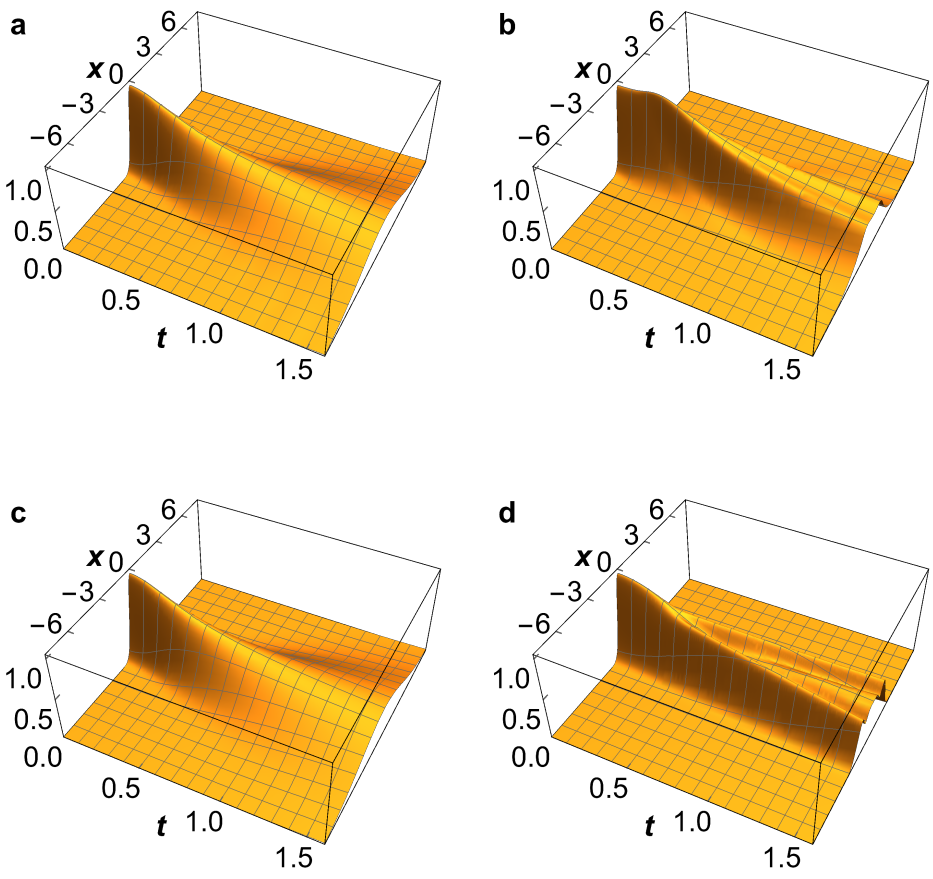

Figure 4 | Illustrations of the 1-dimensional time-dependent diffusion of the Gaussian wave packet e^{-2x^2} as obtained using various methods in natural units. **a**, Computation result of Eq. 40 when the initial condition is $\mathcal{M}_0(x,0)=10^{-13}e^{-2x^2}$. The norm has been magnified ($\times 10^{13}$) to facilitate the shape comparison. **b**, Computation result of Eq. 40 when the initial condition is $\mathcal{M}_0(x,0)=e^{-2x^2}$. **c**, Computation result

of the Schrödinger equation. **d**, Computation result of the Dirac equation.

As illustrated in Fig. 4, there is almost no difference between the visualization of the time-dependent diffusion of the wave packet obtained from Eq. 40 under an appropriate initial condition $\mathcal{M}_0(x,0)=10^{-13}e^{-2x^2}$ (Fig. 4a) and that obtained from the Schrödinger equation (Fig. 4c) (note: for convenience, the norms of wave functions, not the squares of the norms, are discussed in this section). This small difference is illustrated in greater detail in Fig. 5 by presenting the standard deviations of the norms at different diffusion times, from which it can be seen that the profiles of the Gaussian wave packets predicted by the two methods almost completely coincide at each time point. Thus, it is further verified that the equation given in this article well approximates the Schrödinger equation (at least for the problem of a Gaussian wave packet) in a domain with an extremely sparse mass density (such as the distribution of electrons outside the nucleus of an atom, excluding the influence of the electric field of the nucleus), which is consistent with the conclusion presented in Section **3.3.5.1** above. In Part 6 of the Supplementary Information, it is further verified that the visualization of the time-dependent diffusion of a Gaussian wave packet as obtained from Eq. 40 in accordance with the initial condition estimated from the product of Eq. 72 and the norm $|\psi_1|$ of the normalized wave function is still basically consistent with that obtained from the Schrödinger equation in the presence of a nuclear electric field.

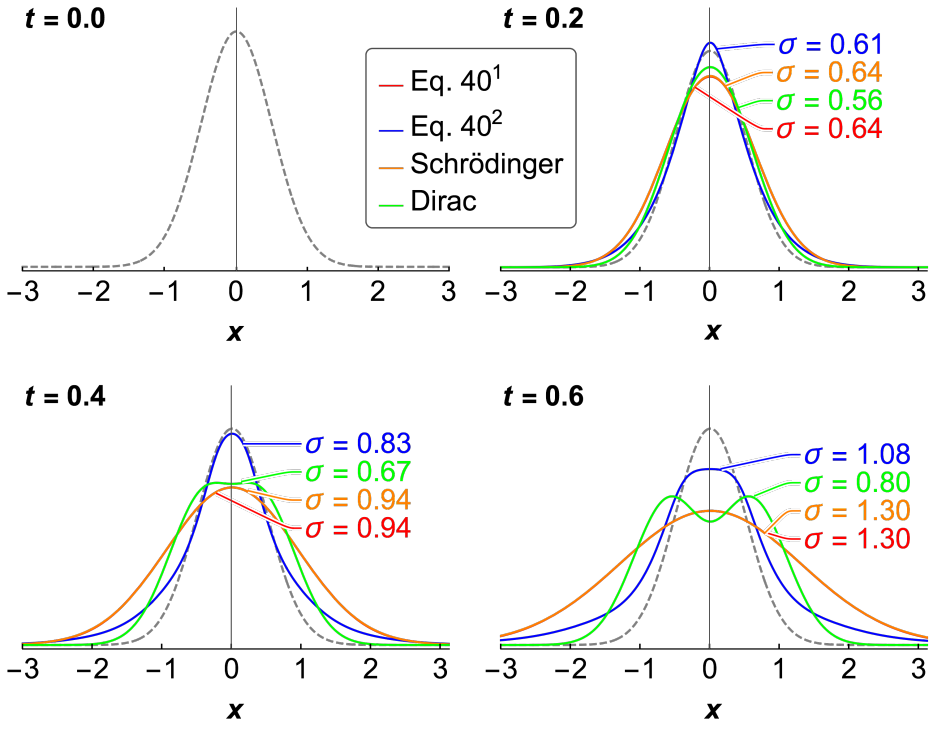

Figure 5 | Visualizations of the time-dependent diffusion trend of a Gaussian wave

packet (norm) as predicted using four methods (for Eq. 40[1], the initial condition is $\mathcal{M}_0(x,0)=10^{-13}e^{-2x^2}$; for Eq. 40[2], the initial condition is $\mathcal{M}_0(x,0)=e^{-2x^2}$) in natural units at various moments in time (t = 0.0, 0.2, 0.4, and 0.6 eV^{-1}).

If the norm of the wave function in the initial condition is large (such as $\mathcal{M}_0(x,0)=e^{-2x^2}$), the profile of the wave packet will show an obvious bulge or particle (position or direction) aggregation near t = 0.3 eV^{-1} (Fig. 4b). Because of self-aggregation, the profile obtained from Eq. 40 is steeper along the direction of the x-axis, which can be clearly seen from the standard deviation of the norm of the Gaussian wave packet in Fig. 5 at the three nonzero times. Under such initial conditions, the diffusion rate predicted by Eq. 40 is not as fast as that predicted by the Schrödinger equation, and the main peak in the profile does not tend to quickly dissipate; this is closer to the situation described by the Dirac equation (Fig. 4d). It can be speculated that this behavior is mainly caused by the gravitation of the wave packet itself. After t = 1 eV^{-1}, the main peak begins to split into two peaks (for more obvious splitting, see the case in which the coefficient of e^{-2x^2} is 1.4 in Part 7 of the Supplementary Information); in the case described by the Dirac equation, strong splitting occurs after t = 0.5 eV^{-1} (the main peak splits into two secondary peaks, and then each secondary peak splits into two smaller peaks). This phenomenon is considered to be caused by the fact that the gravitation of the wave packet itself is not considered in the Dirac equation and the corresponding correction to the real result is excessive. This is also confirmed by the standard deviation profiles illustrated in Fig. 5.

To study the influence of the norm in the initial condition on the diffusion of the wave packet in greater detail, we also compare the shapes of the key parts of the profiles (the time-dependent trend of the norm for the wave packet at x = 0 and the wave packet at the maximum value of the norm) after assigning various initial conditions ($10^{-13}e^{-2x^2}$, e^{-2x^2}, $1.2e^{-2x^2}$ and $1.4e^{-2x^2}$) for Eq. 40 (see the description of the process of generating Fig. 6 in Part 7 of the Supplementary Information for the detailed Mathematica code for the solution process); the results are illustrated in Fig. 6. It can be seen from this figure that when different initial conditions are specified, with norms ranging from small to large, the wave-packet diffusion profiles predicted by Eq. 40 (at x = 0) are initially consistent with those predicted by the Schrödinger equation and then gradually tend to continue to agglomerate near 0.3 eV^{-1} (the profile gradually begins to bulge); the corresponding trend is shown in Fig. 6a. In addition, Fig. 6b shows the shape

of the wave packet at the highest point (see Part 7 of the Supplementary Information for the full spectrum waveforms for the initial conditions of $\mathcal{M}_0(x,0)=1.2e^{-2x^2}$ and $\mathcal{M}_0(x,0)=1.4e^{-2x^2}$ and the corresponding comparisons with the Dirac equation). As the initial norm gradually increases, the wave packet initially will gradually shrink, and when the norm reaches the maximum, the waveform will gradually become steeper and steeper and (presumably) will gradually approach that of the function satisfying Eq. 43. It can also be seen from this trend that as the mass density of the wave packet increases, the attenuation speed of the wave packet becomes slower.

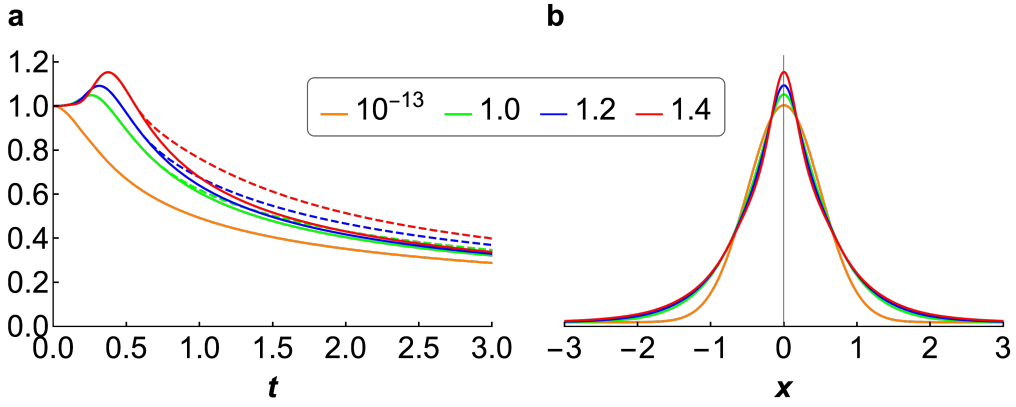

Figure 6 | Comparison of the shapes of the Gaussian wave packets obtained when assuming different initial conditions $\mathcal{M}_0 = (10, 1.0, 1.2, 1.4)\,e^{-2x^2}$ in natural units. **a**, Time-dependent trends of the norm for the wave packet at $x = 0$ (solid line) and for the wave packet at the maximum value of the norm (dashed line of the same color). **b**, Profiles at the maximum values of the norms. The numbers in the legend are the coefficients of e^{-2x^2} corresponding to the different initial conditions. The initial norm at $t = 0$ eV^{-1} in each case is normalized to facilitate the shape comparison.

3.5 Adding External Fields to the Equation

Theoretically, the particle motion law for the whole system, as described by Eq. 40, is basically sufficient. All forces and phenomena in nature are caused by the generalized diffusion of particles. However, when dealing with practical problems, to reduce the scale of computation, etc., a local process is often studied. Therefore, it is necessary to add external fields to Eq. 40.

In Section **3.7**, we speculate on the essence of the four fundamental forces of nature that have been discovered by human beings. Since the strong force can be regarded as describing the energy interaction between a single point and another single point, it is not necessary to use the form of external fields. Therefore, it is easy to

address this force directly with Eq. 40; hence, this kind of interaction is not considered here. Only the gravitational, electromagnetic and weak interaction fields are considered in the following. In view of the different forms (in particular, there is no repulsion in gravitation) of gravitation and other forces (such as the electromagnetic force and weak force) and the understanding of gravitation in this article, it is considered that the possible external fields should be divided into two types: gravitational fields and other potential fields. A gravitational field originates from the difference in the spatiotemporal probability of the spatial anisotropy of (randomly moving) larger-mass-level particles (or tiny particles) formed by the local background density produced by the equiprobable distribution of randomly moving tiny particles in space-time, which is a statistical effect dominated by position aggregation. Other fields originate from the acceleration (or change in direction) of particles of higher mass levels (or tiny particles) induced by the spin field, which is a statistical effect dominated by direction aggregation. For a gravitational field, the acceleration effect can generally be ignored; for other potential fields, the gravitational effect can generally be ignored. A more detailed description follows.

First, let us consider the principle of the generation of random spins for particles with a large mass level. If relativistic effects (statistical effects of moving particles) are not considered, then the agglomeration of particles in space can be regarded as following the Poisson distribution given above (Eq. 20). Here, we study the aggregation of particles in one box (or several adjacent boxes), under the assumptions that the aggregation is spherical and that there is no aggregation caused by relativistic effects. This is the case when the particle volume and the density differences of the vectors are both sufficiently small. Given particles of a certain mass level, the more microscopic the investigated system is (where the property of being microscopic is relative), the closer the situation is to this case. Given a number of particles with the same speed and random direction agglomeration in 3-dimensional space, there must be a corresponding movement component to produce a spin effect on the overall centroid at a certain moment in time. To illustrate this problem, the particles with equal speed and random directions are still regarded as random vectors with equal norms, and the analysis is divided into the following two steps: first, the distribution of the norm of the angular velocity generated by a single random vector relative to the total centroid is obtained, and then, this distribution is extended to the distribution of the norm of the angular

velocity generated by a number of random vectors relative to their centroid.

First, let us study the distribution of the norm $|\boldsymbol{\Omega}_S|$ of the random angular velocity generated by a random vector $\boldsymbol{V}_S$ with a given norm (the linear velocity of the random points on the sphere) uniformly distributed on a unit sphere S. The contribution of $\boldsymbol{V}_S$ to the random angular velocity of the center of the sphere is in all possible directions in space. How can multiple rotation contributions be added together to specify the overall rotation? The vector product $\boldsymbol{\omega}_S$ of the linear velocity $\boldsymbol{v}_S$ of a point on the sphere and the radius $\boldsymbol{r}$ of the unit sphere S on which this point located can easily explain the total rotation contribution, or the distribution of the contribution to the angular velocity by a single random vector (here, $|\boldsymbol{r}|=1$; if $|\boldsymbol{r}|\neq 1$, then $\frac{\boldsymbol{\omega}_S}{|\boldsymbol{r}|}$ is the contribution of the linear velocity $\boldsymbol{v}_S$ to the angular velocity $\boldsymbol{\omega}_S$), namely,

$$\boldsymbol{\omega}_S = \boldsymbol{r}\times\boldsymbol{v}_S. \tag{53}$$

The process of solving the above problem can be divided into two independent steps. The first step is to determine the direction of the unit vector $\boldsymbol{r}$ in space, that is, to determine the position of the end point of the vector $\boldsymbol{r}$ on the unit sphere S. This position is uniformly distributed over the whole sphere S and is represented by a random vector $\boldsymbol{R}$. The second step is to determine the direction of the linear velocity $\boldsymbol{v}_S$ of the point at this position, which is also uniformly distributed throughout the whole space and is represented by the random vector $\boldsymbol{V}_S$. Suppose that there is a sphere S' of radius $|\boldsymbol{v}_S|$ at the end of $\boldsymbol{r}$ (specifically, the end that lies on the sphere S). Then, the random vector $\boldsymbol{V}_S$ is equivalent to the vector formed by connecting the uniformly distributed points on the sphere S' to the center of S'. Considering that $|\boldsymbol{r}|=1$ and the definition of the cross product, when the direction of $\boldsymbol{r}$ is determined, $|\boldsymbol{r}\times\boldsymbol{v}_S|$ is equivalent to the norm of the vector obtained by connecting the center of the sphere S' to the projection of the uniformly distributed points on the sphere S' along a direction parallel to $\boldsymbol{r}$ onto a tangent disk D' that passes through the center of the sphere S' and is perpendicular to $\boldsymbol{r}$; this vector norm is denoted by $|\boldsymbol{\omega}'|$ (Fig. 7).

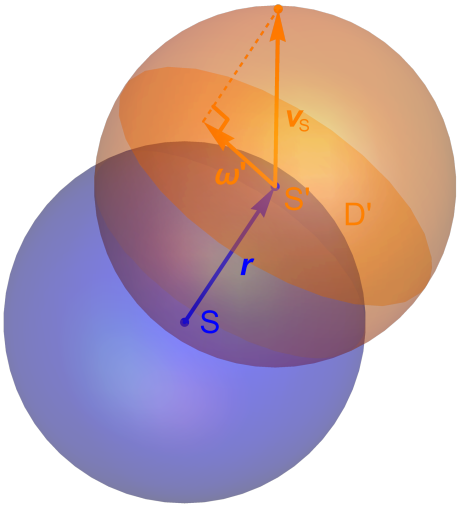

Figure 7 | Schematic diagram of the generation method for the vector $\boldsymbol{\omega}'$.

When the random vector $\boldsymbol{R}$ changes, it is equivalent to driving the tangent disk D' on the unit sphere S to move. Since the sum of two uniform distributions is also a uniform distribution, the result of $\boldsymbol{R}\times\boldsymbol{V}_{\mathrm{S}}$ can be regarded as the uniform distribution of the random vector $\boldsymbol{\Omega}'$ throughout the entire space. Thus, one can find the distribution of the norm $|\boldsymbol{\Omega}'|$ of the random vector on the disk D' and assign it a random direction in space to obtain the distribution of the norm $|\boldsymbol{\Omega}_{\mathrm{S}}|$ of the angular velocity generated by the contribution of $\boldsymbol{V}_{\mathrm{S}}$ to the center of the sphere S.

Under the assumption that the random variables $N_1\sim N(0, 1)$, $N_2\sim N(0, 1)$ and $N_3\sim N(0, 1)$ are independent of each other, one coordinate X that is equivalent to the three coordinates of $\boldsymbol{R}$, which is the unit random vector, can be written as[14,15]

$$X=\frac{N_1}{\sqrt{N_1^{\,2}+N_2^{\,2}+N_3^{\,2}}}, \tag{54}$$

the probability density of which is

$$f_X(x)=\begin{cases}\dfrac{1}{2}, & -1<x<1,\\ 0, & \text{otherwise.}\end{cases} \tag{55}$$

Let us establish a 3-dimensional Cartesian coordinate system for S'. Suppose that the disk D' is perpendicular to the z-axis and consider the random variables $\Theta\sim U(-1, 1)$ and $H\sim U(-\pi, \pi)$. Then, the coordinates of the random vector $\boldsymbol{\Omega}'$ obtained by projecting the uniformly distributed points on sphere S' onto disc D' are $X=c\cdot\sin\cos^{-1}\Theta\cdot\cos H$, $Y=c\cdot\sin\cos^{-1}\Theta\cdot\cos H$ and $Z=0$, and the norm of this random vector is

$$\left|\boldsymbol{\Omega}'\right| = \sqrt{X^2 + Y^2 + Z^2} = c \cdot \sqrt{1 - \Theta^2}. \tag{56}$$

Therefore, the probability of $\left|\boldsymbol{\Omega}'\right|$ is

$$\left|\boldsymbol{\omega}'\right|(x) = \begin{cases} \dfrac{x}{c \cdot \sqrt{c^2 - x^2}}, & 0 < x < c, \\ 0, & \text{otherwise.} \end{cases} \tag{57}$$

Note that the distribution of the random variable $\left|\boldsymbol{\Omega}_{\mathrm{S}}\right|$ is the random distribution generated by the random motion of $\boldsymbol{\Omega}'$ in space driven by $\boldsymbol{R}$. Therefore, by taking a product $F_X(x) \cdot \left|\boldsymbol{\Omega}'\right|(x)$ of random variables, we can obtain the probability density of X, which represents one of the three equivalent coordinates of the angular velocity $\boldsymbol{\Omega}_{\mathrm{S}}$ contributed by the random vector $\boldsymbol{V}_{\mathrm{S}}$, namely,

$$\boldsymbol{\omega}_{\mathrm{S},X}(x) = \begin{cases} \dfrac{1}{2c}\sin^{-1}\dfrac{x}{c} + \dfrac{\pi}{4c}, & -c < x < 0, \\ \dfrac{1}{2c}\cos^{-1}\dfrac{x}{c}, & 0 \le x < c, \\ 0, & \text{otherwise.} \end{cases} \tag{58}$$

The angular velocity $\boldsymbol{\Omega}_{\mathrm{B}}$ contribution of the random vector $\boldsymbol{V}_{\mathrm{B}}$, which is uniformly distributed throughout the whole unit ball enclosed by the sphere S, is also multiplied by the reciprocal $\dfrac{1}{r}$ of the norm r of the radius $\boldsymbol{r}$ at which the starting point of this vector $\boldsymbol{V}_{\mathrm{B}}$ is located within the ball. Therefore, the contribution of $\boldsymbol{V}_{\mathrm{B}}$ to the equivalent coordinate $\boldsymbol{\Omega}_{\mathrm{B},X}$ of $\boldsymbol{\Omega}_{\mathrm{B}}$ is calculated as follows:

$$\boldsymbol{\Omega}_{\mathrm{B},X}(x,r) = \frac{1}{r} \cdot \boldsymbol{\Omega}_{\mathrm{S},X}(x). \tag{59}$$

Hence, the new probability density is

$$\boldsymbol{\omega}_{\mathrm{B},X}(x,r) = \begin{cases} \dfrac{1}{2c} r \sin^{-1}\dfrac{rx}{c} + \dfrac{\pi r}{4c}, & -\dfrac{c}{r} < x < 0, \\ \dfrac{1}{2c} r \cos^{-1}\dfrac{rx}{c}, & 0 \le x < \dfrac{c}{r}, \\ 0, & \text{otherwise.} \end{cases} \tag{60}$$

Thus, the distribution function $\boldsymbol{\Omega}_{\mathrm{B},X}(r)$ of the contribution of $\boldsymbol{V}_{\mathrm{B}}$ to one of the equivalent coordinates of $\boldsymbol{\Omega}_{\mathrm{B}}$ is obtained. Next, $\boldsymbol{\Omega}_{\mathrm{B},X}(r)$ is integrated over the whole unit ball:

$$\int_0^1 4\pi r^2 \cdot \boldsymbol{\Omega}_{\mathrm{B},X}(r)\mathrm{d}r. \tag{61}$$

Eq. 61 describes the case in which the particles are uniformly distributed in the ball. If the particles are instead distributed in the (nondispersive) shape described by Eq. 43, the integration should be performed approximately in accordance with this density function; however, this analytical function is not available at present. Nevertheless, even if only the case of a uniform distribution is considered, the discussion of the following problems will not be affected. The case described by Eq. 43 is a spherical particle swarm with an nonuniform particle density distribution along the radial direction. It can be inferred that this is still a similar case with a rotation effect (in fact, for every layer of the sphere, a spin vector with random norm and direction can be generated; according to the central limit theorem, the norm of the total vector must follow the Maxwell distribution with a certain parameter). The probability density of the contribution of $\boldsymbol{V}_{\mathrm{B}}$ in the whole unit ball to an equivalent coordinate X of the angular velocity $\boldsymbol{\Omega}_{\mathrm{B}}$ can be obtained by finding the derivative of Eq. 61 with respect to x and normalizing it, as follows:

$$\boldsymbol{\omega}_{\mathrm{B},X}(x)=\begin{cases}\dfrac{9\pi c^3}{128x^4}, & x>c\vee x\le -c,\\[2ex] \dfrac{3\left(8x^4\sin^{-1}\dfrac{x}{c}+4\pi x^4+U_1\right)}{64cx^4}, & -c<x<0,\\[2ex] \dfrac{3\left(8x^4\cos^{-1}\dfrac{x}{c}-U_1\right)}{64cx^4}, & 0<x\le c,\\[2ex] 0, & \text{otherwise,}\end{cases} \tag{62}$$

where $U_1=x(2x^2+3c^2)\sqrt{c^2-x^2}-3c^4\sin^{-1}\dfrac{x}{c}$. This is the case of a random vector $\boldsymbol{V}_{\mathrm{B}}$ inside the unit sphere S (including S).

Next, we extend the analysis to the case in which the radius of the ball has an arbitrary value R. When the radius of the ball is R, the above situation scales to

$\frac{\boldsymbol{\Omega}_{\mathrm{B},X}(x)}{R}$. Accordingly, the probability density of the contribution of the random vector $\boldsymbol{V}$ to the single equivalent coordinate X of angular velocity $\boldsymbol{\Omega}$ is

$$\boldsymbol{\omega}_X(x)=\begin{cases}\dfrac{9\pi c^3}{128R^3x^4}, & x>\dfrac{c}{R}\vee x\le -\dfrac{c}{R},\\[2ex] \dfrac{3\left(8R^4x^4\sin^{-1}\dfrac{Rx}{c}+4\pi R^4x^4+U_2\right)}{64cR^3x^4}, & -\dfrac{c}{R}<x<0,\\[2ex] \dfrac{3\left(8R^4x^4\cos^{-1}\dfrac{Rx}{c}-U_2\right)}{64cR^3x^4}, & 0<x\le\dfrac{c}{R},\\[2ex] 0, & \text{otherwise},\end{cases} \tag{63}$$

where $U_2=Rx(2R^2x^2+3c^2)\sqrt{c^2-R^2x^2}-3c^4\sin^{-1}\dfrac{Rx}{c}$, the standard deviation of which is $\dfrac{\sqrt{6}c}{3R}$. If $R=3$ and $c=1$, the above probability density (Eq. 63) of the angular velocity can be plotted as shown in Fig. 8.

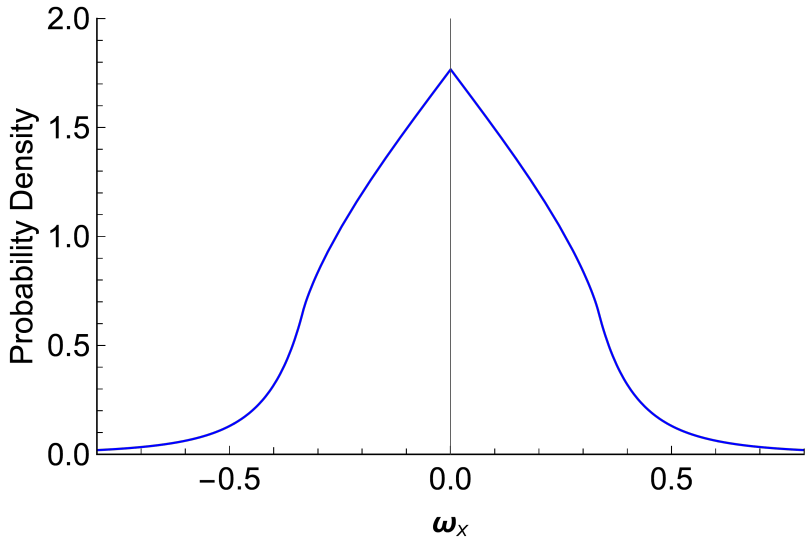

Figure 8 | The contribution of the random vector $\boldsymbol{V}$ to the distribution of the single equivalent coordinate $\boldsymbol{\Omega}_X$ of the angular velocity $\boldsymbol{\Omega}$ when $R=3$ and $c=1$.

Therefore, when k independent and identically distributed random vectors $\boldsymbol{V}$ move randomly in space, according to the central limit theorem (when they are grouped together), the norm $|\boldsymbol{\Omega}|$ of the average angular velocity generated by all of their components relative to their total centroid follows the Maxwell distribution with scale

parameter $\frac{\sqrt{6}c}{3R\sqrt{k}}$. To verify this conclusion, values of $k = 10^3$, $R = 3$ and $c = 100$ are considered here, and this theoretical distribution is compared with the results of simulating 10^6 samples with the same parameters. The results are illustrated in Fig. 9 (see the description of the process of generating Fig. 9 in Part 8 of the Supplementary Information for the details of the simulation). It can be seen from this figure that the analytical expression derived in this article is in good agreement with the simulated results.

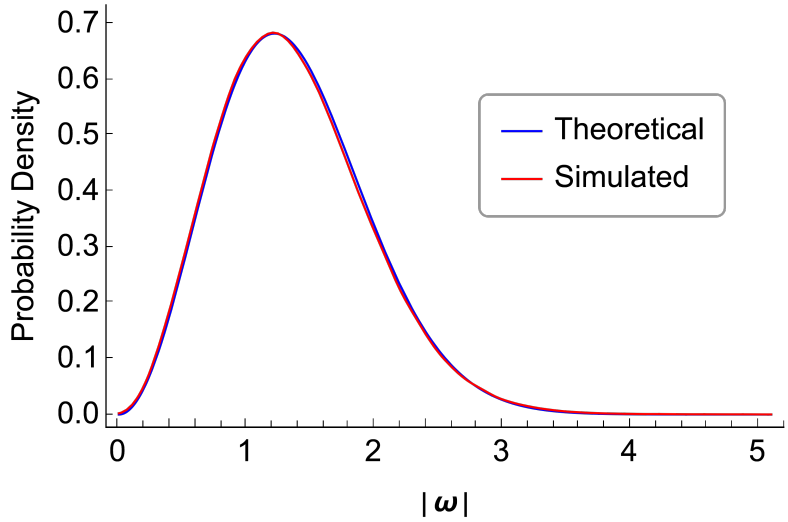

Figure 9 | The distribution of the norm $|\boldsymbol{\Omega}|$ of the total angular velocity when 10^3 random vectors with a norm of 100 are grouped together (with $R = 3$).

See Part 4 of Supplementary Information for the detailed Mathematica code of the above calculation process. So far, this article proves that there are more or less rotational components in the agglomeration (even if there is no aggregation) generated by the aggregation of randomly moving particles in space, and the angular velocity of the agglomeration follows the Maxwell distribution with a certain parameter. If the strengthening influence of the statistical effect of moving particles is added to this agglomeration and rotation, it can be seen that, like aggregation, spin is the general characteristics of the universe.

It is believed that the acceleration in a certain direction that we can perceive is essentially a time-dependent rate of change in the average velocity of the tiny particles in the target domain towards that direction (if it is only the average velocity without a time-dependent change, it has been proven in Section **3.3.2** that the target object will form an inertial system, with no difference in physical laws compared with the previous

state, and the target object will then lose the sense of acceleration). The essence of gravitational acceleration is a time-dependent rate of change in the average velocity of tiny particles at a lower vector density to a higher vector density due to the statistical effect of the moving particles (e.g., when a particle agglomeration that meets the condition of Eq. 43 is located in a gravitational field, the particles in it are replaced by the particles of higher density in the gravitational field, resulting in the deformation of the agglomeration and causing the movement trend of particles forming the agglomeration weakly towards the low-density domain and strongly towards the high-density domain). The essence of other types of acceleration is an increase in the time-dependent rate of change in the average velocity in the opposite direction in a (moving) reference system composed of tiny particles. Fundamentally, the causes of these forces or potentials are the same, but they are of different types.

For uniform circular motion, the acceleration direction is perpendicular to the velocity direction, and the principle of acceleration generation is the same as above, but the form is special. When a spherical agglomeration domain of particles produces spin (which can be approximately thought of as uniform circular motion), from the overall view (ignoring the behavior of single particles), the spherical matter domain rotates continuously and is subject to a continuous centripetal force that changes the direction of motion. If there is no spin, a particle $\mathcal{S}$ can be formed that satisfies the condition of Eq. 43. As the rotation intensifies, more centripetal force is needed to maintain the acceleration. In this case, $\mathcal{S}$ must satisfy the condition of Eq. 43 again by changing its previous shape, that is, by increasing the norm $|\mathcal{M}|$ of the wave function near the center of rotation (from another point of view, if the norm of the wave function at each point near the edge of $\mathcal{S}$ becomes larger, $|\mathcal{M}|$ must become larger near the center to meet the condition of Eq. 43). Thus, a larger $|\mathcal{M}|$ can indicate not only a higher particle concentration but also a faster particle speed. In this article, we study only the case in which a faster speed results in an increase in $|\mathcal{M}|$. There are four cases in which the particle speed is faster at the center of rotation, as shown in Fig. 10a–d.

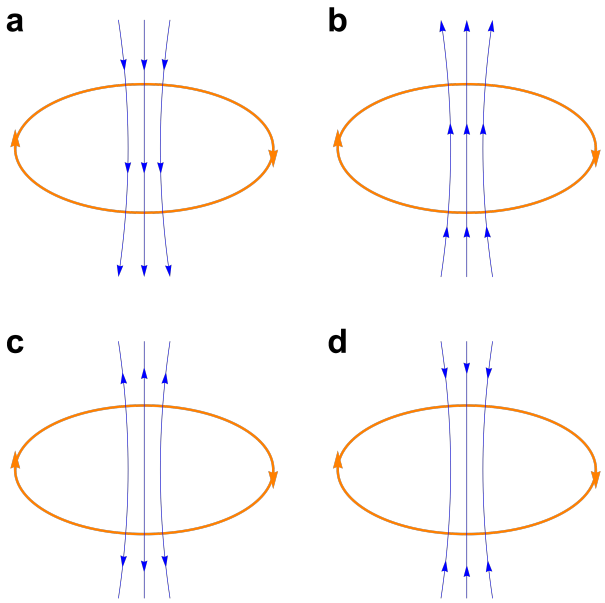

Figure 10 | Possible cases with a faster velocity of particles at the center of rotation, satisfying the condition of Eq. 43.

On the other hand, if $\mathcal{S}$ does not rotate, a certain number of tiny particles escape along the radial direction (in balance with the number of tiny particles absorbed by $\mathcal{S}$). With increasing rotation, according to the above analysis of acceleration, there may be either more tiny particles escaping along the radial direction or almost no particles escaping. Considering the gravitation and mass stability of the particle swarm (which must basically satisfy the condition given in Eq. 43), if some particles escape, the whole particle swarm needs to be replenished. This replenishment can only be provided in the axial direction perpendicular to the plane of rotation. This causes the particle swarm to be in a state of suction along the direction of the spin axis (excluding the possibility of Fig. 10c), and the particle swarm will tend to be in the state shown in Fig. 10d. When there is almost no particle escape, the particle swarm is more likely to be in one of the states shown in Fig. 10a and Fig. 10b. We will study only the latter case in the following. As a result, the spin results in a field of direction aggregation in both the axial and radial directions (especially in the axial direction), resulting in a radial spin axis (similar to the formation mechanism of the solar wind[16]). When a series of such spin particle swarms come together, if the axes of radiation are consistent with each other, there will be an obvious direction aggregation field of velocity (similar to the mechanism of the passive magnetic field generation of iron bars). In addition, particles of different mass levels (larger particle groups) formed by the spin particles will form direction aggregation fields of different intensities. Such a direction aggregation field is

considered to be another type of potential field (electromagnetic field or weak interaction field). When studying single particles of the spin particle swarms, strings similar to those in string theory may be found, and the lengths of these strings should also be computable (although this problem will not be studied in depth here). Other potential fields generated in this way will change only the aggregation state of particles in space (including the aggregation of velocity direction) but not the original velocity of the particles. Since spin is also spontaneously formed and exists in the background field, the aggregation of the velocity direction will also be limited by the background field in accordance with statistical laws.

It is believed that the reason for the change in the movement speed of an agglomerate caused by gravitational potential energy is the accumulation of the position-aggregation-dominated statistical effects produced by the moving particles in the gravitational field. By contrast, the reason that other types of potential energy cause changes in the movement speed of an agglomerate is the accumulation of the direction-aggregation-dominated statistical effects produced by the moving particles in other types of potential fields. The mechanism by which a gravitational field realizes acceleration process is the gradual aggregation of the positions of the particles forming the target object (after being replaced by particles with a position aggregation effect), which leads to an unbalanced diffusion trend that promotes the accumulation of velocity. For other potential fields, the particles forming the target object are constantly replaced by particles with a velocity aggregation effect, which leads to a gradual accumulation of the velocity aggregation effect and thus causes acceleration. At first, such a process can only manifest as a trend, that is, a so-called force. Once the target object begins to move along the trend line, the trend will continue to accumulate. In these potential fields, the particles that form the potential fields will continue to follow the statistical laws together with the particles forming the target object in the fields (exhibiting the generalized diffusion behavior described by Eq. 40). When the particles of the target object are studied separately, the phenomenon of continuous aggregation of position or direction will appear. This phenomenon is characterized by an increase in the potential energy of the target particles. In Section **3.7**, we deduce the particle structure of the matrix for an electron. It is considered that other external fields (electromagnetic fields and weak interaction fields) possess similar structures. The existence of other external fields leads to an increase in the potential energy of particles in this structure, while the

existence of a gravitational field leads to an increase in the potential energy caused by the aggregation of particles in a unit of volume. In this way, most of the mass (in accordance with the viewpoint in Section **3.3.5.2**) in the whole target particle can be accelerated by an external potential field. The scale of the target wave function is generally much smaller than the particle structure of the electron matrix, and the point at which the wave function is located is generally among these larger particles; while it can be equivalently treated in a gravitational field. The wave function (norm) at a point before the action of the external field is much smaller than that after the action of the external field (if the wave function created by an external field, such as a gravitational field, is small, it can be either ignored or studied together with the target object). The superposition of the wave functions at this point can be approximately regarded as characterizing only the speed of these larger particles after acceleration.

Therefore, the contribution of other external fields to the time-dependent rate of change in the density $\mathcal{M}$ of the total relative vector at a point can be regarded as consisting of two superposable components. On the one hand, since the diffusion part of this (infinitesimal) microdomain is still in the background field, regardless of the effect of acceleration, the diffusion behavior of the affected vector is no different from that of a spontaneously formed vector that is not affected by acceleration and still follows the same generalized diffusion law. On the other hand, it exhibits the direction aggregation effect induced by the accelerating field in the (infinitesimal) microdomain, which needs to satisfy the corresponding change in the average potential energy, and the direction is approximately the direction of $\mathcal{M}$ at this point; it is an additional time-dependent change in $\mathcal{M}$ that cannot be affected by diffusion. Throught the joint action of these two vectors, the time-dependent rate of change in the total relative vector density at a certain point is the sum of these two terms. Regarding the additional time-dependent rate of change in $\mathcal{M}$ caused by other potential fields, a potential field here can be understood as an additional particle diffusion coefficient (since the diffusion coefficient is related to the square of the speed and such a potential field changes the velocity of the particle swarm; for example, in a gravitational field, $\frac{GM}{r}m=\frac{1}{2}mv^2$, and the diffusion coefficient is $D=\frac{v^2}{2}t^1$, where $t^1 = 1$ s). In addition, relativistic effects do not need to be considered to determine the potential energy of large monopole

particles because regardless of whether there are relativistic effects, $\rho_m v^2$ is a fixed value that depends on the potential energy where the monopole particles are located. From another perspective, since the potential energy of a particle with a larger mass level is related only to its position, no matter what its motion state is, whether it is affected by special relativistic effects or not, its potential energy will not change. Moreover, the existing particles must be dispersed throughout the whole field, so a change in a particle's potential energy will inevitably lead to a corresponding change in the particle's kinetic energy. With regard to this additional diffusion behavior in an external field, in Fig. 1a, it can be seen that the wave function at A is a certain value $\mathcal{M}$, and at B, it is 0. The same wave function ($\mathcal{M}$) can be obtained by taking A and B as one point at which to find the second derivative. Therefore, the current wave function is numerically consistent with the second derivative, and the corresponding diffusion coefficient is also consistent with the current coefficient. Therefore, regardless of their dimensions, the numerically study will not be affected. Since $\mathcal{M}$ is a plane vector, its direction should be perpendicular to $\frac{\partial \mathcal{M}}{\partial t}$. Since $\mathcal{M}$ is a plane vector, its direction should be perpendicular to $\frac{\partial \mathcal{M}}{\partial t}$. Therefore, the product of another potential energy $\mathcal{E}$ as a diffusion coefficient and $\mathcal{M}$ at a certain point is directly proportional to the change in the diffusion rate of the relative vector. The specific form of this expression is verified by the Schrödinger equation, namely,

$$-\boldsymbol{i}\cdot\frac{\mathcal{E}}{\hbar}\cdot\mathcal{M}. \tag{64}$$

In summary, the final form of the equation for characterizing the generalized diffusion of relative momenta (vectors) in the presence of external fields can be written as

$$\boxed{\boldsymbol{i}\hbar\frac{\partial \mathcal{M}}{\partial t}=-\frac{\hbar^2}{2m}e^{-\mathcal{M}}\left[\Delta\mathcal{M}-T^2(\mathcal{M})\right]+\mathcal{E}\cdot\mathcal{M}}. \tag{65}$$

Here, again, it is emphasized that Eq. 65 is not a final solution; it is only a compromise solution to reduce the computational scale in certain specific cases. If the whole universe is represented by the physical model established in this article, and considering the essential origins of the four fundamental forces (as speculated in Section **3.7**), then either Eq. 40 or Eq. 65 derived in this article can even be called the

real Theory of Everything. Since it describes the most basic laws of motion in nature (if a spin description is added, where the method used for this addition is the same as the traditional method), it can reveal the essence of all phenomena and characteristics of objects in the universe. In accordance with the logic of particle classification by mass put forward in this article, there is no need to add a spin description. The spin effect is also caused by the generalized diffusion behavior of moving particles, and therefore, spin information can be obtained by considering the generalized diffusion behavior of particles of lower mass levels.

3.6 Preliminary Exploration of the Spin Magnetic Moment of the Electron

First, the expression for the momentum operator is determined following the logic of this article, as follows. To find the first derivative of Eq. 22 with respect to position (x, y, z), we obtain

$$\nabla R(\mathcal{M},k). \tag{66}$$

In view of the statistical effect of moving particles, the actual momentum of the particle swarm of each order will not be directly proportional to Eq. 66 but rather will be "weakened" by corresponding diffusion coefficient factors $\frac{1}{k}$. Therefore, by multiplying Eq. 66, representing each complex value, by $\frac{1}{k}$ and adding each order together, we can obtain

$$\sum_{k=1}^{\infty}\left[\frac{1}{k}\cdot\nabla R(\mathcal{M},k)\right]=e^{-\mathcal{M}}\cdot\nabla\mathcal{M}. \tag{67}$$

Accordingly, following this logic, the momentum operator can be expressed as

$$\boldsymbol{p}\rightarrow -\boldsymbol{i}\hbar e^{-\varphi}\nabla\varphi=\boldsymbol{i}\hbar\nabla e^{-\varphi}, \tag{68}$$

where φ is the applied quantity.

Based on the analysis of Eq. 46 and the discussion of Eq. 64 in Section **3.5**, the effect of external potential fields on the velocity of a tiny particle swarm can be quantitatively expressed as

$$\frac{\bar{V}^2}{2}t^1=\frac{\bar{\mathcal{E}}}{\hbar}, \tag{69}$$

where t^1 = 1 s. Here, we take the situation of the electron in the hydrogen atom as the basic reference (note that the same conclusion could be obtained using another atom as the reference) to construct the expression of interest. The average electric potential

energy of the electron in the hydrogen atom is

$$\bar{\mathcal{E}} = \frac{{e_{\mathrm{g}}}^2}{4\pi\varepsilon_0 \bar{r}}, \tag{70}$$

where e_{g} = –1.602 177 33(49) × 10^{-10} C is the charge of the electron, $\varepsilon_0 = \frac{10^7}{4\pi c^2}\ \mathrm{F\cdot m^{-1}}$ is the permittivity of vacuum, and $\bar{r}$ is the average electron radius of the hydrogen atom, for which the Bohr radius is adopted, namely, $\bar{r} = \frac{4\pi\varepsilon_0\hbar^2}{m_e {e_g}^2}$. For the same reasons as in Eq. 47, t^1 is temporarily ignored. By substituting Eq. 70 into Eq. 69, we can obtain a quantitative expression for the norm of the average velocity $\bar{V}$ of a particle swarm in a domain $\mathcal{V}$, namely,

$$\left|\bar{V}\right| = \sqrt{\frac{2{e_{\mathrm{g}}}^2}{4\pi\varepsilon_0 \bar{r}\hbar}} = \alpha c\sqrt{\frac{2m_e}{\hbar}}, \tag{71}$$

where $\alpha = \frac{{e_g}^2}{4\pi\varepsilon_0\hbar c}$ is the fine structure constant, m_e is the mass of the electron, and c is the speed of light. This average velocity in $\mathcal{V}$ is a constant that does not change with the number of particles. In the electron dispersion region, the number of tiny particles forming the electron matrix is $\frac{m_e}{\mu}$, which can be substituted into Eq. 48 together with Eq. 71 before dividing by the speed and number density of tiny particles in the background field to obtain the norm of the relative vector of the whole electron or the norm of the total wave function in the electron dispersion region, namely,

$$\left|\mathcal{M}_{\mathrm{A},e}\right| = \hat{\lambda}_e \cdot \frac{\sqrt{2}\,\alpha m_e^{\frac{3}{2}}}{\bar{\rho}_{m,0}\sqrt{\hbar}}, \tag{72}$$

where $\hat{\lambda}_e = 1\,\mathrm{m^{-2}\cdot s^{-\frac{1}{2}}}$, the purpose of which is to correct the dimensional difference caused by the transformation between different physical quantities. The expression for the equivalent wave function of the whole electron in the potential field is determined above (the product of Eq. 72 and the norm of the normalized wave function is the initial wave function here). However, the contribution of the mass density to the wave function is not considered here because it is negligible compared with the contribution of the electric potential field.

Suppose that the Hamiltonian of a free electron can be written as

$$H = \frac{(\boldsymbol{\sigma} \cdot \boldsymbol{p})^2}{2m_e}, \tag{73}$$

where $\boldsymbol{\sigma}$ is the Pauli operator and $\boldsymbol{p}$ is the electron momentum. Under an external magnetic field $\boldsymbol{B} = \nabla \times \boldsymbol{A}$ (where $\boldsymbol{A}$ is the electric vector potential), H can be transformed into

$$H = \frac{\left[\boldsymbol{\sigma} \cdot \left(\boldsymbol{p} + e_g \boldsymbol{A}\right)\right]^2}{2m_e}. \tag{74}$$

If $\boldsymbol{A}$ and $\boldsymbol{p}$ both commute with $\boldsymbol{\sigma}$, then

$$H = \frac{\left(\boldsymbol{p} + e_g \boldsymbol{A}\right)^2}{2m_e} + \frac{\boldsymbol{i}}{2m_e}\boldsymbol{\sigma} \cdot \left[\left(\boldsymbol{p} + e_g \boldsymbol{A}\right) \times \left(\boldsymbol{p} + e_g \boldsymbol{A}\right)\right]. \tag{75}$$

After the above treatment, the terms describing the interaction of the orbital magnetic moment with the external magnetic field (the first term on the right-hand side of Eq. 75) and the spin term of the electron (the second term on the right-hand side of Eq. 75) have been successfully separated. Next, we will study the spin term separately.

The experimentally measured spin magnetic moment of an electron actually reflects the effect of the external magnetic field on the whole atom. Therefore, the whole wave function of the electron is of great significance here. In view of the discussion in Section **3.5**, Eq. 72 is the intrinsic relative wave function of the whole electron, which does not vary with time. Therefore, it (Eq. 72) appears only in the natural exponential term of Eq. 68 and is not affected by the Hamiltonian operator ∇. When the external magnetic field $\boldsymbol{B}$ is weak, its relativistic effect on the electron momentum can also be ignored. Therefore, only $\left|\mathcal{M}_{\mathrm{A},e}\right|$ alone affects the natural exponential term in Eq. 68. If the distribution of the electron matrix outside the nucleus is regarded as a flat field, only the real part of the system is contributed by the wave function that denotes the flat field. Since it is in the position of the natural exponential term, indicating a statistical effect that is independent of the tiny particle location, the real wave function can be superposed together to denotes a whole particle, which can be expressed as a real $\left|\mathcal{M}_{\mathrm{A},e}\right|$. Because of the special structure of the electron (see the speculations on the

electronic structure presented in Section **3.7**), its diffusion trend is exactly opposite to the usual behavior of the density gradient, so this scalar must be negative; therefore, the negative value $-\left|\mathcal{M}_{\mathrm{A},e}\right|$ of the norm of $\mathcal{M}_{\mathrm{A},e}$ is the best choice. On these grounds, the second term on the right-hand side of Eq. 75 can be transformed into

$$\begin{aligned}\frac{\boldsymbol{i}e_{\mathrm{g}}}{2m_e}\boldsymbol{\sigma}\cdot(\boldsymbol{p}\times\boldsymbol{A}+\boldsymbol{A}\times\boldsymbol{p}) &= \frac{\boldsymbol{i}e_{\mathrm{g}}}{2m_e}\boldsymbol{\sigma}\cdot(-\boldsymbol{i}\hbar e^{\left|\mathcal{M}_{\mathrm{A},e}\right|}\nabla\times\boldsymbol{A}),\\ &= \frac{e_{\mathrm{g}}\hbar}{2m_e}e^{\left|\mathcal{M}_{\mathrm{A},e}\right|}\boldsymbol{\sigma}\cdot\boldsymbol{B}.\end{aligned} \tag{76}$$

Therefore, the expression for the spin magnetic moment of the electron derived in this article is

$$\mu_{\mathrm{g}} = \frac{e_{\mathrm{g}}\hbar}{2m_e}e^{\left|\mathcal{M}_{\mathrm{A},e}\right|}, \tag{77}$$

where $e^{\left|\mathcal{M}_{\mathrm{A},e}\right|}$ can be calculated using Eq. 72. If the average mass density $\overline{\rho}_{m,0}=2\times10^{-28}\,\mathrm{kg\cdot m^{-3}}$ of a broader space is used, then $\mu_{\mathrm{g}}\approx1.004\,38\,\mu_{\mathrm{B}}$, where $\mu_{\mathrm{B}}=\frac{e_g\hbar}{2m_e}$ is the Bohr magneton. However, when a larger value is used, such as the average mass density near the earth (from a comparison with the experimental value measured on earth, it is obvious that this value should be used, but the specific form of this value cannot be obtained at present; hence, we can only assume $\overline{\rho}_{m,\mathrm{E}}$ = 7.537 648 754 4 × 10^{-28} kg·m^{-3}), we can obtain $\mu_{\mathrm{g}}\approx1.001\,159\,652\,2\,\mu_{\mathrm{B}}$. Thus, in turn, the average mass density near the earth can be deduced from the spin magnetic moment of the electrons located there.

It is amazing that small electrons can form such an enormous spin magnetic moment. It is estimated that this spin magnetic moment is induced by the total spin of the tiny particles of the background in the whole atomic domain, and the details of their motion need to be further investigated on the basis of Eq. 40. However, no further in-depth exploration will be presented here.

3.7 Speculations Based on the Physical Model

Following the logic of this article, the black holes observed in the universe should not be very small singularities, as they are considered in the traditional theory. A black hole should have a certain or huge volume with a relatively large density. The mass of

photons is at a sufficiently high level that they cannot escape from the event horizon. However, not all substances cannot escape, at least gravitational effects can escape and be perceived (if there were no substance that could convey this information, it would obviously be impossible for it to be perceived). Therefore, there may be other worlds, even dense forms of life or civilized societies, in some black holes. These civilized life forms in black holes (if they exist) may regard us as being as light, loose and meaningless as we regard clouds in the sky on earth. They may even be able to communicate through particles of lower mass levels.

In light of the model presented in this article, it is speculated that outer space can be divided into interstellar space of varying degrees of emptiness at the levels of interplanetary, interstellar, intergalactic and galactic clusters, etc. The matter in these spaces becomes increasingly sparse until it reaches a certain threshold at which even photons cannot be formed, so that light cannot traverse it. This broad outer space is a field that is untouchable by the electromagnetic wave detection technology that has currently been mastered by human beings. However, gravitation can travel through it.

If we regard the galactic groups with lower connections with each other as multiple universes (these universes as a whole can still be regarded as part of the larger universe), then if one of them could be observed, it would be born at a certain moment in time and eventually die. Such a dead universe, like dead stars, will eventually evaporate. If these multiple universes (multiverses) were completely unconnected, they might be regarded as parallel universes; however, according to the logic of this article, there should be connections between these universes. They must be distributed symmetrically due to their mutual influence. Therefore, parallel universes cannot exist, and only a symmetrical universe can appear.

The concept of the Big Bang is not accepted according to the logic of this article. The idea that the universe originated from an infinitesimal point is absurd. General relativity can be applied only under certain conditions and should not be extended unconditionally. For example, the earth or the sun may be treated as a point mass to calculate gravitation in Newtonian mechanics, but they are not infinitesimal points themselves. The sun is constantly radiating and spreading, and its main body will expand farther in the future, but no one believes that the sun originated from an infinitesimal point. Therefore, according to the view of multiple universes, our universe should have a life cycle similar to that of stars. The universe that we can observe is

constantly spreading (which may be the cause of the repulsion between celestial bodies) or expanding, but the total matter of the larger universe will not change, nor will its total entropy. Following the logic of this article, the concept of the ratio of the abundances of hydrogen and helium in the universe is very easy to understand.

Speculations on photonic structure: It is believed that photons are composed of particles of a lower mass level (*k*th-order) than that of a photon energy agglomeration itself. According to the above discussion, the average speed of these lower-mass-level particles is a fixed value, and they can form structures with different spin periods ($\mathcal{S}_1$ or $\mathcal{S}_2$). Two kinds of photonic structures with different spin periods (frequencies) are illustrated in Fig. 11.

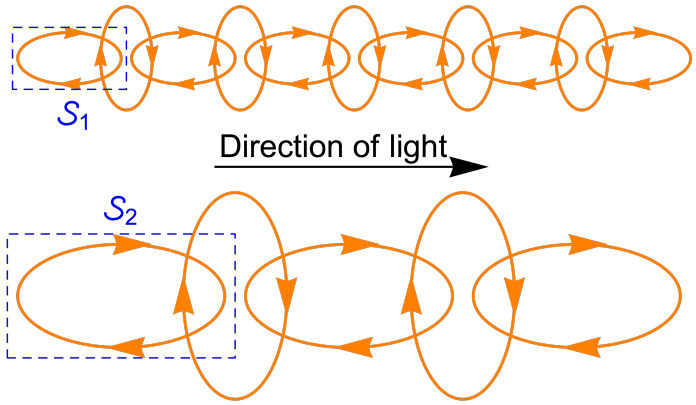

Figure 11 | Schematic diagram of two photonic structures with different frequencies. Ellipses with arrows pointing in different directions represent perpendicular rotations.

According to the logic of this article, the standard for measuring the energy of a photon in a given location is the density of *k*th-order particles present there, or the number of *k*th-order particles passing through that location per unit time. Therefore, from the model structures shown in Fig. 11, it can be seen that frequency is directly proportional to energy. Since the speed of all *k*th-order particles is the same, when they form the structures $\mathcal{S}_1$ and $\mathcal{S}_2$, which are of different sizes, the spin periods of these two structures will be different, and thus, photons of different frequencies will appear. However, in any case, it is obvious that the overall speed of a *k*th-order particle swarm is certain (it is directly proportional to the speed of *k*th-order particles, by a factor of $\frac{1}{\pi}$). Therefore, although the particles have mass, the photons of different frequencies that are formed by them still move at the same speed. The *k*th-order particles do not move in a straight line, and they move faster than the speed of light. However, the norm

of their group velocity is the speed of light. Therefore, we can think of such groups as larger particles (photons), whose speed is the speed of light. This conceptualization does not affect the use of the photon frequency as a tool for measuring the expansion of the universe, nor does it affect the method of taking the speed of light as the representative speed of particles at this mass level. However, from the perspective of general relativity, photons of different frequencies have different energies and cause different degrees of space-time distortion. Therefore, photons of higher frequency or energy will move more slowly due to the influence of their own energy fields. By following the logic of this article, we can obtain the same conclusion. However, because a photon's own energy is so low, the impact of this phenomenon is negligible.

Understanding of the cosmic microwave background radiation: The background radiation in the universe is the measurable agglomeration produced by the tiny particles in the gravitational background field. According to the perspective presented in this article, this gravitational background is everywhere, but in different interstellar spaces, its sparsity is different.

This article holds that it is necessary to return to the concept of the "ether", but it should have different connotations. If the ether is regarded as "absolute space-time", it can be understood as follows: The ether is a gravitational background field composed of tiny particles moving randomly. The ether in the broadest space is the purest absolute space-time. The ether near different types of celestial bodies can be approximated as absolute space-time to varying degrees. For example, the ether near the earth can be approximated as absolute space-time; the ether near the sun can be approximated as absolute space-time to different extent. However, the approximation of the ether near the earth is not as close to absolute space-time as that near the sun because it is also affected by the ether near the sun.

To analyze the natural exponential term in the equation (Eq. 40) presented in this article, when the momentum density reaches infinity (that is, the velocity density or the mass density or both are infinite), the diffusion rate is infinitesimal. If the speed v is infinite and the energy density has a certain value at a particular location, then the mass density ρ_m at that location must be infinitesimal, and it is an infinitesimal of higher order than $\frac{1}{v}$. In this case, the momentum density $\rho_m v$ would also be infinitesimal, and there would be no concept of momentum aggregation; therefore, this situation is

meaningless. However, if the mass density is relatively large, even if the mass distribution does not satisfy the condition in Eq. 43, the diffusion will be extremely slow, and the distribution will be relatively stable on the time scale that is perceptible to humans. This conclusion, together with the situation described by Eq. 43, explains the mechanism of the formation of "stable particles" in the universe. With such a formation mechanism, particles of different mass levels will appear and will be effectively equivalent. In view of the above considerations, there is no interaction between particles of different mass levels, and particles of different mass levels are equivalent. Therefore, it is understandable that the universe is subject to fractal laws and that the universe is a "large organism" that also has a theoretical basis.

The plane wave function given in Eq. 40 and Eq. 65 in this article has certain requirements in terms of direction. This plane wave function is a simplification of a three-dimensional vector wave function. For this reason, the uniqueness of the three-dimensional function determines the uniqueness of the plane wave function described in this article. Therefore, this article does not support the idea that the wave function $\mathcal{M}$ should be equivalent in all directions in the plane. As mentioned above, the wave function presented in this article also requires a suitable norm of the wave function in the initial condition.

Understanding of the wave nature of solid particles (such as protons and electrons): The solid particle's matrix (background field) consists of particle waves of a low mass level, which diffuse in accordance with the corresponding laws. Solid particles are produced by this matrix and thus follow the dense regime of matrix diffusion. The diffusion rate of solid particles can be thought of as the apparent diffusion rate corresponding to the mass assignment under the diffusion law of the matrix wave function.

Understanding of the process of electrons escaping from atoms: Since electrons have a fixed mass aggregation degree, when they escape by forming fixed-mass-level particles (at this time, the electron wave function collapses, where the so-called process of wave function collapse refers to the disturbed aggregation of the tiny particles forming the abovementioned matrix), the remaining mass (atomic nucleus, etc.) will immediately follow the aggregation law described by Eq. 43 to a different extent. For the effect of direction aggregation generated by the spin in atomic nucleus, this (the state of electrons escaping from atom) is an unstable state. Due to the lack of a

corresponding spin request (for the energy released by the nuclear spin) in electron, the energy released by the nuclear spin can only be spread out, thus resulting in the manifestation of an electric field of a certain magnitude.

Speculations on electronic structure: As described above, the electron is not a particle with a mass of 9.109 389 7(54) × 10^{-31} kg, as it is traditionally considered, but rather consists of a matrix (consisting of particles of a lower mass level than the electron) dispersed in space. Now, we analyze the structure of the particles forming the electron matrix (we assume that they are k_1 th-order particles). There is a strong interaction between the electron matrix and the nucleus, which has a positive charge, and the k_1 th-order particles forming the matrix must also be negative monopoles. For negative monopoles with such a small mass to produce such a large force, each of them must have a spin acceleration structure, as described in Section 3.5. A single spin acceleration structure cannot achieve such a function (omnidirectional attraction); therefore, a complex of multiple spin structures must be formed. One possible structure of a spherical 3-dimensional composite is illustrated in Fig. 12, simplified to the form of a plane.

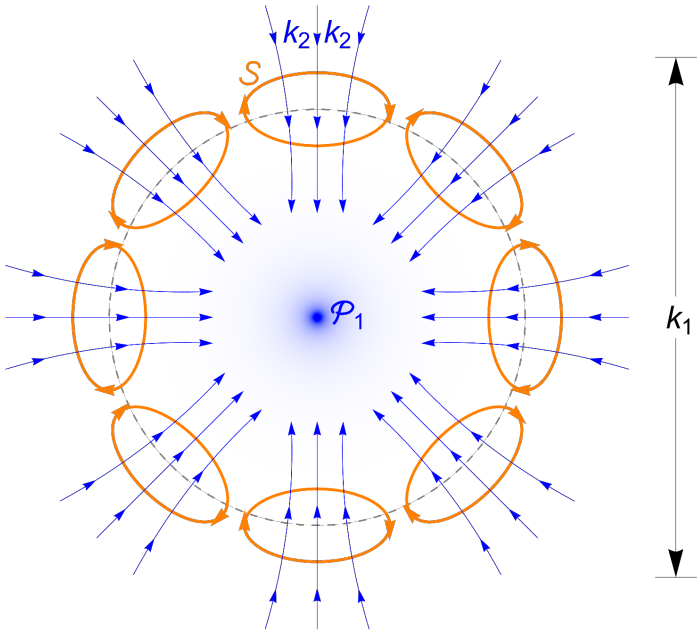

Figure 12 | Speculative schematic of the structure of a k_1 th-order particle forming the electron matrix. Here, we use a plane diagram to illustrate the 3-dimensional spherical structure, where each blue line with arrows represents a track of k_2 th-order particles and each orange elliptical ring with arrows represents an $\mathcal{S}$-structure.

There is a black-hole-like structure (the blue diffusion point $\mathcal{P}_1$ in Fig. 12) with a great

mass density in the center of the k_1 th-order particle (composite structure), of which the outer sphere accumulates at least one layer of spin acceleration structures $\mathcal{S}$, the orange structures shown in Fig. 12. On the one hand, these $\mathcal{S}$ structures are attracted by $\mathcal{P}_1$; on the other hand, because of the escape of the smaller particles (k_2 th-order particles) in the radial direction, these $\mathcal{S}$ structures will repel each other. The jets formed in the axial direction are exactly suctioned into $\mathcal{P}_1$. All of the constraining mechanisms above make the k_1 th-order particle a stable composite structure. Such a composite structure can continuously and rapidly pull in k_2 th-order particles from the outside, thus forming a strong attractive force. Because of relativistic effects, the k_2 th-order particles pulled in by the k_1 th-order particle from the outside will gather together in a highly concentrated form (similar to a black hole), temporarily forming a stable suction structure ($\mathcal{P}_1$ and k_1 th-order particles). However, in the long term, the continuous suction of materials from the outside will inevitably lead to instability of the k_1 th-order particle structure. As a result, such structures will continue to be generated and collapse on a longer time scale, but the total number of these structures in a specific region will remain unchanged.

Based on the electronic matrix model, we can deduce the principles of action of the four known fundamental forces in the following way: The strong interaction force is a statistical effect between a few energy aggregations very close to each other, which has the same form as gravitation. This is a type of energy-level force (for example, it is quite difficult to merge or separate two peaks in Fig. 4b). Such a force is strong and e^{-x} -like. The action principle of the electromagnetic force is that both sides of the interaction are composed of electron matrix structures. The action principle of the weak interaction force is that only one side of the interaction is composed of an electron matrix structure. The action principle of gravitation is that neither side of the interaction is composed of an electron matrix structure, or the electronic matrix structure exerts no effect; instead, gravitation is a statistical effect between particle aggregations at a long distance.

Understanding of antimatter: As mentioned above, space is infinitesimal relative to infinitesimal moving particles in it, and particles exist in space as if nothing were present in that space. Accordingly, we can also suppose that infinitely many spaces exist for one particle, such spaces move among a particle, and this particle can be divided into entities with the same number of spaces. If the empty boxes in space are instead

taken as the research objects, then in a way analogous to that described above, antiparticles, white holes and negative energy will arise. Since our world consists of agglomerations of matter, the proportion of antimatter is relatively small. In this way, the understanding of antimatter is complete and self-consistent.

Understanding of quantum entanglement: If two particle states are entangled with each other, then information must be transmitted between them. In this article, the way in which different particles are classified according to their mass can well explain this kind of action at a distance. Similarly, there is also the strange phenomenon of Wheeler's delayed-choice experiment. However, if we understand it in accordance with the logic of this article, it is no longer mysterious.

4. Conclusions

In this article, a physical model of the whole universe has been constructed from the most basic philosophical paradoxes. Based on this model, a mathematical equation has been established to describe the generalized diffusion behavior of moving particles, for which the corresponding form without an external field has been simply verified. For the first time, relativistic effects have been interpreted as statistical effects of moving particles, based on the understanding that the higher the degree of aggregation of particles is (in terms of either position or movement direction), the more of their average velocity in other directions is consumed. Thus, the gravitational force and (special) relativistic effects can be actually integrated into the derived equation (achieved by selecting an initial wave function with a specific norm when solving it), thus avoiding the problem of nonrenormalizability when gravitation is introduced into quantum mechanics. Further analysis has shown that the gravitation between objects is also caused by a statistical effect of randomly moving particles. These particles can also form stable nondispersive particle swarms, which, as larger-mass-level particles, can further unite into stable nondispersive particle swarms, and so on. No matter the mass level of the particles that are regarded as infinitesimal particles, and no matter how slow the speed that is regarded as an infinite speed, the equations derived in this article are equivalent at the scale of human understanding. On the one hand, based on the hypotheses stated in **HYPO 1–3**, this article has deduced the form of the Schrödinger equation and the conclusions of special relativity, thus further confirming the rationality of these hypotheses concerning the universe. On the other hand, based on these assumptions, the derived equation contains the conditions for the generation of stable

particles, which, in turn, form a logical self-consistency with the previous assumptions. Therefore, the basic physical model of the universe established in this article is a relatively reliable and complete logical model, and the universe is likely to be a product of the movement of noninteracting random particles and to obey the mathematical equation given in Eq. 40.

Based on this physical model, we can answer the questions raised at the beginning of this article. The universe is both large and small, and its size is only a relative logical concept. From this relative point of view, the universe is boundless (for human beings). The current appearance of the universe is only one stage of its evolution, and this evolution is a process without beginning or end. The constant random motion or generalized diffusion of particle swarms is the mechanism by which it operates, and there is no beginning or end point of this diffusive movement (although there may be a beginning and end in local space). The energy in the universe cannot be designated as existing or not; it is merely a relative concept arising from the movement of infinitesimal particles. If we observe the group behavior of these particles, their average speed will decrease, giving rise to the concepts of time, space, speed and energy. Therefore, these concepts (including force) are all statistical effects that arise when observing these moving particles from different angles. Energy will never be exhausted, nor will it increase or decrease. According to this view, the total entropy in the whole universe also will not increase or decrease.

However, due to various conditions, the viewpoints advanced in some paragraphs of this article have not been supported by rigorous derivations and proofs. The equations have not been tested on rigorous cases, and some conjectures presented at the end of this article were not based on rigorous theories. In view of the above problems, additional efforts will be needed in the future to develop the ideas proposed here into a more mature theory.

Acknowledgments I thank the engineers at *Wolfram Inc*. for technical support.

References

1 Harris, P. *Three Hundred Tang Poems*. (Everyman's Library, 2009).

2 Sun, T. *The art of war · Attacking by stratagem*. (Zhonghua Book Company, 2001).

3 Hawking, S. *A Brief History of Time*. (Bantam Dell Publishing Group, 1988).

4 Dirac, P. A. M. *General theory of relativity*. (Princeton University Press, 1975).

5 Kaku, M. *Hyperspace: A scientific odyssey through parallel universes, time warps, and the tenth dimension*. (Oxford University Press, 2016).

6 Kant, I. *Critique of pure reason*. (Cambridge university press, 1999).

7 Darwin, C. *On the Origin of Species*. (Routledge, 1859).

8 Marx, K. H. *Capital*. (Progress Publisher, Moscow, USSR, 1887).

9 Hegel, G. W. F. *The Science of Logic*. (Cambridge University Press, 1929).

10 Einstein, A. & de-Sitter, W. On the relation between the expansion and the mean density of the universe. *Proc. Natl. Acad. Sci.* **18**, 213–214 (1932).

11 Scaramella, R. *et al.* The ESO Slice Project [ESP] galaxy redshift survey⋆ V. Evidence for a D=3 sample dimensionality. *Astronomy and Astrophysics* **334**, 404–408 (1998).

12 Martínez, V. J., Pons-Bordería, M. J., Moyeed, R. A. & Graham, M. J. Searching for the scale of homogeneity. *Mon. Not. R. Astron. Soc.* **298**, 1212–1222 (1998).

13 Maxwell, J. C. *Illustrations of the dynamical theory of gases*. Vol. 20 (The London, Edinburgh, and Dublin Philosophical Magazine and Journal of Science, 1860).

14 Marsaglia, G. Choosing a point from the surface of a sphere. *Ann. Math. Stat.* **43**, 645–646 (1972).

15 Muller, M. E. A note on a method for generating points uniformly on n-dimensional spheres. *Comm. Assoc. Comput. Mach.* **2**, 19–20 (1959).

16 Kasper, J. C., Maruca, B. A., Stevens, M. L. & Zaslavsky, A. Sensitive Test for Ion-Cyclotron Resonant Heating in the Solar Wind. *Phys. Rev. Lett.* **110**, 091102-1–091102-5 (2013).

Supplementary Information
(Mathematica v12.0 code of TraditionalForm)

Part 1. The Square of the Norm of the Average Velocity is Proportional to the Number of Vectors

Definition: Particles with a higher mass level composed of k particles are called kth-order particles. Then, the velocity of a kth-order particle is the velocity of the overall center of mass of the k particles, which is the average of the velocity vectors of all these particles.
Assumption: Each particle is moving at the same speed and in a random direction in space.
Thus, the projection of the velocity vector of a kth-order particle onto one of the three equivalent coordinate axes of the 3-dimensional Cartesian coordinate system is the mean value of the projection (onto the same axis) of the velocity vectors of the 1st-order particles forming the kth-order particle, which follow the same distribution; therefore, it approximately follows a normal distribution (central limit theorem).
There are three equivalent (approximate) normal distributions, one on each of the three axes, which are not completely independent. However, James Clerk Maxwell and Ludwig Boltzmann proved that these distribution can, in fact, be equivalently treated as completely independent. This is because randomly selecting a vector is equivalent to randomly determining a three-axis coordinate; moreover, the problem of the momentum transfer of gas molecules participating in random collisions is also equivalent to the problem discussed in this article.

First, the probability density of the norm of the 3-dimensional vectors formed by three normal distribution $N(0, \sigma_2)$ components that are independent on three coordinate axes is calculated.

In[•]:=
```
Clear["Global`*"];
𝒟 = Simplify[PDF[TransformedDistribution[x^2 + y^2 + z^2,
        {x, y, z} ≈ ProductDistribution[{NormalDistribution[0, σ2], 3}]], x], Assumptions → σ2 > 0];
𝒟1 = PDF[TransformedDistribution[ Sqrt[x], x ≈ ProbabilityDistribution[𝒟, {x, 0, +∞}]], x]
```

Out[•]=
$$\begin{cases} \frac{\sqrt{\frac{2}{\pi}}\, x^2\, e^{-\frac{x^2}{2\sigma_2^2}}}{\sigma_2^3} & x > 0 \\ 0 & \text{True} \end{cases}$$

Then, we find the probability density of the Maxwell distribution with scale parameter σ_2:

In[•]:=
```
𝒟2 = PDF[MaxwellDistribution[σ2], x]
```

Out[•]=
$$\begin{cases} \frac{\sqrt{\frac{2}{\pi}}\, x^2\, e^{-\frac{x^2}{2\sigma_2^2}}}{\sigma_2^3} & x > 0 \\ 0 & \text{True} \end{cases}$$

Therefore, these two probability densities are equal:

In[•]:=
```
𝒟1 - 𝒟2
```

Out[•]= 0

We verify the above conclusion (c is the speed of the 1st-order; n is the number of vectors) (This code takes approximately 1.74 hours):

In[•]:=
```
c = 1;
n = 1000;
m = 1 000 000;
dd = {};
ProgressIndicator[Dynamic[i], {1, m}]
For[i = 1, i < m, i++,
    ℋ = RandomPoint[Sphere[{0, 0, 0}, c], n];
    ℋℋ = Norm[Total /@ Transpose[ℋ]];
    dd = AppendTo[dd, ℋℋ]];
𝒟 = SmoothKernelDistribution[dd, {"Adaptive", Automatic, Automatic}];
Plot[{PDF[𝒟, x], PDF[MaxwellDistribution[c/Sqrt[3] Sqrt[n]], x]},
  {x, 0, 100 c}, PlotStyle → {{Red, Thickness → 0.0032}, {Blue, Thickness → 0.0032}},
  Frame → {{True, False}, {True, False}}, FrameStyle → Directive[Black, Thickness → 0.0017],
  LabelStyle → Directive[Black, FontFamily → "Arial", FontSize → 14],
  Epilog → Inset[LineLegend[{Directive[Blue, Thickness[0.0032]], Directive[Red, Thickness[0.0032]]},
      {Style["Theoretical", FontFamily → "Arial", FontSize → 14],
       Style["Simulated", FontFamily → "Arial", FontSize → 14]}, LegendFunction →
       (Framed[#, RoundingRadius → 4, FrameStyle → GrayLevel[.6]] &)], Scaled[{0.732, 0.644}]]]
```

Out[•]=

Out[•]=

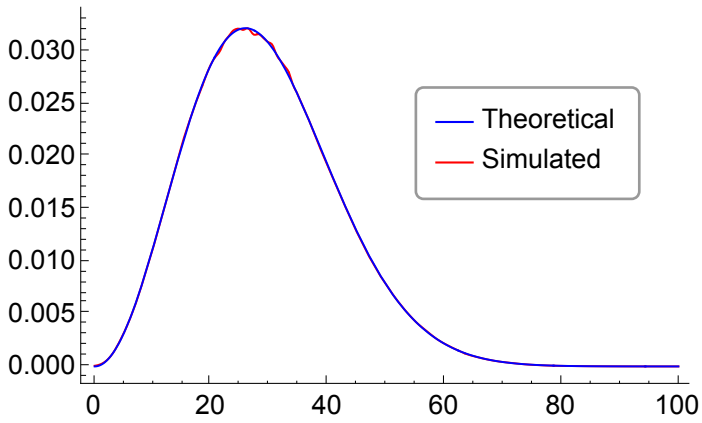

Accordingly, the norm of the 3-dimensional vectors formed by three normal distribution $N(0, \sigma_2)$ components which are independent on three coordinate axes follows the Maxwell distribution with the scale parameter σ_2.

Suppose that the standard deviation of the projection of the velocity of any one of the k equivalent particles forming a kth-order particle onto each equivalent coordinate axis is σ. Then, the standard deviation of the projection of the velocity of a kth-order particle onto each equivalent coordinate axis (i.e., the mean value of the projection of the velocity of 1st-order particle) is $\frac{\sigma}{\sqrt{k}}$, namely, the projection onto each coordinate axis (approximate) follows a normal distribution with a mean value of 0 and a standard deviation of $\frac{\sigma}{\sqrt{k}}$. As a result, the speed of kth-order particles follows the Maxwell distribution with scale parameter $\frac{\sigma}{\sqrt{k}}$.

Then, the average velocity of the kth-order particles is

In[•]:= $\bar{v} = \text{Mean}\left[\text{MaxwellDistribution}\left[\frac{\sigma}{\sqrt{k}}\right]\right]$

Out[•]= $\frac{2\sqrt{\frac{2}{\pi}}\,\sigma}{\sqrt{k}}$

For the kth-order particles in different references ($\mathcal{R}_u$ and $\mathcal{R}_0$) and with different standard deviations (σ_u and σ_0), the ratio of their average velocity $\bar{v}_u / \bar{v}_0$ =

In[•]:= $\frac{2\sqrt{\frac{2}{\pi}}\,\sigma_u}{\sqrt{k}} \Big/ \frac{2\sqrt{\frac{2}{\pi}}\,\sigma_0}{\sqrt{k}}$

Out[•]= $\frac{\sigma_u}{\sigma_0}$

Therefore, the ratio of σ_u to σ_0 is the ratio between the average speeds of particles of higher mass levels in $\mathcal{R}_u$ and $\mathcal{R}_0$.

For k_1- and k_2-order particles, the ratio of their average velocity $\bar{v}_1 / \bar{v}_2$ =

In[•]:= $\frac{2\sqrt{\frac{2}{\pi}}\,\sigma}{\sqrt{k_1}} \Big/ \frac{2\sqrt{\frac{2}{\pi}}\,\sigma}{\sqrt{k_2}}$

Out[•]= $\frac{\sqrt{k_2}}{\sqrt{k_1}}$

And because: $m_1 = \mu\, k_1$ and $m_2 = \mu\, k_2$, where μ is the scale factor or the mass of 1-order particle. $\bar{v}_1 / \bar{v}_2$ also equals:

In[•]:= $\text{Simplify}\left[\frac{\sqrt{\frac{m_2}{\mu}}}{\sqrt{\frac{m_1}{\mu}}}, \text{Assumptions} \to \mu > 0\right]$

Out[•]= $\frac{\sqrt{m_2}}{\sqrt{m_1}}$

Therefore, the square of the average velocity of particles is directly proportional to the mass of particles or the number of 1-order particles forming it.

Part 2. Special Relativistic Effects on Infinitesimal Particles

Correspondence:

The mixed distribution of $\mathcal{D}_1$and $\mathcal{D}_2$ is represented by $\mathcal{D}12$;

The mixed distribution of $\mathcal{D}_3$and $\mathcal{D}_4$ is represented by $\mathcal{D}34$;

The rest of the symbols are consistent with those in the main text.

```
In[•]:= Clear["Global`*"];
        𝒟 = TransformedDistribution[c Cos[θ] Sin[ArcCos[η]],
            {θ ≈ UniformDistribution[{-π, π}], η ≈ UniformDistribution[{-1, 1}]}];
        𝒟1 = TransformedDistribution[c Cos[θ] Sin[ArcCos[η]],
            {θ ≈ UniformDistribution[{-π, π}], η ≈ UniformDistribution[{u/c, 1}]}];
        𝒟2 = TransformedDistribution[c Cos[θ] Sin[ArcCos[η]],
            {θ ≈ UniformDistribution[{-π, π}], η ≈ UniformDistribution[{-1, u/c}]}];
        𝒟3 = TruncatedDistribution[{u, c}, UniformDistribution[{-c, c}]];
        𝒟4 = TruncatedDistribution[{-c, u}, UniformDistribution[{-c, c}]];
        𝒟34 = MixtureDistribution[{w, 1 - w}, {𝒟3, 𝒟4}];
        Simplify[Mean[𝒟34], Assumptions → 0 < u < c]
```

$$\text{Out[•]=}\ \frac{1}{2}(c\,(2\,w-1)+u)$$

Let the mean value expression be $\frac{1}{2}(c\,(2\,w-1)+u)=u$, then find the weight w

```
In[•]:= Reduce[1/2 (c (2 w - 1) + u) == u, w]
```

$$\text{Out[•]=}\ (u=0\land c=0)\lor\left(c\neq 0\land w=\frac{c+u}{2\,c}\right)$$

Then, the mixed distribution $\mathcal{D}12$ consisting of $\mathcal{D}_1$ and $\mathcal{D}_2$ can be calculated in accordance with this weight w. The analytical form of $\mathcal{D}12$ cannot be given by Mathematica. Therefore, the standard deviation of $\mathcal{D}12$ is calculated directly (This code takes approximately 91 seconds).

```
In[•]:= w = (c + u)/(2 c);
        𝒟12 = MixtureDistribution[{w, 1 - w}, {𝒟1, 𝒟2}];
        σu = Simplify[StandardDeviation[𝒟12], Assumptions → 0 < u < c]
```

$$\text{Out[•]=}\ \frac{\sqrt{c^2-u^2}}{\sqrt{3}}$$

The standard deviation of $\mathcal{D}34$ is the same.

```
In[•]:= Simplify[StandardDeviation[𝒟34], Assumptions → 0 < u < c]
```

$$\text{Out[•]=}\ \frac{\sqrt{c^2-u^2}}{\sqrt{3}}$$

Then, the ratio between σ_u and the velocity components on the x-axis of the particles in $\mathcal{R}_0$ can be obtained.

```
In[•]:= Simplify[σu / StandardDeviation[𝒟], Assumptions → 0 < u < c]
```

$$\text{Out[•]=}\ \frac{\sqrt{c^2-u^2}}{c}$$

The same factor can also be obtained by evaluating the ratio of the standard deviation of $\mathcal{D}34$ to the standard deviation of the velocity components on the z-axis in $\mathcal{R}_0$.

In[•]:=
```
Simplify[StandardDeviation[𝒟34]/StandardDeviation[UniformDistribution[{-c, c}]],
  Assumptions → 0 < u < c]
```

Out[•]=
$$\frac{\sqrt{c^2-u^2}}{c}$$

Part 3. The Norm of the Component Vector is Proportional to the Number of Vectors Forming It

When the total vector value of a specified vector swarm is determined, the mean norms between different component vectors should be proportional to the number forming them. The following proves this viewpoint in detail.

It has been proven that the degree of slowdown on all three axes is the same in Part 2 of the Supplementary Information. Therefore, when observing all of the moving particles in $\mathcal{R}_u$ from $\mathcal{R}_0$, all the randomly moving particles in $\mathcal{R}_u$ can be considered to have an additional velocity component u along the z-axis. Then, according to cosine theorem, the probability density of the particles in $\mathcal{R}_u$ observed in $\mathcal{R}_0$ can be expressed as (where k is the number of the particles, u is the speed of $\mathcal{R}_u$ and v is the norm of momentum of these k particles observed from $\mathcal{R}_u$):

In[•]:=
```
Clear["Global`*"];
𝒟 = TransformedDistribution[ Sqrt[(k u)^2 + v^2 - 2 k u v Cos[ArcCos[η]]] ,
    {v ≈ MaxwellDistribution[ Sqrt[k] Sqrt[c^2 - u^2] / Sqrt[3] ], η ≈ UniformDistribution[{-1, 1}]}];
FullSimplify[PDF[𝒟, x], Assumptions → c > 0 ∧ 0 < u < c]
```

Out[•]=
$$\begin{cases} \dfrac{\sqrt{3}\, x \left(e^{\frac{6 u x}{c^2-u^2}}-1\right) e^{-\frac{3(k u-x)^2}{2k\left(c^2-u^2\right)}}}{k u \sqrt{2\pi c^2 k - 2\pi k u^2}} & k>0 \wedge ((x>0 \wedge k u > x) \vee k u < x) \\ -\dfrac{\sqrt{6\pi}\ \sqrt{c^2 k - u x}\left(5 u x - 2 c^2 k\right)\operatorname{erf}\left(\frac{\sqrt{6}\, x}{\sqrt{c^2 k - u x}}\right) + 4 x\, e^{\frac{6x^2}{u x - c^2 k}}\left(c^2(6k+2) - u(2u+3x)\right) - 8x(c-u)(c+u)}{4\sqrt{6\pi}\, k^{5/2} u ((c-u)(c+u))^{3/2}} & k u = x \wedge k > 0 \end{cases}$$

The meaningful part (first branch) is selected to be verified. Note that the sampling with the replacement method in the particle swarm with a mean speed of u can simulate all of the cases of the particle swarm with a mean speed of u. (The following code takes averagely 108 + 77 minutes)

In[•]:=
```
c = 1;
n = 1 000 000;
ℋℋ = 0;
While[ℋℋ < 2700,
    ℋ = RandomPoint[Sphere[{0, 0, 0}, c], n];
    ℋℋ = Norm[Total /@ Transpose[ℋ]]];
m = 100 000;
dd = {};
ProgressIndicator[Dynamic[j], {1, m}]
For[j = 1, j < m, j++,
    ℋ0 = RandomChoice[ℋ, 0.3 n];
    ℋℋ0 = Norm[Total /@ Transpose[ℋ0]];
    dd = AppendTo[dd, ℋℋ0]];
𝒟 = SmoothKernelDistribution[dd, {"Adaptive", Automatic, Automatic}];
k = 0.3 n;
u = ℋℋ / n;
Plot[{PDF[𝒟, x], Sqrt[3] x (E^(6 u x/(c^2 - u^2)) - 1) E^(-3 (k u + x)^2/(2 k (c^2 - u^2)))/(k u Sqrt[2 π c^2 k - 2 π k u^2])}, {x, 0, 2500},
  PlotStyle → {{Red, Thickness → 0.0032}, {Blue, Thickness → 0.0032}},
  Frame → {{True, False}, {True, False}}, FrameStyle → Directive[Black, Thickness → 0.0017],
  LabelStyle → Directive[Black, FontFamily → "Arial", FontSize → 14],
  Epilog → Inset[LineLegend[{Directive[Blue, Thickness[0.0032]], Directive[Red, Thickness[0.0032]]},
      {Style["Theoretical", FontFamily → "Arial", FontSize → 14],
       Style["Simulated", FontFamily → "Arial", FontSize → 14]}, LegendFunction →
       (Framed[#, RoundingRadius → 4, FrameStyle → GrayLevel[.6]] &)], Scaled[{0.753, 0.644}]]]
```

Out[•]=

Out[•]=

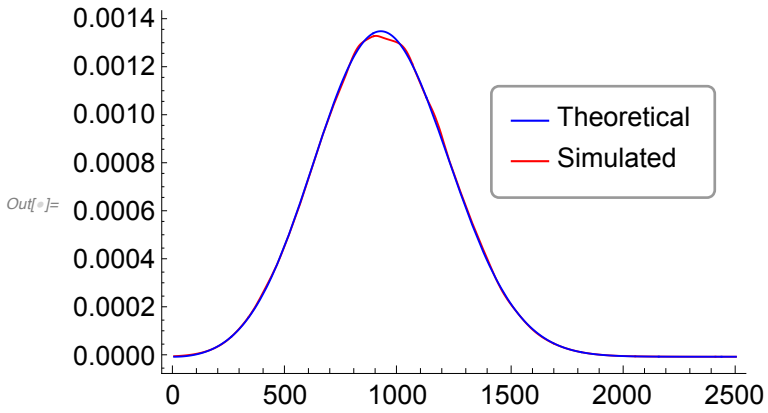

In view of the above conclusions, we find the mean value of this distribution (This code takes approximately 166 seconds).

In[•]:=
$$\overline{\mathcal{V}}_k = \text{FullSimplify}\left[\text{Mean}\left[\text{ProbabilityDistribution}\left[\frac{\sqrt{3}\, x \left(e^{\frac{6ux}{c^2-u^2}} - 1\right) e^{-\frac{3(ku+x)^2}{2k(c^2-u^2)}}}{ku\sqrt{2\pi c^2 k - 2\pi k u^2}}, \{x, 0, +\infty\}\right]\right], \text{Assumptions} \to c > u > 0 \wedge k > 0\right]$$

Out[•]=
$$\frac{\left(c^2 + (3k-1)u^2\right)\text{erf}\left(\frac{\sqrt{\frac{3}{2}}\, ku}{\sqrt{k(c-u)(c+u)}}\right) + \sqrt{\frac{6}{\pi}}\, u\, e^{\frac{3ku^2}{2(u^2-c^2)}}\sqrt{k(c-u)(c+u)}}{3u}$$

We find the limit of the ratio of this mean value $\overline{\mathcal{V}}_k$ and k when k approaches $+\infty$.

In[•]:=
$$\text{Simplify}\left[\text{Limit}\left[\frac{\overline{\mathcal{V}}_k}{k}, k \to +\infty\right], \text{Assumptions} \to u > 0\right]$$

Out[•]=
$$\begin{cases} -u & \arg\left(c^2 - u^2\right) \geq \pi \\ u & \text{True} \end{cases}$$

Therefore, when k is a large number, the norm of the mean value $\overline{\mathcal{V}}_k$ is directly proportional to the number k forming $\overline{\mathcal{V}}_k$, namely $\overline{\mathcal{V}}_k = k\, u$.

Eq. 21 in the main text determines the proportion of particle number distributed in various boxes partitioned by k, and these particles are distributed in each box of $\mathcal{V}$ with equal probability. That is, the particles are randomly extracted from the micro domain $\mathcal{V}$ to be distributed in each box. When the number of extractions is large enough, the norm of each component vector partitioned by k should be proportional to the number of particles according to the probability.

Next, we verify the standard deviations of this distribution in the three axes.

In[•]:=
```
c = 1;
n = 10 000 000;
ℋℋ = 0;
While[ℋℋ < 6600,
    ℋ = RandomPoint[Sphere[{0, 0, 0}, c], n];
    ℋℋ = Norm[Total /@ Transpose[ℋ]]];
ℋ0 = RandomChoice[ℋ, 0.3 n];
ℋℋx = StandardDeviation[Transpose[ℋ0][[1]]]
ℋℋy = StandardDeviation[Transpose[ℋ0][[2]]]
ℋℋz = StandardDeviation[Transpose[ℋ0][[3]]]
```

Out[•]= 0.57735

Out[•]= 0.577374

Out[•]= 0.577327

The standard deviation in theory is:

In[•]:=
```
u = ℋℋ / n;
k = 0.3 n;
Sqrt[c^2 - u^2] / Sqrt[3]
```

Out[•]= 0.57735

This result verifies that the conclusions in Part 2 and Part 3 are both correct.

Part 4. The 2-Dimensional Drawings Under the Same Conditions

When solving the equation, an equivalent form of multiplying both sides by the power function of e is adopted to make the solution more accurate and obtain it faster (This code takes approximately 72 seconds).

In[1]:=
```
Clear["Global`*"];
Needs["NDSolve`FEM`"];
Ω = ImplicitRegion[0.0016 ≤ x^2 + y^2 ≤ 16, {x, y}];
mesh = ToElementMesh[Ω, MeshRefinementFunction →
       Function[{vertices, area}, area > 0.00003 (0.1 + 80 Norm[Mean[vertices]])]];

uif = NDSolveValue[{e^-u[x,y] (∂^2 u[x, y]/∂ x^2 + ∂^2 u[x, y]/∂ y^2 - (∂ u[x, y]/∂ x)^2 - (∂ u[x, y]/∂ y)^2) == 0,
       DirichletCondition[u[x, y] == 1 + 2 i, x^2 + y^2 == 0.0016],
       DirichletCondition[u[x, y] == 0, x^2 + y^2 == 16]}, u, {x, y} ∈ mesh];
p4 = Plot3D[(Abs[uif[x, y]])^2, {x, y} ∈ mesh, PlotRange → {0, 5},
      ColorFunction → (Hue[0.65, #3] &), AxesLabel → {"x", "y", "z"},
      LabelStyle → Directive[Black, FontFamily → "Times New Roman", FontSize → 21],
      BoxStyle → Directive[Gray, Thickness → 0.002], BoxRatios → 1, ViewPoint → {15, -26, 16}];

ImageResize[p4, 700]
```

Out[7]=

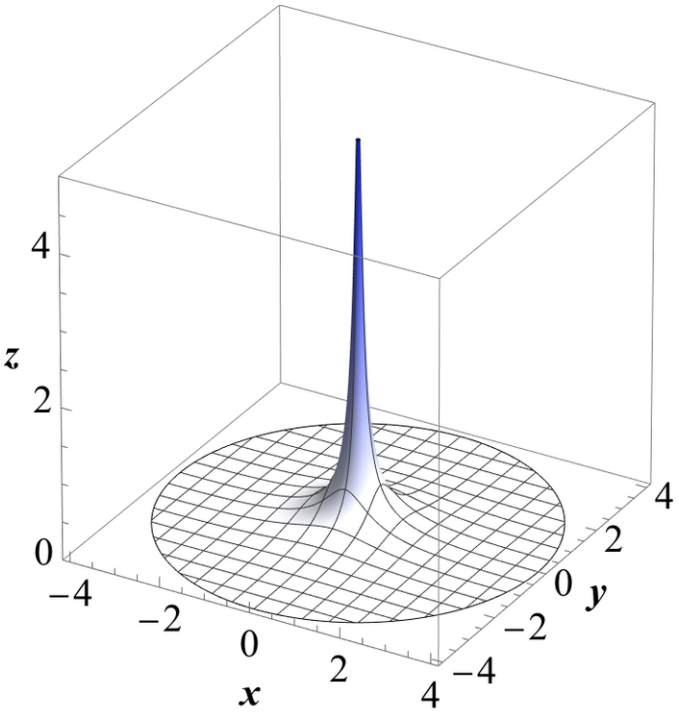

It can be seen from the figure that it is a circular symmetrical structure.

Part 5. Angular Speed Distribution of Random Spin Particles

```
Clear["Global`*"];
X = TransformedDistribution[ N1 / Sqrt[N1^2 + N2^2 + N3^2],
    {N1, N2, N3} ≈ ProductDistribution[{NormalDistribution[], 3}]];
PDF[X, x]
```

Out[•]=
$$\begin{cases} \frac{1}{2} & -1 \le x \le 1 \\ 0 & \text{True} \end{cases}$$

The expression of $|\Omega'|$ in the main text is calculated as follows.

```
In[•]:= X = c Sin[ArcCos[Θ]] Cos[H];
Y = c Sin[ArcCos[Θ]] Sin[H];
Z = 0;
FullSimplify[ Sqrt[X^2 + Y^2 + Z^2] , Assumptions → c > 0]
```

Out[•]= $c\ \sqrt{1-\Theta^2}$

NOTE: $|\omega'|(x)$ in the main text is substituted by ω' as the probability expression here.

```
In[•]:= ω' = TransformedDistribution[c Sqrt[1 - Θ^2] , Θ ≈ UniformDistribution[{-1, 1}]];
FullSimplify[PDF[ω', x], Assumptions → c > 0]
```

Out[•]=
$$\begin{cases} \frac{x}{c\ \sqrt{c^2-x^2}} & x > 0 \wedge c > x \\ 0 & \text{True} \end{cases}$$

NOTE: $\omega_{S,X}(x)$ in the main text is substituted by ωsx here. Then, the probability density of X, which represents one of the three equivalent coordinates of the angular velocity $\mathbf{\Omega}_S$ contributed by the random vector $\boldsymbol{V}_S$, can be obtained:

```
In[•]:= ωsx = TransformedDistribution[F1 F2,
    {F1 ≈ ProbabilityDistribution[1/2, {x, -1, 1}], F2 ≈ ProbabilityDistribution[ x / (c Sqrt[c^2 - x^2]), {x, 0, c}]}];
FullSimplify[PDF[ωsx, x], Assumptions → c > 0]
```

Out[•]=
$$\begin{cases} \frac{\cos^{-1}\left(\frac{x}{c}\right)}{2c} & x = 0 \vee (x > 0 \wedge c > x) \\ \frac{2\sin^{-1}\left(\frac{x}{c}\right)+\pi}{4c} & c + x > 0 \wedge x < 0 \end{cases}$$

NOTE: $\omega_{B,X}(x,r)$ in the main text is substituted by ωbx here. Then, the probability density of the norm r of the radius $\boldsymbol{r}$ at which the starting point of the vector $\boldsymbol{V}_B$ is located within the ball can be obtained:

$$\omega\text{bx} = \text{TransformedDistribution}\left[\frac{1}{r}x,\ x \approx \text{ProbabilityDistribution}\left[\begin{cases} \frac{\text{ArcCos}\left[\frac{x}{c}\right]}{2c} & 0 \le x < c \\ \frac{2\,\text{ArcSin}\left[\frac{x}{c}\right]+\pi}{4c} & -c < x < 0 \end{cases}, \{x, -c, c\}\right], \text{Assumptions} \to r > 0 \wedge c > 0\right];$$

$$\text{PDF}[\omega\text{bx}, x]$$

Out[•]=
$$\begin{cases} \frac{r\cos^{-1}\left(\frac{rx}{c}\right)}{2c} & c + rx > 0 \wedge c - rx > 0 \wedge rx \ge 0 \\ \frac{r\left(2\sin^{-1}\left(\frac{rx}{c}\right)+\pi\right)}{4c} & c + rx > 0 \wedge c - rx > 0 \wedge rx < 0 \end{cases}$$

The distribution function of the contribution of V_B to the equivalent coordinate $\Omega_{B,X}$ of Ω_B is calculated as follows (NOTE: This is the result in Mathematica 11.2):

$$\text{CDF}\left[\text{ProbabilityDistribution}\left[\begin{cases} \frac{r\,\text{ArcCos}\left[\frac{rx}{c}\right]}{2c} & 0 \le x < \frac{c}{r} \\ \frac{r\left(2\,\text{ArcSin}\left[\frac{rx}{c}\right]+\pi\right)}{4c} & -\frac{c}{r} < x < 0 \end{cases}, \left\{x, -\frac{c}{r}, \frac{c}{r}\right\}, \text{Assumptions} \to r > 0 \wedge c > 0\right], x\right]$$

$$\begin{cases} \frac{1}{2} & \frac{c}{r} - x > 0 \wedge x = 0 \\ 1 & \frac{c}{r} - x < 0 \wedge x \ge 0 \\ \frac{-\sqrt{c^2-r^2x^2}+rx\cos^{-1}\left(\frac{rx}{c}\right)+2c}{2c} & \left(\frac{c}{r} - x = 0 \wedge x \ge 0\right) \vee \left(\frac{c}{r} - x \ge 0 \wedge x > 0\right) \\ \frac{2\sqrt{c^2-r^2x^2}+2rx\sin^{-1}\left(\frac{rx}{c}\right)+\pi rx}{4c} & x < 0 \wedge \frac{c}{r} - x > 0 \wedge \frac{c}{r} + x > 0 \end{cases}$$

We remove the meaningless parts of the above function and integrate the function in the whole unit ball (NOTE: This is the result in Mathematica 11.2):

$$\text{FullSimplify}\left[\int_0^1 4\pi r^2 \left(\begin{cases} \frac{2\sqrt{c^2-r^2x^2}+2rx\,\text{ArcSin}\left[\frac{rx}{c}\right]+\pi rx}{4c} & -\frac{c}{r} < x < 0 \\ \frac{-\sqrt{c^2-r^2x^2}+rx\,\text{ArcCos}\left[\frac{rx}{c}\right]+2c}{2c} & 0 \le x < \frac{c}{r} \end{cases}\right) dr, \text{Assumptions} \to c > 0\right]$$

$$\begin{cases} -\frac{\pi^2 c^3}{32x^3} & c + x \le 0 \\ \frac{(128-3\pi)\pi c^3}{96x^3} & c < x \\ \frac{\pi\left(3c^2 x\sqrt{(c-x)(c+x)}+3c^4\left(3\sin^{-1}\left(\frac{x}{c}\right)-4\tan^{-1}\left(\frac{x}{\sqrt{c^2-x^2}}\right)\right)+24x^4\sec^{-1}\left(\frac{c}{x}\right)+64cx^3-30x^3\sqrt{(c-x)(c+x)}\right)}{48cx^3} & c \ge x \wedge x \ge 0 \\ \frac{\pi\left(\left(8x^4-3c^4\right)\sin^{-1}\left(\frac{x}{c}\right)+x\sqrt{(c-x)(c+x)}\left(10x^2-c^2\right)+4c^4\tan^{-1}\left(\frac{x}{\sqrt{c^2-x^2}}\right)+4\pi x^4\right)}{16cx^3} & \text{True} \end{cases}$$

We find the first derivative of the above result with respect to x (NOTE: This is the result in Mathematica 11.2):

$$\textbf{FullSimplify}\Big[D\Big[\begin{cases} -\frac{\pi^2 c^3}{32 x^3} & x \le -c \\ \frac{(128-3\pi)\pi c^3}{96 x^3} & x > c \\ \frac{\pi\left(3c^2 x\sqrt{(c-x)(c+x)}+3c^4\left(3\,\text{ArcSin}\left[\frac{x}{c}\right]-4\,\text{ArcTan}\left[\frac{x}{\sqrt{c^2-x^2}}\right]\right)+24x^4\,\text{ArcSec}\left[\frac{c}{x}\right]+64cx^3-30x^3\sqrt{(c-x)(c+x)}\right)}{48cx^3} & 0 < x \le c \\ \frac{\pi\left(\left(8x^4-3c^4\right)\text{ArcSin}\left[\frac{x}{c}\right]+x\sqrt{(c-x)(c+x)}\left(10x^2-c^2\right)+4c^4\,\text{ArcTan}\left[\frac{x}{\sqrt{c^2-x^2}}\right]+4\pi x^4\right)}{16cx^3} & -c < x < 0 \end{cases}, x \Big]\Big]$$

$$\begin{cases} \frac{3\pi^2 c^3}{32x^4} & c + x \le 0 \\ \frac{\pi(3\pi-128)c^3}{32x^4} & c < x \\ \frac{\pi\left(-x\sqrt{(c-x)(c+x)}\left(3c^2+2x^2\right)+3c^4\left(4\tan^{-1}\left(\frac{x}{\sqrt{c^2-x^2}}\right)-3\sin^{-1}\left(\frac{x}{c}\right)\right)+8x^4\sec^{-1}\left(\frac{c}{x}\right)\right)}{16cx^4} & x > 0 \wedge c \ge x \\ \frac{\pi\left(x\sqrt{(c-x)(c+x)}\left(3c^2+2x^2\right)+\left(9c^4+8x^4\right)\sin^{-1}\left(\frac{x}{c}\right)-12c^4\tan^{-1}\left(\frac{x}{\sqrt{c^2-x^2}}\right)+4\pi x^4\right)}{16cx^4} & c + x > 0 \wedge x < 0 \end{cases}$$

We modify the above results to the form of a continuous function and integrate the function in the whole interval (-∞, ∞).

In[•]:=
$$\textbf{Integrate}\Big[\begin{cases} \frac{3\pi^2 c^3}{32x^4} & c + x \le 0 \\ \frac{3\pi^2 c^3}{32x^4} & c < x \\ \frac{\pi\left(-x\sqrt{(c-x)(c+x)}\left(3c^2+2x^2\right)+3c^4\left(4\,\text{ArcTan}\left[\frac{x}{\sqrt{c^2-x^2}}\right]-3\,\text{ArcSin}\left[\frac{x}{c}\right]\right)+8x^4\,\text{ArcSec}\left[\frac{c}{x}\right]\right)}{16cx^4} & x > 0 \wedge c \ge x \\ \frac{\pi\left(\left(9c^4+8x^4\right)\text{ArcSin}\left[\frac{x}{c}\right]+x\sqrt{(c-x)(c+x)}\left(3c^2+2x^2\right)-12c^4\,\text{ArcTan}\left[\frac{x}{\sqrt{c^2-x^2}}\right]+4\pi x^4\right)}{16cx^4} & c + x > 0 \wedge x < 0 \end{cases}, \{x, -\infty, \infty\}, \textbf{Assumptions} \to c > 0 \Big]$$

Out[•]=
$$\frac{4\pi}{3}$$

The above function is normalized according to the integration results (NOTE: This is the result in Mathematica 11.2):

$$\textbf{FullSimplify}\Big[\frac{1}{\frac{4\pi}{3}} \begin{cases} \frac{3\pi^2 c^3}{32x^4} & c + x \le 0 \\ \frac{3\pi^2 c^3}{32x^4} & c < x \\ \frac{\pi\left(-x\sqrt{(c-x)(c+x)}\left(3c^2+2x^2\right)+3c^4\left(4\,\text{ArcTan}\left[\frac{x}{\sqrt{c^2-x^2}}\right]-3\,\text{ArcSin}\left[\frac{x}{c}\right]\right)+8x^4\,\text{ArcSec}\left[\frac{c}{x}\right]\right)}{16cx^4} & x > 0 \wedge c \ge x \\ \frac{\pi\left(\left(9c^4+8x^4\right)\text{ArcSin}\left[\frac{x}{c}\right]+x\sqrt{(c-x)(c+x)}\left(3c^2+2x^2\right)-12c^4\,\text{ArcTan}\left[\frac{x}{\sqrt{c^2-x^2}}\right]+4\pi x^4\right)}{16cx^4} & c + x > 0 \wedge x < 0 \end{cases} \Big]$$

$$\begin{cases} \frac{9\pi c^3}{128x^4} & c < x \vee c + x \le 0 \\ \frac{3\left(-x\sqrt{(c-x)(c+x)}\left(3c^2+2x^2\right)+3c^4\left(4\tan^{-1}\left(\frac{x}{\sqrt{c^2-x^2}}\right)-3\sin^{-1}\left(\frac{x}{c}\right)\right)+8x^4\sec^{-1}\left(\frac{c}{x}\right)\right)}{64cx^4} & x > 0 \wedge c \ge x \\ \frac{3\left(\left(9c^4+8x^4\right)\sin^{-1}\left(\frac{x}{c}\right)+x\sqrt{(c-x)(c+x)}\left(3c^2+2x^2\right)-12c^4\tan^{-1}\left(\frac{x}{\sqrt{c^2-x^2}}\right)+4\pi x^4\right)}{64cx^4} & c + x > 0 \wedge x < 0 \end{cases}$$

In view of $\tan^{-1}\frac{x}{\sqrt{c^2-x^2}} = \sin^{-1}\frac{x}{c}$ and $\sec^{-1}\frac{c}{x} = \cos^{-1}\frac{x}{c}$,

the probability density of the contribution of $\boldsymbol{V}_{\mathrm{B}}$ in the whole unit ball to an equivalent coordinate X of the angular velocity $\boldsymbol{\Omega}_{\mathrm{B}}$ can be obtained by simplifying the above results (Note : $\omega_{\mathrm{B},X}(x)$ in the main text is substituted by ωBx here) (NOTE : This is the result in Mathematica 11.2) :

ωBx = **FullSimplify**[

$$\begin{cases} \frac{9\pi c^3}{128 x^4} & c < x \vee c + x \le 0 \\ \frac{3\left(-x\sqrt{(c-x)(c+x)}\left(3c^2+2x^2\right)+3c^4\left(4\,\mathrm{ArcSin}\left[\frac{x}{c}\right]-3\,\mathrm{ArcSin}\left[\frac{x}{c}\right]\right)+8x^4\,\mathrm{ArcCos}\left[\frac{x}{c}\right]\right)}{64 c x^4} & x > 0 \wedge c \ge x \\ \frac{3\left(\left(9c^4+8x^4\right)\mathrm{ArcSin}\left[\frac{x}{c}\right]+x\sqrt{(c-x)(c+x)}\left(3c^2+2x^2\right)-12c^4\,\mathrm{ArcSin}\left[\frac{x}{c}\right]+4\pi x^4\right)}{64 c x^4} & c + x > 0 \wedge x < 0 \end{cases}, \textbf{Assumptions} \to c > 0 \Big]$$

$$\begin{cases} \frac{9\pi c^3}{128 x^4} & c < x \vee c + x \le 0 \\ \frac{3\left(3c^4\sin^{-1}\left(\frac{x}{c}\right)-x\sqrt{c^2-x^2}\left(3c^2+2x^2\right)+8x^4\cos^{-1}\left(\frac{x}{c}\right)\right)}{64 c x^4} & x > 0 \wedge c \ge x \\ \frac{3\left(\left(8x^4-3c^4\right)\sin^{-1}\left(\frac{x}{c}\right)+x\sqrt{c^2-x^2}\left(3c^2+2x^2\right)+4\pi x^4\right)}{64 c x^4} & c + x > 0 \wedge x < 0 \end{cases}$$

Further more, when the radius of the ball is R, the above situation scales to $\frac{\Omega_{\mathrm{B},X}(x)}{R}$. Accordingly, the probability density of the contribution of the random vector $\boldsymbol{V}$ to the single equivalent coordinate X of angular velocity $\boldsymbol{\Omega}$ is (Note: $\omega_X(x)$ in the main text is substituted by ωx here) (NOTE: This is the result in Mathematica 11.2):

ωx = TransformedDistribution$\Big[\frac{x}{R},$

$$x \approx \textbf{ProbabilityDistribution}\Big[\begin{cases} \frac{9\pi c^3}{128 x^4} & x > c \vee x \le -c \\ \frac{3\left(\left(8x^4-3c^4\right)\mathrm{ArcSin}\left[\frac{x}{c}\right]+x\sqrt{c^2-x^2}\left(3c^2+2x^2\right)+4\pi x^4\right)}{64 c x^4} & -c < x < 0 \\ \frac{3\left(3c^4\,\mathrm{ArcSin}\left[\frac{x}{c}\right]-x\sqrt{c^2-x^2}\left(3c^2+2x^2\right)+8x^4\,\mathrm{ArcCos}\left[\frac{x}{c}\right]\right)}{64 c x^4} & 0 < x \le c \\ \textbf{Indeterminate} & \textbf{True} \end{cases}, \{x, -\infty, \infty\}\Big],$$

$$\textbf{Assumptions} \to R > 0 \wedge c > 0\Big];$$

FullSimplify[PDF[ωx, x]]

$$\begin{cases} \frac{9\pi c^3}{128 R^3 x^4} & c < R x \vee c + R x \le 0 \\ \frac{3\left(R x\sqrt{c^2-R^2x^2}\left(3c^2+2R^2x^2\right)+\left(8R^4x^4-3c^4\right)\sin^{-1}\left(\frac{Rx}{c}\right)+4\pi R^4x^4\right)}{64 c R^3 x^4} & c + R x > 0 \wedge R x < 0 \\ \frac{3\left(-R x\sqrt{c^2-R^2x^2}\left(3c^2+2R^2x^2\right)+3c^4\sin^{-1}\left(\frac{Rx}{c}\right)+8R^4x^4\cos^{-1}\left(\frac{Rx}{c}\right)\right)}{64 c R^3 x^4} & R x > 0 \wedge c \ge R x \\ \text{Indeterminate} & \text{True} \end{cases}$$

The standard deviation of ωx is:

StandardDeviation[ωx]

$$\frac{\sqrt{\frac{2}{3}}\, c}{R}$$

This is the end of the whole proof.

Part 6. Differences Between the Two Solving Methods (Schrödinger Equation and Eq. 40)

This code takes approximately 2 days.

In[•]:=
```
Clear["Global`*"];
usol = DSolveValue[{I ∂ψ(x, t)/∂t == -1/2 ∂²ψ(x, t)/∂x², ψ(x, 0) == e^(-2 x²)}, ψ, {x, t}];
F[x_] := e^(-x); L = 20;
vsol = NDSolveValue[{I ∂M(x, t)/∂t == -1/2 F[M(x, t)] (∂²M(x, t)/∂x² - (∂M(x, t)/∂x)²),
    M(x, 0) == 10^-2 e^(-2 x²), M(-L, t) == M(L, t)}, M, {x, -L, L}, {t, 0, 3}, WorkingPrecision → 40];
s1 = Plot3D[Abs[usol[x, t]] - 10^2 Abs[vsol[x, t]], {t, 0, 1.6}, {x, -8, 8}, PlotPoints → 60,
  MaxRecursion → 3, PlotRange → {{0, 1.6}, {-8, 8}, {-0.002, 0.003}},
  AxesLabel → {Style["t ", 22, FontFamily → "Arial", Black, Italic, Bold],
    Style["x", 22, FontFamily → "Arial", Black, Italic, Bold], ""},
  AxesStyle → Directive[Black, Thickness → 0.002], BoxStyle → Directive[Black, Thickness → 0.002],
  Ticks → {{{0, "0.0"}, {0.5, 0.5, {0.01, 0}, Thickness → 0.003}, {1.0, "1.0", {0.01, 0}, Thickness → 0.003},
      {1.5, 1.5, {0.01, 0}, Thickness → 0.003}}, {{-6, -6, {0.011, 0}, Thickness → 0.003},
      {-3, -3, {0.011, 0}, Thickness → 0.003}, {0, 0, {0.011, 0}, Thickness → 0.003},
      {3, 3, {0.011, 0}, Thickness → 0.003}, {6, 6, {0.011, 0}, Thickness → 0.003}},
    {{-0.002, -0.002, {0.012, 0}, Thickness → 0.003}, {-0.001, -0.001, {0.012, 0}, Thickness → 0.003},
      {0, "0.000", {0.012, 0}, Thickness → 0.003}, {0.001, 0.001, {0.012, 0}, Thickness → 0.003},
      {0.002, "0.002", {0.012, 0}, Thickness → 0.003}, {0.003, "0.003", {0.012, 0}, Thickness → 0.003}}},
  LabelStyle → Directive[Black, FontFamily → "Arial", FontSize → 21], ViewPoint → {1, -2, 2.1}]
FindMaxValue[{(Abs[usol[x, t]] - 10^2 Abs[vsol[x, t]]), x > 0, t > 0}, {x, t}, WorkingPrecision → 34] /
 (Abs[usol[x, t]] /. Last[
    FindMaximum[{Abs[usol[x, t]] - 10^2 Abs[vsol[x, t]], x > 0, t > 0}, {x, t}, WorkingPrecision → 34]])
Export["/Users/gotall/Library/Mobile Documents/com~apple~CloudDocs/SPaper/Figures/S 1.png",
  s1, Background → None, ImageResolution → 300];
```

Out[•]=

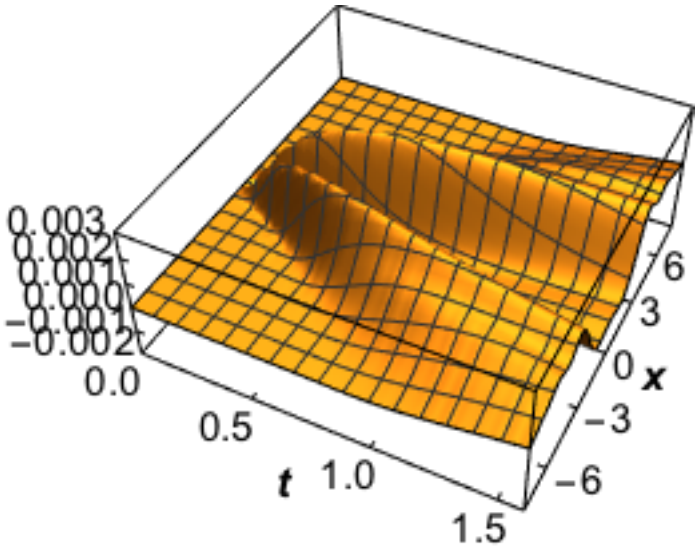

Out[•]= 0.011376093046505820342206378855072 77

Part 7. Another Comparison When the Initial Wave Function Is $1.4\, e^{-2x^2}$

This code takes approximately 3 hours.

```
Clear["Global`*"];
L = 20;
F[x_] := e^(-x);
```

```
usol = NDSolveValue[{I ∂M[x, t]/∂t == -1/2 F[M[x, t]] (∂^2 M[x, t]/∂x^2 - (∂M[x, t]/∂x)^2),
    M[x, 0] == 6/5 E^(-2 x^2), M[-L, t] == M[L, t]}, M, {x, -L, L}, {t, 0, 3}, WorkingPrecision → 22];
vsol = NDSolveValue[{I ∂M[x, t]/∂t == -1/2 F[M[x, t]] (∂^2 M[x, t]/∂x^2 - (∂M[x, t]/∂x)^2), M[x, 0] == 7/5 E^(-2 x^2),
    M[-L, t] == M[L, t]}, M, {x, -L, L}, {t, 0, 3}, WorkingPrecision → 26];
χ[x, t] = {u[x, t], v[x, t]};
σ3 = {{1, 0}, {0, -1}}; σ1 = {{0, 1}, {1, 0}};
xsol = NDSolve[{I D[χ[x, t], t] == -σ1.χ[x, t] - I σ3.D[χ[x, t], x], u[x, 0] == Sqrt[2]/2 E^(-2 x^2), v[x, 0] == Sqrt[2]/2 E^(-2 x^2),
    u[L, t] == u[-L, t], v[L, t] == v[-L, t]}, {u, v}, {x, -L, L}, {t, 0, 3}, WorkingPrecision → 14];
G1 = Plot3D[5/6 Abs[usol[x, t]], {t, 0, 1.6}, {x, -8, 8}, PlotPoints → 60,
    MaxRecursion → 3, PlotRange → {{0, 1.6}, {-8, 8}, {0, 1.23}},
    AxesLabel → {Style["t ", 22, FontFamily → "Arial", Black, Italic, Bold],
      Style["x", 22, FontFamily → "Arial", Black, Italic, Bold], ""},
    AxesStyle → Directive[Black, Thickness → 0.002], BoxStyle → Directive[Black, Thickness → 0.002],
    Ticks → {{{0, "0.0"}, {0.5, 0.5, {0.01, 0}, Thickness → 0.003}, {1.0, "1.0", {0.01, 0}, Thickness → 0.003},
        {1.5, 1.5, {0.01, 0}, Thickness → 0.003}}, {{-6, -6, {0.011, 0}, Thickness → 0.003},
        {-3, -3, {0.011, 0}, Thickness → 0.003}, {0, 0, {0.011, 0}, Thickness → 0.003},
        {3, 3, {0.011, 0}, Thickness → 0.003}, {6, 6, {0.011, 0}, Thickness → 0.003}},
      {{0, "0.0"}, {0.5, 0.5, {0.012, 0}, Thickness → 0.003}, {1, "1.0", {0.012, 0}, Thickness → 0.003}}},
    LabelStyle → Directive[Black, FontFamily → "Arial", FontSize → 21], ViewPoint → {1, -2, 2.1},
    Epilog → Text[Style["a", 22, FontFamily → "Arial", Bold, Black], {-0.09, 0.88}, {-1, 1}]];
G2 = Plot3D[5/7 Abs[vsol[x, t]], {t, 0, 1.6}, {x, -8, 8}, PlotPoints → 60,
    MaxRecursion → 3, PlotRange → {{0, 1.6}, {-8, 8}, {0, 1.23}},
    AxesLabel → {Style["t ", 22, FontFamily → "Arial", Black, Italic, Bold],
      Style["x", 22, FontFamily → "Arial", Black, Italic, Bold], ""},
    AxesStyle → Directive[Black, Thickness → 0.002], BoxStyle → Directive[Black, Thickness → 0.002],
    Ticks → {{{0, "0.0"}, {0.5, 0.5, {0.01, 0}, Thickness → 0.003}, {1.0, "1.0", {0.01, 0}, Thickness → 0.003},
        {1.5, 1.5, {0.01, 0}, Thickness → 0.003}}, {{-6, -6, {0.011, 0}, Thickness → 0.003},
        {-3, -3, {0.011, 0}, Thickness → 0.003}, {0, 0, {0.011, 0}, Thickness → 0.003},
        {3, 3, {0.011, 0}, Thickness → 0.003}, {6, 6, {0.011, 0}, Thickness → 0.003}},
      {{0, "0.0"}, {0.5, 0.5, {0.012, 0}, Thickness → 0.003}, {1, "1.0", {0.012, 0}, Thickness → 0.003}}},
    LabelStyle → Directive[Black, FontFamily → "Arial", FontSize → 21], ViewPoint → {1, -2, 2.1},
    Epilog → Text[Style["b", 22, FontFamily → "Arial", Bold, Black], {-0.09, 0.88}, {-1, 1}]];
G3 = Plot3D[Norm[Evaluate[{u[x, t], v[x, t]} /. xsol]], {t, 0, 1.6}, {x, -8, 8},
    PlotPoints → 60, MaxRecursion → 3, PlotRange → {{0, 1.6}, {-8, 8}, {0, 1.23}},
    AxesLabel → {Style["t ", 22, FontFamily → "Arial", Black, Italic, Bold],
      Style["x", 22, FontFamily → "Arial", Black, Italic, Bold], ""},
    AxesStyle → Directive[Black, Thickness → 0.002], BoxStyle → Directive[Black, Thickness → 0.002],
    Ticks → {{{0, "0.0"}, {0.5, 0.5, {0.01, 0}, Thickness → 0.003}, {1.0, "1.0", {0.01, 0}, Thickness → 0.003},
        {1.5, 1.5, {0.01, 0}, Thickness → 0.003}}, {{-6, -6, {0.011, 0}, Thickness → 0.003},
        {-3, -3, {0.011, 0}, Thickness → 0.003}, {0, 0, {0.011, 0}, Thickness → 0.003},
        {3, 3, {0.011, 0}, Thickness → 0.003}, {6, 6, {0.011, 0}, Thickness → 0.003}},
      {{0, "0.0"}, {0.5, 0.5, {0.012, 0}, Thickness → 0.003}, {1, "1.0", {0.012, 0}, Thickness → 0.003}}},
    LabelStyle → Directive[Black, FontFamily → "Arial", FontSize → 21], ViewPoint → {1, -2, 2.1},
    Epilog → Text[Style["c", 22, FontFamily → "Arial", Bold, Black], {-0.09, 0.88}, {-1, 1}]];
```

```
G4 = Plot[{5/6 Norm[usol[x, 1]], 5/7 Norm[vsol[x, 1]], Norm[Evaluate[{u[x, 1], v[x, 1]} /. xsol]]}, {x, −3.8, 3.8},
    PlotStyle → {{Red, Thickness → 0.005}, {Blue, Thickness → 0.005}, {Black, Thickness → 0.005}},
    PlotRange → {{−3, 3}, {−0.02, 0.9}}, Frame → {{False, False}, {True, False}},
    FrameStyle → Directive[Black, Thickness → 0.002],
    AxesStyle → Directive[GrayLevel[.3], Thickness → 0.0012], FrameTicks →
      {{{−3, −3, {0.01, 0}, Thickness → 0.003}, {−2, −2, {0.01, 0}, Thickness → 0.003}, {−1, −1, {0.01, 0},
          Thickness → 0.003}, {0, 0, {0.01, 0}, Thickness → 0.003}, {1, 1, {0.01, 0}, Thickness → 0.003},
        {2, 2, {0.01, 0}, Thickness → 0.003}, {3, 3, {0.01, 0}, Thickness → 0.003}}, {{0, 0}}},
    FrameLabel → {Style["x", 22, FontFamily → "Arial", Black, Italic, Bold]},
    LabelStyle → Directive[Black, FontFamily → "Arial", FontSize → 22], PlotLegends →
      Placed[LineLegend[{Directive[Red, Thickness[0.0036]], Directive[Blue, Thickness[0.0036]], ,
          Directive[Black, Thickness[0.0036]]}, {"1.2", "1.4", "Dirac"}], {0.873, 0.72}]];
s2 = GraphicsGrid[{{G1, G2}, {G3, G4}}, Alignment → Bottom, ImageSize → 700,
    Epilog → Text[Style["d", 22, FontFamily → "Arial", Black, Bold], Scaled[{0.556, 0.739}]]];
Export["/Users/gotall/Library/Mobile Documents/com~apple~CloudDocs/SPaper/Figures/S 2.png",
  s2, Background → None, ImageResolution → 600];

ImageResize[s2, 1200]
```

NDSolveValue: Warning: scaled local spatial error estimate of 52.4157 at t = 3.000000000000000000000000 in the direction of independent variable x is much greater than the prescribed error tolerance. Grid spacing with 1239 points may be too large to achieve the desired accuracy or precision. A singularity may have formed or a smaller grid spacing can be specified using the MaxStepSize or MinPoints method options.

Out[ ]=

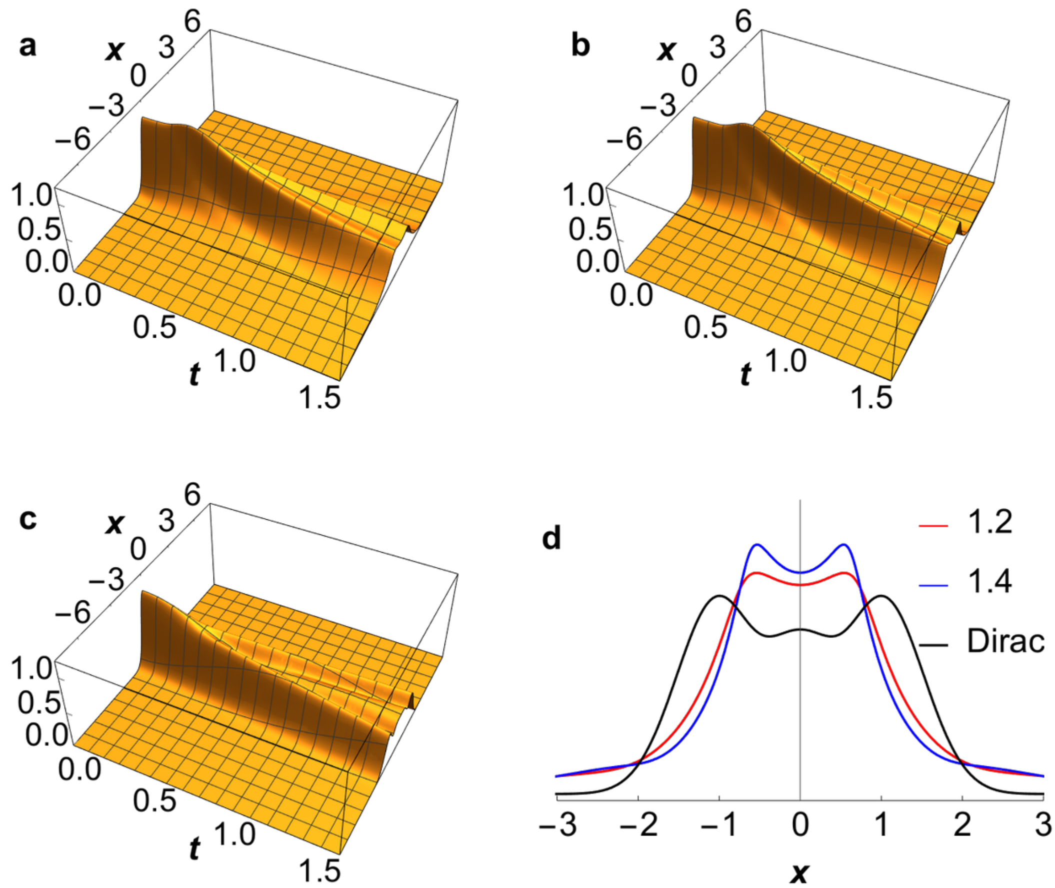

Part 8. Figures Used in This Article

```
## ## ## Figure1 ## ## ## ## ## ## ## ## ## ## ## ## ## ## ## ## ## ## ## ## ## ## ##

Clear["Global`*"];
aa = Graphics[{{RGBColor[178/255, 252/255, 61/255], Rectangle[{0, 0}, {1, 1}]},
    {RGBColor[178/255, 252/255, 61/255, 0.5], Rectangle[{1, 0}, {2, 1}]},
    {RGBColor[250/255, 200/255, 0], Arrowheads[0.06], {Thickness[0.006], Arrow[{{0.7, 0.54}, {1.3, 0.54}}]}},
    {RGBColor[250/255, 200/255, 0], Arrowheads[0.06], {Thickness[0.006], Arrow[{{1.3, 0.46}, {0.7, 0.46}}]}},
    {RGBColor[178/255, 252/255, 61/255, 0.5], Arrowheads[0.06],
     {Thickness[0.006], Arrow[{{0, -1.3}, {1.2, -1.3}}]}},
    {RGBColor[178/255, 252/255, 61/255], Arrowheads[0.06], {Thickness[0.006], Arrow[{{0, -1.3}, {0.8, -0.3}}]}},
    {Orange, {Thickness[0.002], DotDashed, Line[{{1, -0.05}, {1, 1.05}}]}},
    {Orange, {Thickness[0.004], Dashed, Line[{{0.8, -0.3}, {2, -0.3}}]}},
    {Orange, {Thickness[0.004], Dashed, Line[{{1.2, -1.3}, {2, -0.3}}]}},
    {Blue, Arrowheads[0.06], {Thickness[0.006], Arrow[{{1.2, -1.3}, {0.8, -0.3}}]}},
    {Blue, Arrowheads[0.06], {Thickness[0.006], Arrow[{{0, -1.3}, {2, -0.3}}]}},
    {Blue, Arrowheads[0.06], {Thickness[0.006], Arrow[{{0, -1.3}, {1, -0.8}}]}},
    Text[Style["V", 24, FontFamily → "Euclid Math One", White], {0.45, 0.5}],
    Text[Style["A", 17, FontFamily → "Arial", White], {0.513, 0.456}],
    Text[Style["V", 24, FontFamily → "Euclid Math One", White], {1.55, 0.5}],
    Text[Style["B", 17, FontFamily → "Arial", White], {1.616, 0.455}],
    Text[Style["D", 24, FontFamily → "Arial", Orange, Italic], {0.982, 0.63}],
    Text[Style["A", 17, FontFamily → "Arial", Orange], {1.063, 0.59}],
    Text[Style["D", 24, FontFamily → "Arial", Orange, Italic], {0.982, 0.38}],
    Text[Style["B", 17, FontFamily → "Arial", Orange], {1.065, 0.34}],
    Text[Style["Φ", 24, FontFamily → "Arial", Orange], {1.06, 1.08}],
    Text[Style["O", 24, FontFamily → "Arial", Orange], {0, -1.39}],
    Text[Style["B", 24, FontFamily → "Arial", RGBColor[178/255, 252/255, 61/255, 0.5]], {1.2, -1.39}],
    Text[Style["A", 24, FontFamily → "Arial", RGBColor[178/255, 252/255, 61/255]], {0.7, -0.28}],
    Text[Style["C", 24, FontFamily → "Arial", Orange], {2.02, -0.4}],
    Text[Style["M", 24, FontFamily → "Arial", Orange], {0.972, -0.93}],
    Inset[Style["a", Black, Bold, FontFamily → "Arial", FontSize → 24], {0.034, 1.12}],
    Inset[Style["b", Black, Bold, FontFamily → "Arial", FontSize → 24], {0.034, -0.2}]}];
Export["/Users/gotall/Library/Mobile Documents/com~apple~CloudDocs/SPaper/Figures/Figure 1.png",
  aa, Background → None, ImageResolution → 600];

## ## ## Figure1 ## ## ## ## ## ## ## ## ## ## ## ## ## ## ## ## ## ## ## ## ## ## ##

## ## ## Figure2 ## ## ## ## ## ## ## ## ## ## ## ## ## ## ## ## ## ## ## ## ## ## ##
```

```
Clear["Global`*"];
text = Graphics[{Gray, Line[{{1, 0}, {1, 10}}], Line[{{2, 0}, {2, 10}}],
    Line[{{3, 0}, {3, 10}}], Line[{{4, 0}, {4, 10}}], Line[{{5, 0}, {5, 10}}],
    Line[{{6, 0}, {6, 10}}], Line[{{7, 0}, {7, 10}}], Line[{{8, 0}, {8, 10}}], Line[{{9, 0}, {9, 10}}],
    Line[{{0, 1}, {10, 1}}], Line[{{0, 2}, {10, 2}}], Line[{{0, 3}, {10, 3}}], Line[{{0, 4}, {10, 4}}],
    Line[{{0, 5}, {10, 5}}], Line[{{0, 6}, {10, 6}}], Line[{{0, 7}, {10, 7}}], Line[{{0, 8}, {10, 8}}],
    Line[{{0, 9}, {10, 9}}], Orange, Rectangle[{6, 4}, {7, 5}]}, PlotRangePadding → 1/1000];
fg1 = Show[{Plot3D[Sin[x + Cos[y]], {x, -3, 3}, {y, -3, 3}, PlotStyle → Texture[text],
      Mesh → None, Lighting → "Neutral",
      PlotLabels → Placed[Style["dS", 14, FontFamily → "Arial", Orange],
        {0.58, -0.3, 0.21 + Sin[0.88 + Cos[-0.3]]}], BoundaryStyle → None, Boxed → False,
      Axes → None, ViewPoint → {1, -1.9, 1.4}], Graphics3D[{{Thickness[0.007], Black,
        Arrow[{{0, 0, 0}, {-Evaluate[D[Sin[x + Cos[y]], x] /. {x → 0.88, y → -0.3}],
            -Evaluate[D[Sin[x + Cos[y]], y] /. {x → 0.88, y → -0.3}], 1}} +
          {{0.88, -0.3, Sin[0.88 + Cos[-0.3]]}, {0.88, -0.3, Sin[0.88 + Cos[-0.3]]}}]},
       {Text[Style["N", 14, FontFamily → "Arial", Bold, Italic, Black],
         {-Evaluate[D[Sin[x + Cos[y]], x] /. {x → 0.88, y → -0.3}],
          -Evaluate[D[Sin[x + Cos[y]], y] /. {x → 0.88, y → -0.3}], 1} +
         {0.88, -0.3, Sin[0.88 + Cos[-0.3]]} + {0.02, 0.03, 0.23}]},
       {Thickness[0.007], Blue, Arrow[{{0.88, -0.3, Sin[0.88 + Cos[-0.3]]}, {1.88, -0.5, 2}}]},
       {Text[Style["χ", 14, FontFamily → "Arial", Bold, Italic, Blue], {2.01, -0.5, 2.01}]},
       {Text[Style["Σ", 14, FontFamily → "Arial", Italic, Gray], {-2.14, -1.5, 0.7}]}}]}];
fg2 = Rasterize[fg1, "Image", RasterSize → 1500, Background → None];
bb = ImageTake[fg2, {145, 935}, {60, 1455}];
Export[
  "/Users/gotall/Library/Mobile Documents/com~apple~CloudDocs/SPaper/Figures/Figure 2.png", bb];

## ## ## Figure2 ## ## ## ## ## ## ## ## ## ## ## ## ## ## ## ## ## ## ## ## ## ## ## ## ## ## ##

## ## ## Figure3 ## ## ## ## ## ## ## ## ## ## ## ## ## ## ## ## ## ## ## ## ## ## ## ## ## ## ##
```

This code takes approximately 20 minutes.

```
Clear["Global`*"];
Needs["NDSolve`FEM`"];
Ω = ImplicitRegion[16/10000 ≤ x^2 + y^2 + z^2 ≤ 16, {x, y, z}];
nr = 50; nφ = 50; nθ = 50;
coordinates = Flatten[ Table[{r Sin[φ] Cos[θ], r Sin[φ] Sin[θ], r Cos[φ]}, {r, 4/100, 4, (4 - 4/100)/(nr - 1)},
    {φ, 1/10000, π - 1/10000, (π - 2/10000)/(nφ - 1)}, {θ, 0, 2 π, 2 π/(nθ - 1)}], 2];
incidents = Flatten[Table[Block[{p1 = (j - 1)*nr + i, p2 = j*nr + i, p3 = p2 + 1, p4 = p1 + 1, p5, p6, p7, p8},
    {p5, p6, p7, p8} = {p1, p2, p3, p4} + k*nr*nφ;
    {p1, p2, p3, p4} += (k - 1)*nr*nφ;
    {p1, p2, p3, p4, p5, p6, p7, p8}], {i, 1, nr - 1}, {j, 1, nφ - 1}, {k, 1, nθ - 1}], 2];
mesh =
  ToElementMesh["Coordinates" → coordinates, "MeshElements" → {HexahedronElement[incidents]}];
uif = NDSolveValue[{∂^2 M(x, y, z)/∂x^2 + ∂^2 M(x, y, z)/∂y^2 + ∂^2 M(x, y, z)/∂z^2 - (∂M(x, y, z)/∂x)^2 - (∂M(x, y, z)/∂y)^2 -
    (∂M(x, y, z)/∂z)^2 == 0, DirichletCondition[M[x, y, z] == 1 + 2 i, x^2 + y^2 + z^2 == 16/10000]],
```

```
    DirichletCondition[M[x, y, z] == 0, x^2 + y^2 + z^2 == 16]}, M,
   {x, y, z} ∈ mesh, WorkingPrecision → 28];
G1 = SliceDensityPlot3D[(Norm[uif[x, y, z]])^2, "CenterPlanes", {x, -4, 4}, {y, -4, 4},
   {z, -4, 4}, Boxed → False, Axes → None, ColorFunction → (Hue[0.65, #1] &),
   BoundaryStyle → Directive[Thickness[0.001], Gray], PlotRange → {0, 5}, PlotPoints → 100,
   Epilog → Text[Style["a", 23, FontFamily → "Arial", Bold, Black], {0.2478, 0.93}, {0.5, 4}]];
G2 = Plot3D[(Norm[uif[x, y, 0]])^2, {x, -4, 4}, {y, -4, 4},
   PlotRange → {{-4.52, 4.52}, {-4.52, 4.52}, {-1.7, 5}}, MeshStyle →
     {Directive[GrayLevel[0.4], Thickness[0.001]], Directive[GrayLevel[0.4], Thickness[0.001]]},
   BoundaryStyle → Directive[Thickness[0.001], Gray], Boxed → False, Axes → None,
   ColorFunction → (Hue[0.65, #3] &), BoxRatios → Automatic, MeshStyle → Gray,
   ImageSize → {300, 300}, PlotPoints → 30, ViewPoint → {1.2, -2, 0.7},
   Epilog → Text[Style["b", 23, FontFamily → "Arial", Bold, Black], {0.2478, 0.93}, {0.5, 4}]];
G3 = DensityPlot[(Norm[uif[x, y, 0]])^2, {x, -4, 4}, {y, -4, 4}, PlotRange → {{-7.2, 7.2}, {-7.2, 7.2}, {0, 5}},
   ColorFunction → (Hue[0.65, #1] &), Frame → False, PlotPoints → 180,
   Epilog → {Text[Style["c", 23, FontFamily → "Arial", Bold, Black], {-3.73, 4.2}],
     {Directive[Thickness[0.001], Gray], Circle[{0, 0}, 4]}}];
G4 = Plot[(Norm[uif[x, 0, 0]])^2, {x, -4, 4}, PlotRange → {{-7.3, 7.3}, {-0.95, 6}},
   ColorFunction → (Hue[0.65, #2] &), PlotPoints → 180, PlotStyle → {Thickness → 0.0036},
   Frame → False, Axes → None, AspectRatio → Automatic];
G4 = Show[{G4, Plot[(Norm[uif[x, 0, 0]])^2, {x, -4, 4}, PlotRange → {{-7.3, 7.3}, {-0.95, 0.9}},
     PlotStyle → Directive[GrayLevel[0.66], Thickness → 0.0036, Dashed],
     Frame → False, Axes → None, AspectRatio → Automatic]}];
cc = GraphicsGrid[{{G1, G2}, {G3, G4}}, Spacings → {-70, -70}, ImageSize → 700,
   Epilog → Text[Style["d", 22, FontFamily → "Arial", Black, Bold], Scaled[{0.653, 0.38785}]]];
Export["/Users/gotall/Library/Mobile Documents/com~apple~CloudDocs/SPaper/Figures/Figure 3.png",
  cc, Background → None, ImageResolution → 600];
afg =
  Import[
   "/Users/gotall/Library/Mobile Documents/com~apple~CloudDocs/SPaper/Figures/Figure 3.png"];
fg = ImageTake[afg, {550, 5150}, {700, 5120}];
Export[
  "/Users/gotall/Library/Mobile Documents/com~apple~CloudDocs/SPaper/Figures/Figure 3.png", fg];

## ## ## Figure3 ## ## ## ## ## ## ## ## ## ## ## ## ## ## ## ## ## ## ## ## ## ## ## ## ##

## ## ## Figure4 ## ## ## ## ## ## ## ## ## ## ## ## ## ## ## ## ## ## ## ## ## ## ## ## ##
```

This code takes approximately 12 minutes.

```
Clear["Global`*"];
L = 20;
F[x_] := e^-x;
usol = NDSolveValue[{I ∂M(x, t)/∂t == -1/2 F[M(x, t)] (∂^2 M(x, t)/∂x^2 - (∂M(x, t)/∂x)^2),
    M(x, 0) == 10^-13 e^-2 x^2, M(-L, t) == M(L, t)}, M, {x, -L, L}, {t, 0, 3}, WorkingPrecision → 66];
F[x_] := e^-x;
vsol = NDSolveValue[{I ∂M(x, t)/∂t == -1/2 F[M(x, t)] (∂^2 M(x, t)/∂x^2 - (∂M(x, t)/∂x)^2),
    M(x, 0) == e^-2 x^2, M(-L, t) == M(L, t)}, M, {x, -L, L}, {t, 0, 3}, WorkingPrecision → 20];
wsol = NDSolveValue[{I ∂ψ(x, t)/∂t == -1/2 ∂^2 ψ(x, t)/∂x^2, ψ(x, 0) == e^-2 x^2, ψ(-L, t) == ψ(L, t)},
```

```
    ψ, {x, -L, L}, {t, 0, 3}, WorkingPrecision → 18];
χ[x, t] = {u[x, t], v[x, t]};
σ3 = ({{1, 0}, {0, -1}}); σ1 = ({{0, 1}, {1, 0}});
xsol = NDSolve[{i D[χ[x, t], t] == -σ1.χ(x, t) - i σ3.D[χ[x, t], x], u[x, 0] == (Sqrt[2]/2) e^(-2 x^2), v[x, 0] == (Sqrt[2]/2) e^(-2 x^2),
    u[L, t] == u[-L, t], v[L, t] == v[-L, t]}, {u, v}, {x, -L, L}, {t, 0, 3}, WorkingPrecision → 14];
G1 = Plot3D[10^13 Abs[usol[x, t]], {t, 0, 1.6}, {x, -8, 8}, PlotPoints → 60,
  MaxRecursion → 3, PlotRange → {{0, 1.6}, {-8, 8}, {0, 1.05}}, MeshStyle →
    {Directive[GrayLevel[0.4], Thickness[0.006]], Directive[GrayLevel[0.4], Thickness[0.006]]},
  AxesLabel → {Style["t ", 22, FontFamily → "Arial", Black, Italic, Bold],
     Style["x", 22, FontFamily → "Arial", Black, Italic, Bold], ""},
  AxesStyle → Directive[Black, Thickness → 0.002], BoxStyle → Directive[Black, Thickness → 0.002],
  Ticks → {{{0, "0.0"}, {0.5, 0.5, {0.01, 0}, Thickness → 0.003}, {1.0, "1.0", {0.01, 0}, Thickness → 0.003},
      {1.5, 1.5, {0.01, 0}, Thickness → 0.003}}, {{-6, -6, {0.011, 0}, Thickness → 0.003},
      {-3, -3, {0.011, 0}, Thickness → 0.003}, {0, 0, {0.011, 0}, Thickness → 0.003},
      {3, 3, {0.011, 0}, Thickness → 0.003}, {6, 6, {0.011, 0}, Thickness → 0.003}},
    {{0, "0.0"}, {0.5, 0.5, {0.012, 0}, Thickness → 0.003}, {1, "1.0", {0.012, 0}, Thickness → 0.003}}},
  LabelStyle → Directive[Black, FontFamily → "Arial", FontSize → 21], ViewPoint → {1, -2, 2.1},
  Epilog → Text[Style["a", 22, FontFamily → "Arial", Bold, Black], {-0.09, 0.88}, {-1, 1}]];
G2 = Plot3D[Abs[vsol[x, t]], {t, 0, 1.6}, {x, -8, 8}, PlotPoints → 60, MaxRecursion → 3,
  PlotRange → {{0, 1.6}, {-8, 8}, {0, 1.05}}, MeshStyle →
    {Directive[GrayLevel[0.4], Thickness[0.006]], Directive[GrayLevel[0.4], Thickness[0.006]]},
  AxesLabel → {Style["t ", 22, FontFamily → "Arial", Black, Italic, Bold],
     Style["x", 22, FontFamily → "Arial", Black, Italic, Bold], ""},
  AxesStyle → Directive[Black, Thickness → 0.002], BoxStyle → Directive[Black, Thickness → 0.002],
  Ticks → {{{0, "0.0"}, {0.5, 0.5, {0.01, 0}, Thickness → 0.003}, {1.0, "1.0", {0.01, 0}, Thickness → 0.003},
      {1.5, 1.5, {0.01, 0}, Thickness → 0.003}}, {{-6, -6, {0.011, 0}, Thickness → 0.003},
      {-3, -3, {0.011, 0}, Thickness → 0.003}, {0, 0, {0.011, 0}, Thickness → 0.003},
      {3, 3, {0.011, 0}, Thickness → 0.003}, {6, 6, {0.011, 0}, Thickness → 0.003}},
    {{0, "0.0"}, {0.5, 0.5, {0.012, 0}, Thickness → 0.003}, {1, "1.0", {0.012, 0}, Thickness → 0.003}}},
  LabelStyle → Directive[Black, FontFamily → "Arial", FontSize → 21], ViewPoint → {1, -2, 2.1},
  Epilog → Text[Style["b", 22, FontFamily → "Arial", Bold, Black], {-0.09, 0.88}, {-1, 1}]];
G3 = Plot3D[Abs[wsol[x, t]], {t, 0, 1.6}, {x, -8, 8}, PlotPoints → 60, MaxRecursion → 3,
  PlotRange → {{0, 1.6}, {-8, 8}, {0, 1.05}}, MeshStyle →
    {Directive[GrayLevel[0.4], Thickness[0.006]], Directive[GrayLevel[0.4], Thickness[0.006]]},
  AxesLabel → {Style["t ", 22, FontFamily → "Arial", Black, Italic, Bold],
     Style["x", 22, FontFamily → "Arial", Black, Italic, Bold], ""},
  AxesStyle → Directive[Black, Thickness → 0.002], BoxStyle → Directive[Black, Thickness → 0.002],
  Ticks → {{{0, "0.0"}, {0.5, 0.5, {0.01, 0}, Thickness → 0.003}, {1.0, "1.0", {0.01, 0}, Thickness → 0.003},
      {1.5, 1.5, {0.01, 0}, Thickness → 0.003}}, {{-6, -6, {0.011, 0}, Thickness → 0.003},
      {-3, -3, {0.011, 0}, Thickness → 0.003}, {0, 0, {0.011, 0}, Thickness → 0.003},
      {3, 3, {0.011, 0}, Thickness → 0.003}, {6, 6, {0.011, 0}, Thickness → 0.003}},
    {{0, "0.0"}, {0.5, 0.5, {0.012, 0}, Thickness → 0.003}, {1, "1.0", {0.012, 0}, Thickness → 0.003}}},
  LabelStyle → Directive[Black, FontFamily → "Arial", FontSize → 21], ViewPoint → {1, -2, 2.1},
  Epilog → Text[Style["c", 22, FontFamily → "Arial", Bold, Black], {-0.09, 0.88}, {-1, 1}]];
G4 = Plot3D[Norm[Evaluate[{u[x, t], v[x, t]} /. xsol]], {t, 0, 1.6}, {x, -8, 8}, PlotPoints → 60,
  MaxRecursion → 3, PlotRange → {{0, 1.6}, {-8, 8}, {0, 1.05}}, MeshStyle →
    {Directive[GrayLevel[0.4], Thickness[0.006]], Directive[GrayLevel[0.4], Thickness[0.006]]},
  AxesLabel → {Style["t ", 22, FontFamily → "Arial", Black, Italic, Bold],
     Style["x", 22, FontFamily → "Arial", Black, Italic, Bold], ""},
  AxesStyle → Directive[Black, Thickness → 0.002], BoxStyle → Directive[Black, Thickness → 0.002],
  Ticks → {{{0, "0.0"}, {0.5, 0.5, {0.01, 0}, Thickness → 0.003}, {1.0, "1.0", {0.01, 0}, Thickness → 0.003},
      {1.5, 1.5, {0.01, 0}, Thickness → 0.003}}, {{-6, -6, {0.011, 0}, Thickness → 0.003},
      {-3, -3, {0.011, 0}, Thickness → 0.003}, {0, 0, {0.011, 0}, Thickness → 0.003},
      {3, 3, {0.011, 0}, Thickness → 0.003}, {6, 6, {0.011, 0}, Thickness → 0.003}},
```

```
        {{0, "0.0"}, {0.5, 0.5, {0.012, 0}, Thickness → 0.003}, {1, "1.0", {0.012, 0}, Thickness → 0.003}}},
      LabelStyle → Directive[Black, FontFamily → "Arial", FontSize → 21], ViewPoint → {1, −2, 2.1},
      Epilog → Text[Style["d", 22, FontFamily → "Arial", Bold, Black], {−0.09, 0.88}, {−1, 1}]];
dd = GraphicsGrid[{{G1, G2}, {G3, G4}}, ImageSize → 700];
Export["/Users/gotall/Library/Mobile Documents/com~apple~CloudDocs/SPaper/Figures/Figure 4.png",
    dd, Background → None, ImageResolution → 300];
bfg =
    Import[
      "/Users/gotall/Library/Mobile Documents/com~apple~CloudDocs/SPaper/Figures/Figure 4.png"];
fg = ImageTake[bfg, {140, 2917}, {0, 2880}];
Export[
    "/Users/gotall/Library/Mobile Documents/com~apple~CloudDocs/SPaper/Figures/Figure 4.png", fg];

## ## ## Figure4 ## ## ## ## ## ## ## ## ## ## ## ## ## ## ## ## ## ## ## ## ## ## ## ## ## ## ##

## ## ## Figure5 ## ## ## ## ## ## ## ## ## ## ## ## ## ## ## ## ## ## ## ## ## ## ## ## ## ## ##
```

This code takes approximately 11 minutes.

In[•]:=

```
Clear["Global`*"];
L = 20;
F[x_] := e^−x;
usol = NDSolveValue[{i ∂M(x, t)/∂t == −1/2 F[M(x, t)] (∂^2 M(x, t)/∂x^2 − (∂M(x, t)/∂x)^2),
      M(x, 0) == 10^−13 e^−2 x^2, M(−L, t) == M(L, t)}, M, {x, −L, L}, {t, 0, 3}, WorkingPrecision → 66];
F[x_] := e^−x;
vsol = NDSolveValue[{i ∂M(x, t)/∂t == −1/2 F[M(x, t)] (∂^2 M(x, t)/∂x^2 − (∂M(x, t)/∂x)^2),
      M(x, 0) == e^−2 x^2, M(−L, t) == M(L, t)}, M, {x, −L, L}, {t, 0, 3}, WorkingPrecision → 20];
wsol = NDSolveValue[{i ∂ψ(x, t)/∂t == −1/2 ∂^2 ψ(x, t)/∂x^2, ψ(x, 0) == e^−2 x^2, ψ(−L, t) == ψ(L, t)},
    ψ, {x, −L, L}, {t, 0, 3}, WorkingPrecision → 18];
χ[x, t] = {u[x, t], v[x, t]};
σ3 = ({{1, 0}, {0, −1}}); σ1 = ({{0, 1}, {1, 0}});
xsol = NDSolve[{i D[χ[x, t], t] == −σ1.χ(x, t) − i σ3.D[χ[x, t], x], u[x, 0] == √2/2 e^−2 x^2, v[x, 0] == √2/2 e^−2 x^2,
      u[L, t] == u[−L, t], v[L, t] == v[−L, t]}, {u, v}, {x, −L, L}, {t, 0, 3}, WorkingPrecision → 14];
G1 = Plot[e^−2 x^2, {x, −3.8, 3.8}, PlotStyle → {Gray, Thickness → 0.005, Dashed},
      PlotRange → {{−3, 3}, {−0.02, 1.1}}, Frame → {{False, False}, {True, False}},
      FrameStyle → Directive[Black, Thickness → 0.002],
      AxesStyle → Directive[GrayLevel[.3], Thickness → 0.0014], FrameTicks →
        {{{−3, −3, {0.01, 0}, Thickness → 0.003}, {−2, −2, {0.01, 0}, Thickness → 0.003}, {−1, −1, {0.01, 0},
              Thickness → 0.003}, {0, 0, {0.01, 0}, Thickness → 0.003}, {1, 1, {0.01, 0}, Thickness → 0.003},
            {2, 2, {0.01, 0}, Thickness → 0.003}, {3, 3, {0.01, 0}, Thickness → 0.003}}, {{0, 0}}},
      FrameLabel → {Style["x", 22, FontFamily → "Arial", Black, Italic, Bold]},
      LabelStyle → Directive[Black, FontFamily → "Arial", FontSize → 22],
      Epilog → Text[Style["t = 0.0", 22, FontFamily → "Arial", Black, Bold], Scaled[{0.1, 0.96}]]];
datau = Table[{x, 10^13 Norm[usol[x, 0.2]]}, {x, −4, 4}];
fu = Normal[NonlinearModelFit[datau, a Exp[b x^2], {a, b}, x]];
```

```
σu = NumberForm[StandardDeviation[ProbabilityDistribution[(∫_-∞^∞ fu dx)^-1 fu, {x, -∞, ∞}]], {3, 2}];

σv = NumberForm[Sqrt[N[∫_-10^10 N[(∫_-10^10 Norm[vsol[x, 0.2]] dx)^-1] x^2 Norm[vsol[x, 0.2]] dx]], {3, 2}];

dataw = Table[{x, Norm[wsol[x, 0.2]]}, {x, -4, 4}];
fw = Normal[NonlinearModelFit[datau, a Exp[b x^2], {a, b}, x]];

σw = NumberForm[StandardDeviation[ProbabilityDistribution[(∫_-∞^∞ fw dx)^-1 fw, {x, -∞, ∞}]], {3, 2}];

σx = NumberForm[Sqrt[N[∫_-10^10 N[(∫_-10^10 Norm[Evaluate[{u[x, 0.2], v[x, 0.2]} /. xsol]] dx)^-1]
      x^2 Norm[Evaluate[{u[x, 0.2], v[x, 0.2]} /. xsol]] dx]], {3, 2}];

G2 = Plot[{e^-2 x^2, Callout[10^13 Norm[usol[x, 0.2]], StringForm["σ = ``", σu], {0.7, 0.64}, {-0.21, 0.83},
      CalloutStyle → {Red, None}, LabelStyle → {FontFamily → "Arial", FontSize → 22, Red},
      Background → None], Callout[Norm[vsol[x, 0.2]], StringForm["σ = ``", σv],
      {0.7281, 1.03}, {0.11, 1.01}, CalloutStyle → {Blue, None},
      LabelStyle → {FontFamily → "Arial", FontSize → 22, Blue}, Background → None],
    Callout[Norm[wsol[x, 0.2]], StringForm["σ = ``", σw], {0.7, 0.9}, {0.23, 0.84},
      CalloutStyle → {Orange, None}, LabelStyle → {FontFamily → "Arial", FontSize → 22, Orange},
      Background → None], Callout[Norm[Evaluate[{u[x, 0.2], v[x, 0.2]} /. xsol]],
      StringForm["σ = ``", σx], {0.7, 0.77}, {0.42, 0.74}, CalloutStyle → {Green, None},
      LabelStyle → {FontFamily → "Arial", FontSize → 22, Green}, Background → None]}, {x, -3.8, 3.8},
  PlotStyle → {{Gray, Thickness → 0.005, Dashed}, {Red, Thickness → 0.005}, {Blue, Thickness → 0.005},
      {Orange, Thickness → 0.005}, {Green, Thickness → 0.005}}, PlotRange → {{-3, 3}, {-0.02, 1.1}},
  FrameLabel → {Style["x", 22, FontFamily → "Arial", Black, Italic, Bold]},
  Frame → {{False, False}, {True, False}}, FrameStyle → Directive[Black, Thickness → 0.002],
  AxesStyle → Directive[GrayLevel[.3], Thickness → 0.0012], FrameTicks →
    {{{-3, -3, {0.01, 0}, Thickness → 0.003}, {-2, -2, {0.01, 0}, Thickness → 0.003}, {-1, -1, {0.01, 0},
        Thickness → 0.003}, {0, 0, {0.01, 0}, Thickness → 0.003}, {1, 1, {0.01, 0}, Thickness → 0.003},
      {2, 2, {0.01, 0}, Thickness → 0.003}, {3, 3, {0.01, 0}, Thickness → 0.003}}, {{0, 0}}},
  Epilog → Text[Style["t = 0.2", 22, FontFamily → "Arial", Black, Bold], Scaled[{0.1, 0.96}]]];
G2 = Show[G2, LabelStyle → {FontFamily → "Arial", 22, GrayLevel[0]}];
datau = Table[{x, 10^13 Norm[usol[x, 0.4]]}, {x, -4, 4}];
fu = Normal[NonlinearModelFit[datau, a Exp[b x^2], {a, b}, x]];

σu = NumberForm[StandardDeviation[ProbabilityDistribution[(∫_-∞^∞ fu dx)^-1 fu, {x, -∞, ∞}]], {3, 2}];

σv = NumberForm[Sqrt[N[∫_-10^10 N[(∫_-10^10 Norm[vsol[x, 0.4]] dx)^-1] x^2 Norm[vsol[x, 0.4]] dx]], {3, 2}];

dataw = Table[{x, Norm[wsol[x, 0.4]]}, {x, -4, 4}];
fw = Normal[NonlinearModelFit[datau, a Exp[b x^2], {a, b}, x]];

σw = NumberForm[StandardDeviation[ProbabilityDistribution[(∫_-∞^∞ fw dx)^-1 fw, {x, -∞, ∞}]], {3, 2}];

dataw = Table[{x, Norm[wsol[x, 0.4]]}, {x, -4, 4}];
fw = Normal[NonlinearModelFit[datau, a Exp[b x^2], {a, b}, x]];

σw = NumberForm[StandardDeviation[ProbabilityDistribution[(∫_-∞^∞ fw dx)^-1 fw, {x, -∞, ∞}]], {3, 2}];

σx = NumberForm[Sqrt[N[∫_-10^10 N[(∫_-10^10 Norm[Evaluate[{u[x, 0.4], v[x, 0.4]} /. xsol]] dx)^-1]
```

```
        x^2 Norm[Evaluate[{u[x, 0.4], v[x, 0.4]} /. xsol]] dx], {3, 2}];

G3 = Plot[{e^(-2 x^2), Callout[10^13 Norm[usol[x, 0.4]], StringForm["σ = ``", σu], {0.8, 0.54}, {-0.22, 0.7},
      CalloutStyle → {Red, None}, LabelStyle → {FontFamily → "Arial", FontSize → 22, Red},
      Background → None], Callout[Norm[vsol[x, 0.4]], StringForm["σ = ``", σv],
      {0.8, 0.93}, {0.157, 0.93}, CalloutStyle → {Blue, None},
      LabelStyle → {FontFamily → "Arial", FontSize → 22, Blue}, Background → None],
     Callout[Norm[wsol[x, 0.4]], StringForm["σ = ``", σw], {0.8, 0.67}, {0.23, 0.713},
      CalloutStyle → {Orange, None}, LabelStyle → {FontFamily → "Arial", FontSize → 22, Orange},
      Background → None], Callout[Norm[Evaluate[{u[x, 0.4], v[x, 0.4]} /. xsol]],
      StringForm["σ = ``", σx], {0.8, 0.8}, {0.14, 0.756}, CalloutStyle → {Green, None},
      LabelStyle → {FontFamily → "Arial", FontSize → 22, Green}, Background → None]},
    {x, -3.8, 3.8}, PlotStyle → {{Gray, Thickness → 0.005, Dashed}, {Red, Thickness → 0.005},
      {Blue, Thickness → 0.005}, {Orange, Thickness → 0.005}, {Green, Thickness → 0.005}},
    PlotRange → {{-3, 3}, {-0.02, 1.1}}, Frame → {{False, False}, {True, False}},
    FrameStyle → Directive[Black, Thickness → 0.002],
    AxesStyle → Directive[GrayLevel[.3], Thickness → 0.0014], FrameTicks →
     {{{-3, -3, {0.01, 0}, Thickness → 0.003}, {-2, -2, {0.01, 0}, Thickness → 0.003}, {-1, -1, {0.01, 0},
        Thickness → 0.003}, {0, 0, {0.01, 0}, Thickness → 0.003}, {1, 1, {0.01, 0}, Thickness → 0.003},
       {2, 2, {0.01, 0}, Thickness → 0.003}, {3, 3, {0.01, 0}, Thickness → 0.003}}, {{0, 0}}},
    FrameLabel → {Style["x", 22, FontFamily → "Arial", Black, Italic, Bold]},
    Epilog → Text[Style["t = 0.4", 22, FontFamily → "Arial", Black, Bold], Scaled[{0.1, 0.96}]]];
G3 = Show[G3, LabelStyle → {FontFamily → "Arial", 22, GrayLevel[0]}];
datau = Table[{x, 10^13 Norm[usol[x, 0.6]]}, {x, -4, 4}];
fu = Normal[NonlinearModelFit[datau, a Exp[b x^2], {a, b}, x]];
σu = NumberForm[StandardDeviation[ProbabilityDistribution[(∫_-∞^∞ fu dx)^-1 fu, {x, -∞, ∞}]], {3, 2}];
σv = NumberForm[Sqrt[N[∫_-10^10 N[(∫_-10^10 Norm[vsol[x, 0.6]] dx)^-1] x^2 Norm[vsol[x, 0.6]] dx]], {3, 2}];
dataw = Table[{x, Norm[wsol[x, 0.6]]}, {x, -4, 4}];
fw = Normal[NonlinearModelFit[datau, a Exp[b x^2], {a, b}, x]];
σw = NumberForm[StandardDeviation[ProbabilityDistribution[(∫_-∞^∞ fw dx)^-1 fw, {x, -∞, ∞}]], {3, 2}];
dataw = Table[{x, Norm[wsol[x, 0.6]]}, {x, -4, 4}];
fw = Normal[NonlinearModelFit[datau, a Exp[b x^2], {a, b}, x]];
σw = NumberForm[StandardDeviation[ProbabilityDistribution[(∫_-∞^∞ fw dx)^-1 fw, {x, -∞, ∞}]], {3, 2}];
σx = NumberForm[Sqrt[N[∫_-10^10 N[(∫_-10^10 Norm[Evaluate[{u[x, 0.6], v[x, 0.6]} /. xsol]] dx)^-1]
        x^2 Norm[Evaluate[{u[x, 0.6], v[x, 0.6]} /. xsol]] dx], {3, 2}];
G4 = Plot[{e^(-2 x^2), Callout[10^13 Norm[usol[x, 0.6]], StringForm["σ = ``", σu], {1.1, 0.49}, {0.79, 0.52},
      CalloutStyle → {Red, None}, LabelStyle → {FontFamily → "Arial", FontSize → 22, Red},
      Background → None], Callout[Norm[vsol[x, 0.6]], StringForm["σ = ``", σv],
      {1.1, 0.88}, {0.157, 0.815}, CalloutStyle → {Blue, None},
      LabelStyle → {FontFamily → "Arial", FontSize → 22, Blue}, Background → None],
     Callout[Norm[wsol[x, 0.6]], StringForm["σ = ``", σw], {1.1, 0.62}, {0.79, 0.52},
      CalloutStyle → {Orange, None}, LabelStyle → {FontFamily → "Arial", FontSize → 22, Orange},
      Background → None], Callout[Norm[Evaluate[{u[x, 0.6], v[x, 0.6]} /. xsol]],
      StringForm["σ = ``", σx], {1.1, 0.75}, {0.64, 0.69}, CalloutStyle → {Green, None},
      LabelStyle → {FontFamily → "Arial", FontSize → 22, Green}, Background → None]},
```

```
    {x, -3.8, 3.8}, PlotStyle → {{Gray, Thickness → 0.005, Dashed}, {Red, Thickness → 0.005},
      {Blue, Thickness → 0.005}, {Orange, Thickness → 0.005}, {Green, Thickness → 0.005}},
    PlotRange → {{-3, 3}, {-0.02, 1.1}}, Frame → {{False, False}, {True, False}},
    FrameStyle → Directive[Black, Thickness → 0.002],
    AxesStyle → Directive[GrayLevel[.3], Thickness → 0.0012], FrameTicks →
     {{{-3, -3, {0.01, 0}, Thickness → 0.003}, {-2, -2, {0.01, 0}, Thickness → 0.003}, {-1, -1, {0.01, 0},
        Thickness → 0.003}, {0, 0, {0.01, 0}, Thickness → 0.003}, {1, 1, {0.01, 0}, Thickness → 0.003},
       {2, 2, {0.01, 0}, Thickness → 0.003}, {3, 3, {0.01, 0}, Thickness → 0.003}}, {{0, 0}}},
    FrameLabel → {Style["x", 22, FontFamily → "Arial", Black, Italic, Bold]},
    Epilog → Text[Style["t = 0.6", 22, FontFamily → "Arial", Black, Bold], Scaled[{0.1, 0.96}]]];
G4 = Show[G4, LabelStyle → {FontFamily → "Arial", 22, GrayLevel[0]}];
ee = GraphicsGrid[{{G1, G2}, {G3, G4}}, ImageSize → 800, Spacings → {Scaled[-0.2], Scaled[0.16]},
    Epilog → Inset[LineLegend[{Directive[Red, Thickness[0.004]], Directive[Blue, Thickness[0.004]],
       Directive[Orange, Thickness[0.004]], Directive[Green, Thickness[0.004]]},
      {Style["Eq. 40^1", FontFamily → "Arial", FontSize → 22], Style["Eq. 40^2", FontFamily → "Arial",
        FontSize → 22], Style["Schrödinger", FontFamily → "Arial", FontSize → 22],
       Style["Dirac", FontFamily → "Arial", FontSize → 22]}, LegendFunction →
       (Framed[#, RoundingRadius → 5, FrameStyle → GrayLevel[.3]] &)], Scaled[{0.5, 1.081}]]];
Export["/Users/gotall/Library/Mobile Documents/com~apple~CloudDocs/SPaper/Figures/Figure 5.png",
  ee, Background → None, ImageResolution → 300];
cfg =
  Import[
   "/Users/gotall/Library/Mobile Documents/com~apple~CloudDocs/SPaper/Figures/Figure 5.png"];
fg = ImageTake[cfg, {0, 2325}, {130, 3200}];
Export[
  "/Users/gotall/Library/Mobile Documents/com~apple~CloudDocs/SPaper/Figures/Figure 5.png", fg];

## ## ## Figure5 ## ## ## ## ## ## ## ## ## ## ## ## ## ## ## ## ## ## ## ## ## ## ## ## ## ## ##

## ## ## Figure6 ## ## ## ## ## ## ## ## ## ## ## ## ## ## ## ## ## ## ## ## ## ## ## ## ## ## ##
```

This code takes approximately 7 hours.

```
Clear["Global`*"];
L = 20;
F[x_] := e^-x;
usol = NDSolveValue[{I ∂M(x, t)/∂t == -1/2 F[M(x, t)] (∂^2 M(x, t)/∂x^2 - (∂M(x, t)/∂x)^2),
    M(x, 0) == 10^-13 e^-2 x^2, M(-L, t) == M(L, t)}, M, {x, -L, L}, {t, 0, 3}, WorkingPrecision → 66];
vsol = NDSolveValue[{I ∂M(x, t)/∂t == -1/2 F[M(x, t)] (∂^2 M(x, t)/∂x^2 - (∂M(x, t)/∂x)^2), M(x, 0) == e^-2 x^2,
    M(-L, t) == M(L, t)}, M, {x, -L, L}, {t, 0, 3}, WorkingPrecision → 20];
wsol = NDSolveValue[{I ∂M(x, t)/∂t == -1/2 F[M(x, t)] (∂^2 M(x, t)/∂x^2 - (∂M(x, t)/∂x)^2),
    M(x, 0) == 6/5 e^-2 x^2, M(-L, t) == M(L, t)}, M, {x, -L, L}, {t, 0, 3}, WorkingPrecision → 22];
xsol = NDSolveValue[{I ∂M(x, t)/∂t == -1/2 F[M(x, t)] (∂^2 M(x, t)/∂x^2 - (∂M(x, t)/∂x)^2), M(x, 0) == 7/5 e^-2 x^2,
    M(-L, t) == M(L, t)}, M, {x, -L, L}, {t, 0, 3}, WorkingPrecision → 26];
G1 = Plot[{10^13 Norm[usol[0, t]], Norm[vsol[0, t]], FindMaxValue[Norm[vsol[x, t]], {x, 0, 3}],
```

```
        5/6 Norm[wsol[0, t]], FindMaxValue[5/6 Norm[wsol[x, t]], {x, 0, 3}],
        5/7 Norm[xsol[0, t]], FindMaxValue[5/7 Norm[xsol[x, t]], {x, 0, 3}]},
      {t, 0, 3}, PlotStyle → {{Orange, Thickness → 0.005}, {Green, Thickness → 0.005},
        {Green, Thickness → 0.005, Dashed}, {Blue, Thickness → 0.005},
        {Blue, Thickness → 0.005, Dashed}, {Red, Thickness → 0.005}, {Red, Thickness → 0.005, Dashed}},
      PlotRange → {{0, 3}, {0, 1.23}}, Frame → {{True, False}, {True, False}},
      FrameStyle → Directive[Black, Thickness → 0.002], FrameTicks →
        {{{0, "0.0"}, {0.5, 0.5, {0.01, 0}, Thickness → 0.003}, {1.0, "1.0", {0.01, 0}, Thickness → 0.003},
          {1.5, 1.5, {0.01, 0}, Thickness → 0.003}, {2.0, "2.0", {0.01, 0}, Thickness → 0.003},
          {2.5, "2.5", {0.01, 0}, Thickness → 0.003}, {3.0, "3.0", {0.01, 0}, Thickness → 0.003}},
         {{0, "0.0"}, {0.2, 0.2, {0.012, 0}, Thickness → 0.003}, {0.4, "0.4", {0.012, 0}, Thickness → 0.003},
          {0.6, "0.6", {0.012, 0}, Thickness → 0.003}, {0.8, "0.8", {0.012, 0}, Thickness → 0.003},
          {1.0, "1.0", {0.012, 0}, Thickness → 0.003}, {1.2, "1.2", {0.012, 0}, Thickness → 0.003}}},
      FrameLabel → {Style["t", 22, FontFamily → "Arial", Black, Italic, Bold]},
      LabelStyle → Directive[Black, FontFamily → "Arial", FontSize → 22]];
xv = NArgMax[Norm[vsol[0, t]], {t, 0.1, 0.5}];
xw = NArgMax[Norm[wsol[0, t]], {t, 0.1, 0.5}];
xx = NArgMax[Norm[xsol[0, t]], {t, 0.1, 0.5}];
G2 = Plot[{10^13 Norm[usol[x, 0]], Norm[vsol[x, xv]], 5/6 Norm[wsol[x, xw]], 5/7 Norm[xsol[x, xx]]},
      {x, −3, 3}, PlotStyle → {{Orange, Thickness → 0.005}, {Green, Thickness → 0.005},
        {Blue, Thickness → 0.005}, {Red, Thickness → 0.005}}, PlotRange → {{−3, 3}, {−0.02, 1.23}},
      Frame → {{False, False}, {True, False}}, FrameStyle → Directive[Black, Thickness → 0.002],
      AxesStyle → Directive[GrayLevel[.3], Thickness → 0.0012], FrameTicks →
        {{{−3, −3, {0.01, 0}, Thickness → 0.003}, {−2, −2, {0.01, 0}, Thickness → 0.003}, {−1, −1, {0.01, 0},
            Thickness → 0.003}, {0, 0, {0.01, 0}, Thickness → 0.003}, {1, 1, {0.01, 0}, Thickness → 0.003},
          {2, 2, {0.01, 0}, Thickness → 0.003}, {3, 3, {0.01, 0}, Thickness → 0.003}}, {{0, 0}}},
      FrameLabel → {Style["x", 22, FontFamily → "Arial", Black, Italic, Bold]},
      LabelStyle → Directive[Black, FontFamily → "Arial", FontSize → 22]];
ff = Labeled[GraphicsRow[{G1, G2}, ImageSize → 800, Spacings → Scaled[−0.2],
      Epilog → Inset[LineLegend[{Directive[Orange, Thickness[0.004]], Directive[Green, Thickness[0.004]],
          Directive[Blue, Thickness[0.004]], Directive[Red, Thickness[0.004]]},
        {Style["10^−13 ", FontFamily → "Arial", FontSize → 22],
          Style["1.0 ", FontFamily → "Arial", FontSize → 22], Style["1.2 ", FontFamily → "Arial",
            FontSize → 22], Style["1.4", FontFamily → "Arial", FontSize → 22]},
        LegendFunction → (Framed[#, RoundingRadius → 5, FrameStyle → GrayLevel[.3]] &),
        LegendLayout −> "Row"], Scaled[{0.5, 0.8}]]],
    Text[Style["    a                                    b", 22, FontFamily → "Arial", Bold, Black]],
    {{Top, Left}},
    Spacings → {0, −0.3}]
Export["/Users/gotall/Library/Mobile Documents/com~apple~CloudDocs/SPaper/Figures/Figure 6.png",
    ff, Background → None, ImageResolution → 300];
dfg =
    Import[
      "/Users/gotall/Library/Mobile Documents/com~apple~CloudDocs/SPaper/Figures/Figure 6.png"];
fg = ImageTake[dfg, {0, 1250}, {90, 3200}];
Export[
    "/Users/gotall/Library/Mobile Documents/com~apple~CloudDocs/SPaper/Figures/Figure 6.png", fg];
```

NDSolveValue: Warning: scaled local spatial error estimate of 52.4157 at t = 3.000000000000000000000000 in the direction of independent variable x is much greater than the prescribed error tolerance. Grid spacing with 1239 points may be too large to achieve the desired accuracy or precision. A singularity may have formed or a smaller grid spacing can be specified using the MaxStepSize or MinPoints method options.

Figure6

Figure7

In[∘]:= Clear["Global`*"];

$\mathcal{R}_1 = \text{Sphere}[\{0, 0, 0\}, 1];$

$\mathcal{R}\text{S1} = \text{Point}[\{0, 0, 0\}];$

$$\mathcal{R}_2 = \text{Sphere}\left[\left\{\frac{1}{2}, -\frac{\sqrt{3}}{4}, \frac{3}{4}\right\}, 1\right];$$

$$A = \text{Line}\left[\left\{\left\{\frac{1}{2}, \frac{\sqrt{3}}{4}, 0\right\}, \left\{\frac{1}{2}, \frac{\sqrt{3}}{4}, 1\right\}\right\}\right];$$

$\text{pts1} = \text{Solve}[\{x, y, z\} \in \mathcal{R}_1 \;\&\&\; \{x, y, z\} \in A, \{x, y, z\}];$

$$\mathcal{R}_3 = \text{Arrow}\left[\left\{\{0, 0, 0\}, \left\{\frac{1}{2}, -\frac{\sqrt{3}}{4}, z\right\} /.\ \text{Association}[\text{pts1}]\right\}\right];$$

$$\{u, v, w\} = \text{Normalize}\left[\{0, 0, 1\} \times \left\{\frac{1}{2}, -\frac{\sqrt{3}}{4}, z\right\} /.\ \text{Association}[\text{pts1}]\right];$$

$$\theta = \text{VectorAngle}\left[\left\{\frac{1}{2}, -\frac{\sqrt{3}}{4}, z\right\} /.\ \text{Association}[\text{pts1}], \{0, 0, 1\}\right];$$

$$M = \begin{pmatrix} u^2 + (1 - u^2)\cos(\theta) & u\,v\,(1 - \cos(\theta)) - w\sin(\theta) & u\,w\,(1 - \cos(\theta)) + v\sin(\theta) & 0 \\ u\,v\,(1 - \cos(\theta)) + w\sin(\theta) & v^2 + (1 - v^2)\cos(\theta) & v\,w\,(1 - \cos(\theta)) - u\sin(\theta) & 0 \\ u\,w\,(1 - \cos(\theta)) - v\sin(\theta) & v\,w\,(1 - \cos(\theta)) + u\sin(\theta) & w^2 + (1 - w^2)\cos(\theta) & 0 \\ 0 & 0 & 0 & 1 \end{pmatrix};$$

$\mathcal{R}_4 = \text{ParametricPlot3D}[\text{Take}[M.\{r\,\text{Cos}[t], r\,\text{Sin}[t], 1, 1\}, 3],$
$\quad \{r, 0, 1\}, \{t, 0, 2\,\text{Pi}\}, \text{PlotStyle} \to \{\text{Orange}, \text{Opacity}[0.4]\}, \text{Mesh} \to \text{None}];$

$$\mathcal{R}_5 = \text{Arrow}\left[\left\{\left\{\frac{1}{2}, -\frac{\sqrt{3}}{4}, z\right\} /.\ \text{Association}[\text{pts1}], \text{Take}\left[M.\left\{-\frac{1}{2}, \frac{1}{4}, 1, 1\right\}, 3\right]\right\}\right];$$

$$\mathcal{R}\text{S2} = \text{Point}\left[\left\{\frac{1}{2}, -\frac{\sqrt{3}}{4}, z\right\} /.\ \text{Association}[\text{pts1}]\right];$$

$$A = \text{Line}\left[\left\{\text{Take}\left[M.\left\{-\frac{1}{2}, \frac{1}{4}, 1, 1\right\}, 3\right], \text{Take}\left[M.\left\{-\frac{1}{2}, \frac{1}{4}, 2, 1\right\}, 3\right]\right\}\right];$$

$\text{pts2} = \text{Solve}[\{x, y, z\} \in \mathcal{R}_2 \;\&\&\; \{x, y, z\} \in A, \{x, y, z\}];$

$$\mathcal{R}_6 = \text{Line}\left[\left\{\text{Take}\left[M.\left\{-\frac{1}{2}, \frac{1}{4}, 1, 1\right\}, 3\right], \{x, y, z\} /.\ \text{Association}[\text{pts2}]\right\}\right];$$

$$\mathcal{R}_7 = \text{Arrow}\left[\left\{\left\{\frac{1}{2}, -\frac{\sqrt{3}}{4}, z\right\} /.\ \text{Association}[\text{pts1}], \{x, y, z\} /.\ \text{Association}[\text{pts2}]\right\}\right];$$

$\mathcal{R}_8 = \text{Point}[\{x, y, z\} /.\ \text{Association}[\text{pts2}]];$

$$\mathcal{R}_9 = \text{Line}\left[\left\{\text{Take}\left[M.\left\{-\frac{1}{2}, \frac{1}{4}, \frac{20 + \sqrt{5}}{20}, 1\right\}, 3\right], \text{Take}\left[M.\left\{-\frac{1}{2} + \frac{1}{10}, \frac{1}{4} - \frac{1}{20}, \frac{20 + \sqrt{5}}{20}, 1\right\}, 3\right]\right\}\right];$$

$$\mathcal{R}_{10} = \text{Line}\left[\left\{\text{Take}\left[M.\left\{-\frac{1}{2} + \frac{1}{10}, \frac{1}{4} - \frac{1}{20}, 1, 1\right\}, 3\right], \text{Take}\left[M.\left\{-\frac{1}{2} + \frac{1}{10}, \frac{1}{4} - \frac{1}{20}, \frac{20 + \sqrt{5}}{20}, 1\right\}, 3\right]\right\}\right];$$

```
gg = Show[{Graphics3D[{{Blue, Specularity[White, 30], Opacity[0.3], ℛ1},
    {PointSize[Large], Blue, ℛS1}, {Orange, Specularity[White, 20], Opacity[0.3], ℛ2},
    {PointSize[Large], Blue, ℛS2}, {Blue, Thickness[0.0085], ℛ3}, {Thickness[0.0085], Orange, ℛ5},
    {Thickness[0.005], Dashed, Orange, ℛ6}, {Thickness[0.0085], Orange, ℛ7},
    {PointSize[Large], Orange, ℛ8}, {Thickness[0.0085], Orange, ℛ9},
    {Thickness[0.0085], Orange, ℛ10}, {Text[Style["S", 24, FontFamily → "Arial", Blue], {0.14, 0, 0}]},
    {Text[Style["r", 24, FontFamily → "Arial", Bold, Italic, Blue], Take[M.{0.11, 0, 1/2, 1}, 3]]},
    {Text[Style["S'", 24, FontFamily → "Arial", Orange], Take[M.{0.14, 0, 1, 1}, 3]]},
    {Text[Style["D'", 24, FontFamily → "Arial", Orange], Take[M.{1/2, 0.22, 1, 1}, 3]]},
    {Text[Style["v",  24, FontFamily → "Arial", Bold, Italic, Orange],
      Take[M.{-1/4 + 0.12, 0, 1 + Sqrt[3]/4, 1}, 3]]}, {Text[
      Style["S",  13, FontFamily → "Arial", Orange], Take[M.{-1/4 + 0.196, 0, 0.98 + Sqrt[3]/4, 1}, 3]]},
    {Text[Style["ω'", 24, FontFamily → "Arial", Bold, Orange], Take[M.{-1/4, 0, 0.928, 1}, 3]]}}],
   ℛ4}, Lighting → Automatic, Boxed → False, ViewPoint → {0, -∞, 0}]
Export["/Users/gotall/Library/Mobile Documents/com~apple~CloudDocs/SPaper/Figures/Figure 7.png",
  gg, Background → None, ImageResolution → 600];
```

Figure7

Figure8

In[•]:=
```
Clear["Global`*"];
R = 3;
c = 1;
```

$$\text{hh} = \text{Plot}\left[\begin{cases} \frac{9\pi c^3}{128 R^3 x^4} & x > \frac{c}{R} \vee x \le -\frac{c}{R} \\ \frac{3\left(\left(8R^4x^4 - 3c^4\right)\sin^{-1}\left(\frac{Rx}{c}\right) + Rx\sqrt{(c-Rx)(c+Rx)}\left(3c^2+2R^2x^2\right) + 4\pi R^4 x^4\right)}{64 c R^3 x^4} & -\frac{c}{R} < x < 0 \\ \frac{9c^4\sin^{-1}\left(\frac{Rx}{c}\right) - 3Rx\sqrt{(c-Rx)(c+Rx)}\left(3c^2+2R^2x^2\right) + 24R^4x^4\cos^{-1}\left(\frac{Rx}{c}\right)}{64 c R^3 x^4} & 0 < x \le \frac{c}{R} \end{cases},\right.$$

```
{x, -0.8 c, 0.8 c}, PlotStyle → {Blue, Thickness → 0.0032}, PlotRange → {{-0.8 c, 0.8 c}, {0, 2/c}},
Frame → {{True, False}, {True, False}}, FrameStyle → Directive[Black, Thickness → 0.0017],
AxesStyle → Directive[GrayLevel[.3], Thickness → 0.001],
FrameTicks → {{{-0.7, "", {0.008, 0}, Thickness → 0.001}, {-0.6, "", {0.008, 0}, Thickness → 0.001},
    {-0.5, -0.5, {0.012, 0}, Thickness → 0.001}, {-0.4, "", {0.01, 0}, Thickness → 0.001},
    {-0.3, "", {0.008, 0}, Thickness → 0.001}, {-0.2, "", {0.008, 0}, Thickness → 0.001},
    {-0.1, "", {0.008, 0}, Thickness → 0.001}, {0, "0.0", {0.012, 0}, Thickness → 0.0011},
    {0.1, "", {0.008, 0}, Thickness → 0.001}, {0.2, "", {0.008, 0}, Thickness → 0.001},
    {0.3, "", {0.008, 0}, Thickness → 0.001}, {0.4, "", {0.008, 0}, Thickness → 0.001},
    {0.5, "0.5", {0.012, 0}, Thickness → 0.001}, {0.6, "", {0.008, 0}, Thickness → 0.001},
    {0.7, "", {0.008, 0}, Thickness → 0.001}, {0.8, "", {0.008, 0}, Thickness → 0.001}},
  {{0, "0.0"}, {0.1, "", {0.008, 0}, Thickness → 0.001}, {0.2, "", {0.008, 0}, Thickness → 0.001},
    {0.3, "", {0.008, 0}, Thickness → 0.001}, {0.4, "", {0.008, 0}, Thickness → 0.001},
    {0.5, "0.5", {0.012, 0}, Thickness → 0.001}, {0.6, "", {0.008, 0}, Thickness → 0.001},
    {0.7, "", {0.008, 0}, Thickness → 0.001}, {0.8, "", {0.008, 0}, Thickness → 0.001},
    {0.9, "", {0.008, 0}, Thickness → 0.001}, {1, "1.0", {0.012, 0}, Thickness → 0.001},
    {1.1, "", {0.008, 0}, Thickness → 0.001}, {1.2, "", {0.008, 0}, Thickness → 0.001},
    {1.3, "", {0.008, 0}, Thickness → 0.001}, {1.4, "", {0.008, 0}, Thickness → 0.001},
    {1.5, "1.5", {0.012, 0}, Thickness → 0.001}, {1.6, "", {0.008, 0}, Thickness → 0.001},
    {1.7, "", {0.008, 0}, Thickness → 0.001}, {1.8, "", {0.008, 0}, Thickness → 0.001},
    {1.9, "", {0.008, 0}, Thickness → 0.001}, {2, "2.0", {0.012, 0}, Thickness → 0.001}}},
FrameLabel → {"ωx", "Probability Density"}, LabelStyle →
  Directive[Black, FontFamily → "Arial", FontSize → 14]]
Export["/Users/gotall/Library/Mobile Documents/com~apple~CloudDocs/SPaper/Figures/Figure 8.png",
  hh, Background → None, ImageResolution → 600];
```

Figure8

Figure9

NOTE: This code takes approximately 15.6 hours.

```
Clear["Global`*"];
m = 1 000 000;
n = 1000;
R = 3;
c = 100;
sl = {};
ProgressIndicator[Dynamic[j], {1, m}]
For[j = 1, j < m + 1, j++,
  𝓗 = RandomPoint[Ball[{0, 0, 0}, R], n];
  For[i = 1, i < n + 1, i++, 𝓗[[i]] = 𝓗[[i]] / (𝓗[[i]][[1]]^2 + 𝓗[[i]][[2]]^2 + 𝓗[[i]][[3]]^2)];
  𝓗θ = RandomPoint[Sphere[{0, 0, 0}, c], n];
  𝓗𝓗 = {0, 0, 0};
  For[i = 1, i < n + 1, i++, 𝓗𝓗 = 𝓗𝓗 + 𝓗[[i]]×𝓗θ[[i]]];
  Clear[𝓗, 𝓗θ];
  sl = AppendTo[sl, Norm[1/n 𝓗𝓗]]];
𝒟 = SmoothKernelDistribution[sl, InterpolationPoints → 100, MaxRecursion → 3];
ii = Plot[{PDF[MaxwellDistribution[(c Sqrt[2/3])/R / Sqrt[1000]], x], PDF[𝒟, x]},
   {x, 0, 5.1}, PlotRange → {{-0.1, 5.21}, {-0.023, 0.73}},
   PlotStyle → {{Blue, Thickness → 0.0032}, {Red, Thickness → 0.0032}},
   Frame → {{True, False}, {True, False}}, FrameStyle → Directive[Black, Thickness → 0.0017],
   FrameTicks → {{{0, "0", {0.012, 0}, Thickness → 0.001},
       {0.2, "", {0.008, 0}, Thickness → 0.001}, {0.4, "", {0.012, 0}, Thickness → 0.001},
       {0.6, "", {0.01, 0}, Thickness → 0.001}, {0.8, "", {0.008, 0}, Thickness → 0.001},
       {1, "1", {0.012, 0}, Thickness → 0.001}, {1.2, "", {0.008, 0}, Thickness → 0.001},
       {1.4, "", {0.008, 0}, Thickness → 0.001}, {1.6, "", {0.008, 0}, Thickness → 0.001},
       {1.8, "", {0.008, 0}, Thickness → 0.001}, {2, "2", {0.012, 0}, Thickness → 0.001},
       {2.2, "", {0.008, 0}, Thickness → 0.001}, {2.4, "", {0.012, 0}, Thickness → 0.001},
       {2.6, "", {0.008, 0}, Thickness → 0.001}, {2.8, "", {0.008, 0}, Thickness → 0.001},
       {3, "3", {0.012, 0}, Thickness → 0.001}, {3.2, "", {0.008, 0}, Thickness → 0.001},
       {3.4, "", {0.008, 0}, Thickness → 0.001}, {3.6, "", {0.008, 0}, Thickness → 0.001},
       {3.8, "", {0.008, 0}, Thickness → 0.001}, {4, "4", {0.012, 0}, Thickness → 0.001},
       {4.2, "", {0.008, 0}, Thickness → 0.001}, {4.4, "", {0.008, 0}, Thickness → 0.001},
       {4.6, "", {0.008, 0}, Thickness → 0.001}, {4.8, "", {0.008, 0}, Thickness → 0.001},
       {5, "5", {0.012, 0}, Thickness → 0.001}, {5.2, "", {0.008, 0}, Thickness → 0.001}},
      {{0, "0.0", {0.012, 0}, Thickness → 0.001}, {0.1, "0.1", {0.012, 0}, Thickness → 0.001},
       {0.2, "0.2", {0.012, 0}, Thickness → 0.001}, {0.3, "0.3", {0.012, 0}, Thickness → 0.001},
       {0.4, "0.4", {0.012, 0}, Thickness → 0.001}, {0.5, "0.5", {0.012, 0}, Thickness → 0.001},
       {0.6, "0.6", {0.012, 0}, Thickness → 0.001}, {0.7, "0.7", {0.012, 0}, Thickness → 0.001}}},
   FrameLabel → {"|ω|", "Probability Density"}, LabelStyle →
     Directive[Black, FontFamily → "Arial", FontSize → 14],
   Epilog → Inset[LineLegend[{Directive[Blue, Thickness[0.0032]], Directive[Red, Thickness[0.0032]]},
       {Style["Theoretical", FontFamily → "Arial", FontSize → 14],
         Style["Simulated", FontFamily → "Arial", FontSize → 14]}, LegendFunction →
         (Framed[#, RoundingRadius → 4, FrameStyle → GrayLevel[.6]] &)], Scaled[{0.732, 0.644}]]];
Export["/Users/gotall/Library/Mobile Documents/com~apple~CloudDocs/SPaper/Figures/Figure 9.png",
  ii, Background → None, ImageResolution → 600];
```

Out[∘]=

```
## ## ## Figure9 ## ## ## ## ## ## ## ## ## ## ## ## ## ## ## ## ## ## ## ## ## ## ##
```

Figure10

In[•]:=
```
jj = Graphics[{{Directive[Thickness[0.004], Orange], Circle[{0, 0}, {2, 1}], Arrowheads[{{.03, 1}}],
    Arrow[{{−2, 0}, {−2, 0.3}}], Arrowheads[{{.03, 1}}], Arrow[{{2, 0}, {2, −0.3}}], Blue,
    Thickness[0.001], Arrowheads[{{.02, 0.2}, {.02, .6}, {.02, 1}}], Arrow[{{0, 2}, {0, −2}}],
    Arrowheads[{{.02, 0.2}, {.02, .6}, {.02, 1}}], Arrow[BezierCurve[{{−0.4, 2}, {−0.1, 0}, {−0.4, −2}}]],
    Arrowheads[{{.02, 0.2}, {.02, .6}, {.02, 1}}], Arrow[BezierCurve[{{0.4, 2}, {0.1, 0}, {0.4, −2}}]]},
  {Directive[Thickness[0.004], Orange], Circle[{5, 0}, {2, 1}], Arrowheads[{{.03, 1}}],
    Arrow[{{3, 0}, {3, 0.3}}], Arrowheads[{{.03, 1}}], Arrow[{{7, 0}, {7, −0.3}}], Blue,
    Thickness[0.001], Arrowheads[{{−.02, 0}, {−.02, .4}, {−.02, 0.8}}], Arrow[{{5, 2}, {5, −2}}],
    Arrowheads[{{−.02, 0}, {−.02, .4}, {−.02, 0.8}}], Arrow[BezierCurve[{{4.6, 2}, {4.9, 0}, {4.6, −2}}]],
    Arrowheads[{{−.02, 0}, {−.02, .4}, {−.02, 0.8}}], Arrow[BezierCurve[{{5.4, 2}, {5.1, 0}, {5.4, −2}}]]},
  {Directive[Thickness[0.004], Orange], Circle[{0, −5}, {2, 1}], Arrowheads[{{.03, 1}}],
    Arrow[{{2, −5}, {2, −5.3}}], Arrowheads[{{.03, 1}}], Arrow[{{−2, −5}, {−2, −4.7}}],
    Blue, Thickness[0.001], Arrowheads[{{−.02, 0.1}, {.02, 0.9}}], Arrow[{{0, −3}, {0, −7}}],
    Arrowheads[{{−.02, 0.12}, {.02, 0.88}}], Arrow[BezierCurve[{{−0.4, −3}, {−0.1, −5}, {−0.4, −7}}]],
    Arrowheads[{{−.02, 0.12}, {.02, 0.88}}], Arrow[BezierCurve[{{0.4, −3}, {0.1, −5}, {0.4, −7}}]]},
  {Directive[Thickness[0.004], Orange], Circle[{5, −5}, {2, 1}], Arrowheads[{{.03, 1}}],
    Arrow[{{3, −5}, {3, −4.7}}], Arrowheads[{{.03, 1}}], Arrow[{{7, −5}, {7, −5.3}}], Blue,
    Thickness[0.001], Arrowheads[{{.02, 0.13}, {−.02, 0.87}}], Arrow[{{5, −3}, {5, −7}}],
    Arrowheads[{{.02, 0.15}, {−.02, 0.85}}], Arrow[BezierCurve[{{4.6, −3}, {4.9, −5}, {4.6, −7}}]],
    Arrowheads[{{.02, 0.15}, {−.02, 0.85}}], Arrow[BezierCurve[{{5.4, −3}, {5.1, −5}, {5.4, −7}}]]},
  Inset[Style["a", Black, Bold, FontFamily → "Arial", FontSize → 20], {−2, 2}],
  Inset[Style["b", Black, Bold, FontFamily → "Arial", FontSize → 20], {3, 2}],
  Inset[Style["c", Black, Bold, FontFamily → "Arial", FontSize → 20], {−2, −3}],
  Inset[Style["d", Black, Bold, FontFamily → "Arial", FontSize → 20], {3, −3}]}];
Export["/Users/gotall/Library/Mobile Documents/com~apple~CloudDocs/SPaper/Figures/Figure 10.png",
  jj, Background → None, ImageResolution → 600];
```

Figure10

Figure11

In[•]:=
```
kk = Graphics[
  {Directive[Thickness[0.004], Orange], Circle[{0, 0}, {2, 1}], Directive[Thickness[0.004], Orange],
   Circle[{2.2, 0}, {1, 2}], Directive[Thickness[0.004], Orange], Circle[{4.4, 0}, {2, 1}],
   Directive[Thickness[0.004], Orange], Circle[{6.6, 0}, {1, 2}], Directive[Thickness[0.004], Orange],
   Circle[{8.8, 0}, {2, 1}], Directive[Thickness[0.004], Orange], Circle[{−1, 4.6}, {1, 1/2}],
   Directive[Thickness[0.004], Orange], Circle[{0.1, 4.6}, {1/2, 1}], Directive[Thickness[0.004], Orange],
   Circle[{1.2, 4.6}, {1, 1/2}], Directive[Thickness[0.004], Orange], Circle[{2.3, 4.6}, {1/2, 1}],
   Directive[Thickness[0.004], Orange], Circle[{3.4, 4.6}, {1, 1/2}], Directive[Thickness[0.004], Orange],
   Circle[{4.5, 4.6}, {1/2, 1}], Directive[Thickness[0.004], Orange], Circle[{5.6, 4.6}, {1, 1/2}],
   Directive[Thickness[0.004], Orange], Circle[{6.7, 4.6}, {1/2, 1}], Directive[Thickness[0.004], Orange],
   Circle[{7.8, 4.6}, {1, 1/2}], Directive[Thickness[0.004], Orange], Circle[{8.9, 4.6}, {1/2, 1}],
   Directive[Thickness[0.004], Orange], Circle[{10, 4.6}, {1, 1/2}], Directive[Thickness[0.003], Black],
   Arrowheads[Large], Arrow[{{1.8, 2.5}, {7.1, 2.5}}], Directive[Thickness[0.004], Orange],
```

```
    Arrowheads[Large], Arrow[{{0.4, 1}, {0.6, 1}}], Directive[Thickness[0.004], Orange],
    Arrowheads[Large], Arrow[{{0, −1}, {−0.3, −1}}], Directive[Thickness[0.004], Orange],
    Arrowheads[Large], Arrow[{{1.2, 0.2}, {1.2, 0.4}}], Directive[Thickness[0.004], Orange],
    Arrowheads[Large], Arrow[{{3.2, −0.2}, {3.2, −0.4}}], Directive[Thickness[0.004], Orange],
    Arrowheads[Large], Arrow[{{4.8, 1}, {5, 1}}], Directive[Thickness[0.004], Orange],
    Arrowheads[Large], Arrow[{{4.4, −1}, {4.1, −1}}], Directive[Thickness[0.004], Orange],
    Arrowheads[Large], Arrow[{{5.6, 0.2}, {5.6, 0.4}}], Directive[Thickness[0.004], Orange],
    Arrowheads[Large], Arrow[{{7.6, −0.2}, {7.6, −0.4}}], Directive[Thickness[0.004], Orange],
    Arrowheads[Large], Arrow[{{9.2, 1}, {9.4, 1}}], Directive[Thickness[0.004], Orange],
    Arrowheads[Large], Arrow[{{8.8, −1}, {8.5, −1}}], Directive[Thickness[0.004], Orange],
    Arrowheads[Medium], Arrow[{{−0.9, 5.1}, {−0.65, 5.1}}], Directive[Thickness[0.004], Orange],
    Arrowheads[Medium], Arrow[{{−1, 4.1}, {−1.23, 4.1}}], Directive[Thickness[0.004], Orange],
    Arrowheads[Medium], Arrow[{{−0.4, 4.7}, {−0.4, 4.9}}], Directive[Thickness[0.004], Orange],
    Arrowheads[Medium], Arrow[{{0.6, 4.7}, {0.6, 4.4}}], Directive[Thickness[0.004], Orange],
    Arrowheads[Medium], Arrow[{{1.3, 5.1}, {1.55, 5.1}}], Directive[Thickness[0.004], Orange],
    Arrowheads[Medium], Arrow[{{1.2, 4.1}, {0.97, 4.1}}], Directive[Thickness[0.004], Orange],
    Arrowheads[Medium], Arrow[{{1.8, 4.7}, {1.8, 4.9}}], Directive[Thickness[0.004], Orange],
    Arrowheads[Medium], Arrow[{{2.8, 4.7}, {2.8, 4.4}}], Directive[Thickness[0.004], Orange],
    Arrowheads[Medium], Arrow[{{3.5, 5.1}, {3.75, 5.1}}], Directive[Thickness[0.004], Orange],
    Arrowheads[Medium], Arrow[{{3.4, 4.1}, {3.17, 4.1}}], Directive[Thickness[0.004], Orange],
    Arrowheads[Medium], Arrow[{{4, 4.7}, {4, 4.9}}], Directive[Thickness[0.004], Orange],
    Arrowheads[Medium], Arrow[{{5, 4.7}, {5, 4.4}}], Directive[Thickness[0.004], Orange],
    Arrowheads[Medium], Arrow[{{5.7, 5.1}, {5.95, 5.1}}], Directive[Thickness[0.004], Orange],
    Arrowheads[Medium], Arrow[{{5.6, 4.1}, {5.37, 4.1}}], Directive[Thickness[0.004], Orange],
    Arrowheads[Medium], Arrow[{{6.2, 4.7}, {6.2, 4.9}}], Directive[Thickness[0.004], Orange],
    Arrowheads[Medium], Arrow[{{7.2, 4.7}, {7.2, 4.4}}], Directive[Thickness[0.004], Orange],
    Arrowheads[Medium], Arrow[{{7.9, 5.1}, {8.15, 5.1}}], Directive[Thickness[0.004], Orange],
    Arrowheads[Medium], Arrow[{{7.8, 4.1}, {7.57, 4.1}}], Directive[Thickness[0.004], Orange],
    Arrowheads[Medium], Arrow[{{8.4, 4.7}, {8.4, 4.9}}], Directive[Thickness[0.004], Orange],
    Arrowheads[Medium], Arrow[{{9.4, 4.7}, {9.4, 4.4}}], Directive[Thickness[0.004], Orange],
    Arrowheads[Medium], Arrow[{{10.1, 5.1}, {10.35, 5.1}}], Directive[Thickness[0.004], Orange],
    Arrowheads[Medium], Arrow[{{10, 4.1}, {9.77, 4.1}}], Directive[Thickness[0.002], Blue, Dashed],
    Line[{{−2.2, −1.2}, {−2.2, 1.2}, {2.2, 1.2}, {2.2, −1.2}, {−2.2, −1.2}}],
    Directive[Thickness[0.002], Blue, Dashed], Line[{{−2.1, 4}, {−2.1, 5.2}, {0.1, 5.2}, {0.1, 4}, {−2.1, 4}}],
    Inset[Style["Direction of light", Black, FontFamily → "Arial", FontSize → 16], {4.1, 2.9}],
    Inset[Style["S1", Blue, FontFamily → "Arial", FontSize → 16], {−0.9, 3.54}],
    Inset[Style["S2", Blue, FontFamily → "Arial", FontSize → 16], {0, 1.7}]}];
Export["/Users/gotall/Library/Mobile Documents/com~apple~CloudDocs/SPaper/Figures/Figure 11.png",
  kk, Background → None, ImageResolution → 600];

## ## ## Figure11 ## ## ## ## ## ## ## ## ## ## ## ## ## ## ## ## ## ## ## ## ## ## ## ## ## ## ##

## ## ## Figure12 ## ## ## ## ## ## ## ## ## ## ## ## ## ## ## ## ## ## ## ## ## ## ## ## ## ## ##
```

In[•]:=

```
Needs["NDSolve`FEM`"];
Ω = ImplicitRegion[0.0001 ≤ x^2 + y^2 ≤ 16, {x, y}];
mesh = ToElementMesh[Ω, MeshRefinementFunction →
    Function[{vertices, area}, area > 0.00003 (0.1 + 80 Norm[Mean[vertices]])]];

uif = NDSolveValue[{e^(−u(x,y)) (∂^2 u(x, y)/∂x^2 + ∂^2 u(x, y)/∂y^2 − (∂u(x, y)/∂x)^2 − (∂u(x, y)/∂y)^2) == 0,
    DirichletCondition[u[x, y] == 1 + 2 i, x^2 + y^2 == 0.0001],
    DirichletCondition[u[x, y] == 0, x^2 + y^2 == 16]}, u, {x, y} ∈ mesh];
ll = DensityPlot[(Norm[uif[x, y]])^2, {x, −4, 4}, {y, −4, 4}, PlotRange → {{−6.2, 7.4}, {−6.2, 6.2}, {0, 5}},
    ColorFunction → (Hue[0.65, 3 ∗ #1] &), Frame → False,
    AspectRatio → Automatic, PlotPoints → 80, Epilog →
```

```
{{Directive[Thickness[0.002], Gray, Dashed], Circle[{0, 0}, 4]}, {PointSize[0.01], Blue, Point[{0, 0}]},
 {Directive[Thickness[0.004], Orange], Circle[{0, 4}, {1.4, 0.7}], Arrowheads[{{.03, 1}}],
   Arrow[{{-1.4, 4}, {-1.39, 4.3}}], Arrowheads[{{.03, 1}}], Arrow[{{1.4, 4}, {1.39, 3.7}}],
   Blue, Thickness[0.001], Arrowheads[{{.02, 0.2}, {.02, .6}, {.02, 1}}], Arrow[{{0, 6}, {0, 2}}],
   Arrowheads[{{.02, 0.2}, {.02, .6}, {.02, 1}}], Arrow[BezierCurve[{{-1, 6}, {-0.4, 4}, {-0.5, 2}}]],
   Arrowheads[{{.02, 0.2}, {.02, .6}, {.02, 1}}], Arrow[BezierCurve[{{1, 6}, {0.4, 4}, {0.5, 2}}]]},
 {Directive[Thickness[0.004], Orange], Rotate[Circle[{{Cos[Pi/4], -Sin[Pi/4]}, {Sin[Pi/4], Cos[Pi/4]}}.{0, 4}, {1.4, 0.7}], Pi/4],
  Arrowheads[{{.03, 1}}], Arrow[{{{Cos[Pi/4], -Sin[Pi/4]}, {Sin[Pi/4], Cos[Pi/4]}}.{-1.4, 4}, {{Cos[Pi/4], -Sin[Pi/4]}, {Sin[Pi/4], Cos[Pi/4]}}.{-1.39, 4.3}}],
  Arrowheads[{{.03, 1}}], Arrow[{{{Cos[Pi/4], -Sin[Pi/4]}, {Sin[Pi/4], Cos[Pi/4]}}.{1.4, 4}, {{Cos[Pi/4], -Sin[Pi/4]}, {Sin[Pi/4], Cos[Pi/4]}}.{1.39, 3.7}}],
  Blue, Thickness[0.001], Arrowheads[{{.02, 0.2}, {.02, .6}, {.02, 1}}],
  Arrow[{{{Cos[Pi/4], -Sin[Pi/4]}, {Sin[Pi/4], Cos[Pi/4]}}.{0, 6}, {{Cos[Pi/4], -Sin[Pi/4]}, {Sin[Pi/4], Cos[Pi/4]}}.{0, 2}}],
  Arrowheads[{{.02, 0.2}, {.02, .6}, {.02, 1}}], Arrow[BezierCurve[
    {{Cos[Pi/4], -Sin[Pi/4]}, {Sin[Pi/4], Cos[Pi/4]}}.{-1, 6}, {{Cos[Pi/4], -Sin[Pi/4]}, {Sin[Pi/4], Cos[Pi/4]}}.{-0.4, 4}, {{Cos[Pi/4], -Sin[Pi/4]}, {Sin[Pi/4], Cos[Pi/4]}}.{-0.5, 2}}]],
  Arrowheads[{{.02, 0.2}, {.02, .6}, {.02, 1}}], Arrow[BezierCurve[
    {{Cos[Pi/4], -Sin[Pi/4]}, {Sin[Pi/4], Cos[Pi/4]}}.{1, 6}, {{Cos[Pi/4], -Sin[Pi/4]}, {Sin[Pi/4], Cos[Pi/4]}}.{0.4, 4}, {{Cos[Pi/4], -Sin[Pi/4]}, {Sin[Pi/4], Cos[Pi/4]}}.{0.5, 2}}]]},
 {Directive[Thickness[0.004], Orange], Rotate[Circle[{{Cos[Pi/2], -Sin[Pi/2]}, {Sin[Pi/2], Cos[Pi/2]}}.{0, 4}, {1.4, 0.7}], Pi/2],
  Arrowheads[{{.03, 1}}], Arrow[{{{Cos[Pi/2], -Sin[Pi/2]}, {Sin[Pi/2], Cos[Pi/2]}}.{-1.4, 4}, {{Cos[Pi/2], -Sin[Pi/2]}, {Sin[Pi/2], Cos[Pi/2]}}.{-1.39, 4.3}}],
  Arrowheads[{{.03, 1}}], Arrow[{{{Cos[Pi/2], -Sin[Pi/2]}, {Sin[Pi/2], Cos[Pi/2]}}.{1.4, 4}, {{Cos[Pi/2], -Sin[Pi/2]}, {Sin[Pi/2], Cos[Pi/2]}}.{1.39, 3.7}}],
  Blue, Thickness[0.001], Arrowheads[{{.02, 0.2}, {.02, .6}, {.02, 1}}],
  Arrow[{{{Cos[Pi/2], -Sin[Pi/2]}, {Sin[Pi/2], Cos[Pi/2]}}.{0, 6}, {{Cos[Pi/2], -Sin[Pi/2]}, {Sin[Pi/2], Cos[Pi/2]}}.{0, 2}}],
  Arrowheads[{{.02, 0.2}, {.02, .6}, {.02, 1}}], Arrow[BezierCurve[
    {{Cos[Pi/2], -Sin[Pi/2]}, {Sin[Pi/2], Cos[Pi/2]}}.{-1, 6}, {{Cos[Pi/2], -Sin[Pi/2]}, {Sin[Pi/2], Cos[Pi/2]}}.{-0.4, 4}, {{Cos[Pi/2], -Sin[Pi/2]}, {Sin[Pi/2], Cos[Pi/2]}}.{-0.5, 2}}]],
  Arrowheads[{{.02, 0.2}, {.02, .6}, {.02, 1}}], Arrow[BezierCurve[
    {{Cos[Pi/2], -Sin[Pi/2]}, {Sin[Pi/2], Cos[Pi/2]}}.{1, 6}, {{Cos[Pi/2], -Sin[Pi/2]}, {Sin[Pi/2], Cos[Pi/2]}}.{0.4, 4}, {{Cos[Pi/2], -Sin[Pi/2]}, {Sin[Pi/2], Cos[Pi/2]}}.{0.5, 2}}]]}}
```

$$\left\{\text{Directive}[\text{Thickness}[0.004],\ \text{Orange}],\ \text{Rotate}\left[\text{Circle}\left[\begin{pmatrix}\cos\left(\frac{3\pi}{4}\right) & -\sin\left(\frac{3\pi}{4}\right)\\ \sin\left(\frac{3\pi}{4}\right) & \cos\left(\frac{3\pi}{4}\right)\end{pmatrix}.\{0,\ 4\},\ \{1.4,\ 0.7\}\right],\ \frac{3\pi}{4}\right],\right.$$

$$\text{Arrowheads}[\{\{.03,\ 1\}\}],$$

$$\text{Arrow}\left[\left\{\begin{pmatrix}\cos\left(\frac{3\pi}{4}\right) & -\sin\left(\frac{3\pi}{4}\right)\\ \sin\left(\frac{3\pi}{4}\right) & \cos\left(\frac{3\pi}{4}\right)\end{pmatrix}.\{-1.4,\ 4\},\ \begin{pmatrix}\cos\left(\frac{3\pi}{4}\right) & -\sin\left(\frac{3\pi}{4}\right)\\ \sin\left(\frac{3\pi}{4}\right) & \cos\left(\frac{3\pi}{4}\right)\end{pmatrix}.\{-1.39,\ 4.3\}\right\}\right],$$

$$\text{Arrowheads}[\{\{.03,\ 1\}\}],\ \text{Arrow}\left[\left\{\begin{pmatrix}\cos\left(\frac{3\pi}{4}\right) & -\sin\left(\frac{3\pi}{4}\right)\\ \sin\left(\frac{3\pi}{4}\right) & \cos\left(\frac{3\pi}{4}\right)\end{pmatrix}.\{1.4,\ 4\},\ \begin{pmatrix}\cos\left(\frac{3\pi}{4}\right) & -\sin\left(\frac{3\pi}{4}\right)\\ \sin\left(\frac{3\pi}{4}\right) & \cos\left(\frac{3\pi}{4}\right)\end{pmatrix}.\{1.39,\ 3.7\}\right\}\right],$$

$$\text{Blue},\ \text{Thickness}[0.001],\ \text{Arrowheads}[\{\{.02,\ 0.2\},\ \{.02,\ .6\},\ \{.02,\ 1\}\}],$$

$$\text{Arrow}\left[\left\{\begin{pmatrix}\cos\left(\frac{3\pi}{4}\right) & -\sin\left(\frac{3\pi}{4}\right)\\ \sin\left(\frac{3\pi}{4}\right) & \cos\left(\frac{3\pi}{4}\right)\end{pmatrix}.\{0,\ 6\},\ \begin{pmatrix}\cos\left(\frac{3\pi}{4}\right) & -\sin\left(\frac{3\pi}{4}\right)\\ \sin\left(\frac{3\pi}{4}\right) & \cos\left(\frac{3\pi}{4}\right)\end{pmatrix}.\{0,\ 2\}\right\}\right],$$

$$\text{Arrowheads}[\{\{.02,\ 0.2\},\ \{.02,\ .6\},\ \{.02,\ 1\}\}],\ \text{Arrow}\left[\text{BezierCurve}\left[\left\{\begin{pmatrix}\cos\left(\frac{3\pi}{4}\right) & -\sin\left(\frac{3\pi}{4}\right)\\ \sin\left(\frac{3\pi}{4}\right) & \cos\left(\frac{3\pi}{4}\right)\end{pmatrix}.\{-1,\ 6\},\right.\right.$$

$$\left.\left.\begin{pmatrix}\cos\left(\frac{3\pi}{4}\right) & -\sin\left(\frac{3\pi}{4}\right)\\ \sin\left(\frac{3\pi}{4}\right) & \cos\left(\frac{3\pi}{4}\right)\end{pmatrix}.\{-0.4,\ 4\},\ \begin{pmatrix}\cos\left(\frac{3\pi}{4}\right) & -\sin\left(\frac{3\pi}{4}\right)\\ \sin\left(\frac{3\pi}{4}\right) & \cos\left(\frac{3\pi}{4}\right)\end{pmatrix}.\{-0.5,\ 2\}\right\}\right]\right],$$

$$\text{Arrowheads}[\{\{.02,\ 0.2\},\ \{.02,\ .6\},\ \{.02,\ 1\}\}],\ \text{Arrow}\left[\text{BezierCurve}\left[\right.\right.$$

$$\left.\left.\left\{\begin{pmatrix}\cos\left(\frac{3\pi}{4}\right) & -\sin\left(\frac{3\pi}{4}\right)\\ \sin\left(\frac{3\pi}{4}\right) & \cos\left(\frac{3\pi}{4}\right)\end{pmatrix}.\{1,\ 6\},\ \begin{pmatrix}\cos\left(\frac{3\pi}{4}\right) & -\sin\left(\frac{3\pi}{4}\right)\\ \sin\left(\frac{3\pi}{4}\right) & \cos\left(\frac{3\pi}{4}\right)\end{pmatrix}.\{0.4,\ 4\},\ \begin{pmatrix}\cos\left(\frac{3\pi}{4}\right) & -\sin\left(\frac{3\pi}{4}\right)\\ \sin\left(\frac{3\pi}{4}\right) & \cos\left(\frac{3\pi}{4}\right)\end{pmatrix}.\{0.5,\ 2\}\right\}\right]\right]\right\},$$

$$\left\{\text{Directive}[\text{Thickness}[0.004],\ \text{Orange}],\ \text{Rotate}\left[\text{Circle}\left[\begin{pmatrix}\cos(\pi) & -\sin(\pi)\\ \sin(\pi) & \cos(\pi)\end{pmatrix}.\{0,\ 4\},\ \{1.4,\ 0.7\}\right],\ \pi\right],\right.$$

$$\text{Arrowheads}[\{\{.03,\ 1\}\}],\ \text{Arrow}\left[\left\{\begin{pmatrix}\cos(\pi) & -\sin(\pi)\\ \sin(\pi) & \cos(\pi)\end{pmatrix}.\{-1.4,\ 4\},\ \begin{pmatrix}\cos(\pi) & -\sin(\pi)\\ \sin(\pi) & \cos(\pi)\end{pmatrix}.\{-1.39,\ 4.3\}\right\}\right],$$

$$\text{Arrowheads}[\{\{.03,\ 1\}\}],\ \text{Arrow}\left[\left\{\begin{pmatrix}\cos(\pi) & -\sin(\pi)\\ \sin(\pi) & \cos(\pi)\end{pmatrix}.\{1.4,\ 4\},\ \begin{pmatrix}\cos(\pi) & -\sin(\pi)\\ \sin(\pi) & \cos(\pi)\end{pmatrix}.\{1.39,\ 3.7\}\right\}\right],$$

$$\text{Blue},\ \text{Thickness}[0.001],\ \text{Arrowheads}[\{\{.02,\ 0.2\},\ \{.02,\ .6\},\ \{.02,\ 1\}\}],$$

$$\text{Arrow}\left[\left\{\begin{pmatrix}\cos(\pi) & -\sin(\pi)\\ \sin(\pi) & \cos(\pi)\end{pmatrix}.\{0,\ 6\},\ \begin{pmatrix}\cos(\pi) & -\sin(\pi)\\ \sin(\pi) & \cos(\pi)\end{pmatrix}.\{0,\ 2\}\right\}\right],$$

$$\text{Arrowheads}[\{\{.02,\ 0.2\},\ \{.02,\ .6\},\ \{.02,\ 1\}\}],\ \text{Arrow}\left[\text{BezierCurve}\left[\right.\right.$$

$$\left.\left.\left\{\begin{pmatrix}\cos(\pi) & -\sin(\pi)\\ \sin(\pi) & \cos(\pi)\end{pmatrix}.\{-1,\ 6\},\ \begin{pmatrix}\cos(\pi) & -\sin(\pi)\\ \sin(\pi) & \cos(\pi)\end{pmatrix}.\{-0.4,\ 4\},\ \begin{pmatrix}\cos(\pi) & -\sin(\pi)\\ \sin(\pi) & \cos(\pi)\end{pmatrix}.\{-0.5,\ 2\}\right\}\right]\right],$$

$$\text{Arrowheads}[\{\{.02,\ 0.2\},\ \{.02,\ .6\},\ \{.02,\ 1\}\}],\ \text{Arrow}\left[\text{BezierCurve}\left[\right.\right.$$

$$\left.\left.\left\{\begin{pmatrix}\cos(\pi) & -\sin(\pi)\\ \sin(\pi) & \cos(\pi)\end{pmatrix}.\{1,\ 6\},\ \begin{pmatrix}\cos(\pi) & -\sin(\pi)\\ \sin(\pi) & \cos(\pi)\end{pmatrix}.\{0.4,\ 4\},\ \begin{pmatrix}\cos(\pi) & -\sin(\pi)\\ \sin(\pi) & \cos(\pi)\end{pmatrix}.\{0.5,\ 2\}\right\}\right]\right]\right\},$$

$$\left\{\text{Directive}[\text{Thickness}[0.004],\ \text{Orange}],\ \text{Rotate}\left[\text{Circle}\left[\begin{pmatrix}\cos\left(\frac{5\pi}{4}\right) & -\sin\left(\frac{5\pi}{4}\right)\\ \sin\left(\frac{5\pi}{4}\right) & \cos\left(\frac{5\pi}{4}\right)\end{pmatrix}.\{0,\ 4\},\ \{1.4,\ 0.7\}\right],\ \frac{5\pi}{4}\right],\right.$$

$$\text{Arrowheads}[\{\{.03,\ 1\}\}],$$

$$\text{Arrow}\left[\left\{\begin{pmatrix}\cos\left(\frac{5\pi}{4}\right) & -\sin\left(\frac{5\pi}{4}\right)\\ \sin\left(\frac{5\pi}{4}\right) & \cos\left(\frac{5\pi}{4}\right)\end{pmatrix}.\{-1.4,\ 4\},\ \begin{pmatrix}\cos\left(\frac{5\pi}{4}\right) & -\sin\left(\frac{5\pi}{4}\right)\\ \sin\left(\frac{5\pi}{4}\right) & \cos\left(\frac{5\pi}{4}\right)\end{pmatrix}.\{-1.39,\ 4.3\}\right\}\right],$$

```
Arrowheads[{{.03, 1}}], Arrow[{{{Cos[5 π/4], -Sin[5 π/4]}, {Sin[5 π/4], Cos[5 π/4]}}.{1.4, 4}, {{Cos[5 π/4], -Sin[5 π/4]}, {Sin[5 π/4], Cos[5 π/4]}}.{1.39, 3.7}}],
Blue, Thickness[0.001], Arrowheads[{{.02, 0.2}, {.02, .6}, {.02, 1}}],
Arrow[{{{Cos[5 π/4], -Sin[5 π/4]}, {Sin[5 π/4], Cos[5 π/4]}}.{0, 6}, {{Cos[5 π/4], -Sin[5 π/4]}, {Sin[5 π/4], Cos[5 π/4]}}.{0, 2}}],
Arrowheads[{{.02, 0.2}, {.02, .6}, {.02, 1}}], Arrow[BezierCurve[{{{Cos[5 π/4], -Sin[5 π/4]}, {Sin[5 π/4], Cos[5 π/4]}}.{-1, 6},
  {{Cos[5 π/4], -Sin[5 π/4]}, {Sin[5 π/4], Cos[5 π/4]}}.{-0.4, 4}, {{Cos[5 π/4], -Sin[5 π/4]}, {Sin[5 π/4], Cos[5 π/4]}}.{-0.5, 2}}]],
Arrowheads[{{.02, 0.2}, {.02, .6}, {.02, 1}}], Arrow[BezierCurve[
  {{{Cos[5 π/4], -Sin[5 π/4]}, {Sin[5 π/4], Cos[5 π/4]}}.{1, 6}, {{Cos[5 π/4], -Sin[5 π/4]}, {Sin[5 π/4], Cos[5 π/4]}}.{0.4, 4}, {{Cos[5 π/4], -Sin[5 π/4]}, {Sin[5 π/4], Cos[5 π/4]}}.{0.5, 2}}]]},
{Directive[Thickness[0.004], Orange], Rotate[Circle[{{Cos[3 π/2], -Sin[3 π/2]}, {Sin[3 π/2], Cos[3 π/2]}}.{0, 4}, {1.4, 0.7}], 3 π/2]},
Arrowheads[{{.03, 1}}],
Arrow[{{{Cos[3 π/2], -Sin[3 π/2]}, {Sin[3 π/2], Cos[3 π/2]}}.{-1.4, 4}, {{Cos[3 π/2], -Sin[3 π/2]}, {Sin[3 π/2], Cos[3 π/2]}}.{-1.39, 4.3}}],
Arrowheads[{{.03, 1}}], Arrow[{{{Cos[3 π/2], -Sin[3 π/2]}, {Sin[3 π/2], Cos[3 π/2]}}.{1.4, 4}, {{Cos[3 π/2], -Sin[3 π/2]}, {Sin[3 π/2], Cos[3 π/2]}}.{1.39, 3.7}}],
Blue, Thickness[0.001], Arrowheads[{{.02, 0.2}, {.02, .6}, {.02, 1}}],
Arrow[{{{Cos[3 π/2], -Sin[3 π/2]}, {Sin[3 π/2], Cos[3 π/2]}}.{0, 6}, {{Cos[3 π/2], -Sin[3 π/2]}, {Sin[3 π/2], Cos[3 π/2]}}.{0, 2}}],
Arrowheads[{{.02, 0.2}, {.02, .6}, {.02, 1}}], Arrow[BezierCurve[{{{Cos[3 π/2], -Sin[3 π/2]}, {Sin[3 π/2], Cos[3 π/2]}}.{-1, 6},
  {{Cos[3 π/2], -Sin[3 π/2]}, {Sin[3 π/2], Cos[3 π/2]}}.{-0.4, 4}, {{Cos[3 π/2], -Sin[3 π/2]}, {Sin[3 π/2], Cos[3 π/2]}}.{-0.5, 2}}]],
Arrowheads[{{.02, 0.2}, {.02, .6}, {.02, 1}}], Arrow[BezierCurve[
  {{{Cos[3 π/2], -Sin[3 π/2]}, {Sin[3 π/2], Cos[3 π/2]}}.{1, 6}, {{Cos[3 π/2], -Sin[3 π/2]}, {Sin[3 π/2], Cos[3 π/2]}}.{0.4, 4}, {{Cos[3 π/2], -Sin[3 π/2]}, {Sin[3 π/2], Cos[3 π/2]}}.{0.5, 2}}]]},
{Directive[Thickness[0.004], Orange], Rotate[Circle[{{Cos[7 π/4], -Sin[7 π/4]}, {Sin[7 π/4], Cos[7 π/4]}}.{0, 4}, {1.4, 0.7}], 7 π/4]},
Arrowheads[{{.03, 1}}],
```

```
Arrow[{{{Cos[7 π/4], -Sin[7 π/4]}, {Sin[7 π/4], Cos[7 π/4]}}.{-1.4, 4}, {{Cos[7 π/4], -Sin[7 π/4]}, {Sin[7 π/4], Cos[7 π/4]}}.{-1.39, 4.3}}],

Arrowheads[{{.03, 1}}], Arrow[{{{Cos[7 π/4], -Sin[7 π/4]}, {Sin[7 π/4], Cos[7 π/4]}}.{1.4, 4}, {{Cos[7 π/4], -Sin[7 π/4]}, {Sin[7 π/4], Cos[7 π/4]}}.{1.39, 3.7}}],

Blue, Thickness[0.001], Arrowheads[{{.02, 0.2}, {.02, .6}, {.02, 1}}],

Arrow[{{{Cos[7 π/4], -Sin[7 π/4]}, {Sin[7 π/4], Cos[7 π/4]}}.{0, 6}, {{Cos[7 π/4], -Sin[7 π/4]}, {Sin[7 π/4], Cos[7 π/4]}}.{0, 2}}],

Arrowheads[{{.02, 0.2}, {.02, .6}, {.02, 1}}], Arrow[BezierCurve[{{{Cos[7 π/4], -Sin[7 π/4]}, {Sin[7 π/4], Cos[7 π/4]}}.{-1, 6},
  {{Cos[7 π/4], -Sin[7 π/4]}, {Sin[7 π/4], Cos[7 π/4]}}.{-0.4, 4}, {{Cos[7 π/4], -Sin[7 π/4]}, {Sin[7 π/4], Cos[7 π/4]}}.{-0.5, 2}}]],

Arrowheads[{{.02, 0.2}, {.02, .6}, {.02, 1}}], Arrow[BezierCurve[
  {{{Cos[7 π/4], -Sin[7 π/4]}, {Sin[7 π/4], Cos[7 π/4]}}.{1, 6}, {{Cos[7 π/4], -Sin[7 π/4]}, {Sin[7 π/4], Cos[7 π/4]}}.{0.4, 4}, {{Cos[7 π/4], -Sin[7 π/4]}, {Sin[7 π/4], Cos[7 π/4]}}.{0.5, 2}}]]},

{Black, Thickness[0.0005], Arrowheads[0.04], Arrow[{{6.9, -0.4}, {6.9, -5}}]},
{Black, Thickness[0.0005], Arrowheads[0.04], Arrow[{{6.9, 0.4}, {6.9, 5}}]},
{Black, Thickness[0.0005], Line[{{6.5, 5}, {7.3, 5}}]},
{Black, Thickness[0.0005], Line[{{6.5, -5}, {7.3, -5}}]},
Inset[Style["𝒫1", Blue, FontFamily → "Arial", FontSize → 16], {0.6, 0.1}],
Inset[Style["𝒮", Orange, FontFamily → "Arial", FontSize → 16], {-1.3, 4.7}],
Inset[Style["k2", Blue, FontFamily → "Arial", FontSize → 16], {-0.39, 5.5}],
Inset[Style["k2", Blue, FontFamily → "Arial", FontSize → 16], {0.4, 5.5}],
Inset[Style["k1", Black, FontFamily → "Arial", FontSize → 16], {6.98, 0}]}];

Export["/Users/gotall/Library/Mobile Documents/com~apple~CloudDocs/SPaper/Figures/Figure 12.png",
  ll, Background → None, ImageResolution → 300];

## ## ## Figure12 ## ## ## ## ## ## ## ## ## ## ## ## ## ## ## ## ## ## ## ## ## ## ## ## ## ## ##
```